Introduction to Neutron (and X-ray) Scattering Techniques

Jeffrey Lynn
NIST Center for Neutron Research

FQM School
January, 2018

Outline

- Scattering Basics
  - Cross sections, form factors, x-rays vs. neutrons
- Powder Diffraction (crystal and magnetic diffraction)
  - Profile refinement, subtraction technique, polarized neutrons
- Single Crystal Diffraction (structure and magnetic)
- Small Angle Neutron Scattering (SANS)
  - Nanoparticles, Vortex lattice, ferromagnetic superconductor, skyrmions
- Reflectometry (thin films and multilayers)
  - Structural and Magnetic Depth Profile
- Inelastic Scattering
  - Phonons, Magnons, Spin Ice, Spin Liquid

- Reference Materials

Main Message: Neutron (and x-ray) scattering

Neutron scattering experiments measure the flux of neutrons scattered by a sample into a detector as a function of the change in neutron wave vector ($\vec{Q}$) and energy ($\hbar\omega$).

$$\Phi(Q,\hbar\omega) = \frac{\text{neutrons}}{\text{sec–cm}^2}$$

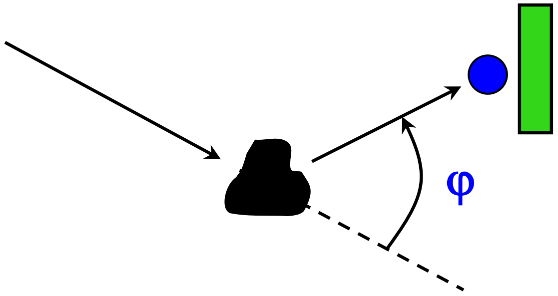

Momentum	Energy
$\hbar k_n = \hbar(2\pi/\lambda_n)$	$E = \hbar^2 k_n{}^2/2m$
$\hbar\vec{Q} = \hbar\vec{k}_i - \hbar\vec{k}_f$	$E = E_i - E_f$

The expressions for the scattered neutron flux Φ depend on the positions and motions of atomic nuclei or unpaired electron spins.

$$\Phi = \mathcal{F}\{\vec{r}_i(t), \vec{r}_j(t), \vec{S}_i(t), \vec{S}_j(t)\}$$

Φ provides information about all of these quantities!

Conservation of Momentum and Energy

$$\mathbf{Q} = \mathbf{k}_i - \mathbf{k}_f$$

$$\Delta E = \frac{\hbar^2 k_i^2}{2m} - \frac{\hbar^2 k_f^2}{2m}$$

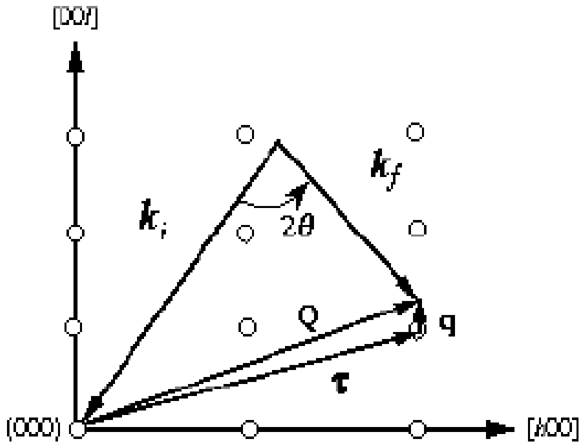

$$\mathbf{Q}_C = \tau + \mathbf{q}$$

Reciprocal (Scattering) Space

Periodic array of atoms in Real Space

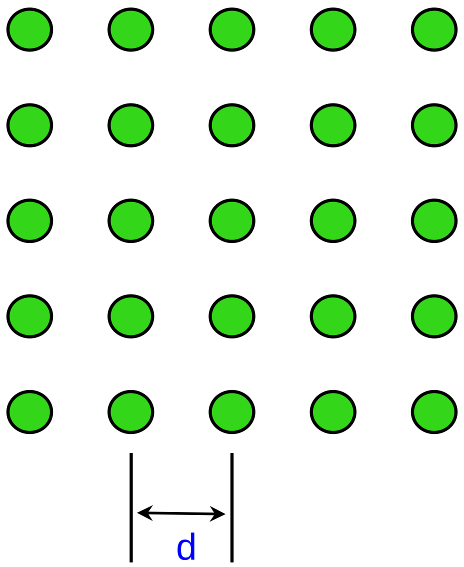

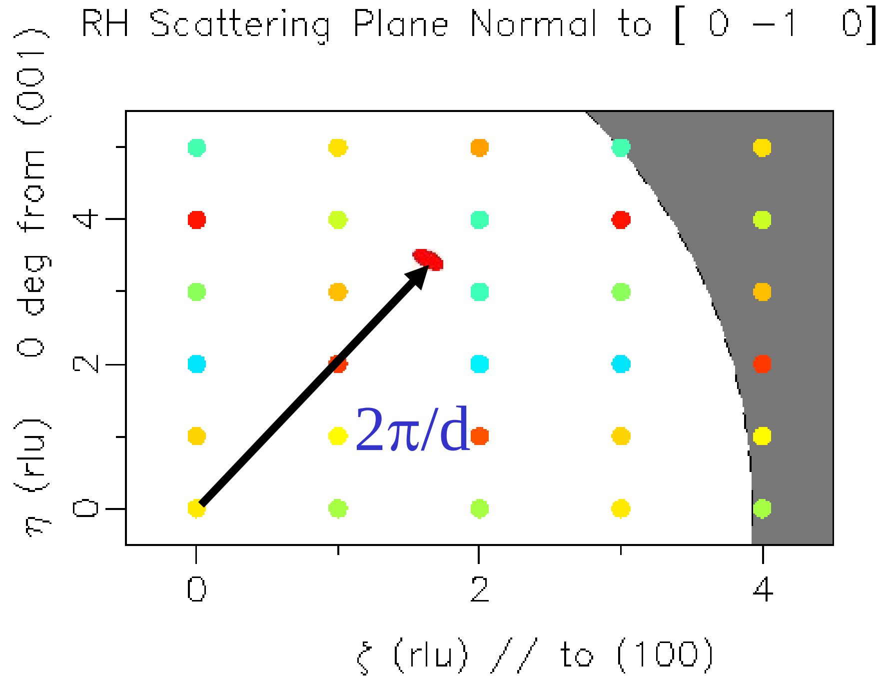

Real space ↔ Reciprocal (Fourier) Space

Other Probes

$$E_{neutron}(meV) = 2.0719k^2 = 81.7968/\lambda^2$$

$$E_{photon}(keV) = 2.0k = 12.4/\lambda$$

$$E_{electron}(eV) = 3.8k^2 = 150/\lambda^2$$

λ = 1 Å: E_n=82 meV; E_p=12,400,000 meV; E_e=150,000 meV

$$1\,meV = 11.6\,K \quad (k_B T)$$

300 K → 25 meV

$$1\,meV = 8.06\,cm^{-1} \quad (E/hc)$$

$$1\,meV = 0.2418\,THz \quad (E/h)$$

$$1\,meV/\mu_B = 17.3\,T \quad (E/\mu_B)$$

Neutron Source: Moderation

Maxwellian Distribution

$$\Phi \sim v^3 e^{(-mv^2/2k_BT)}$$

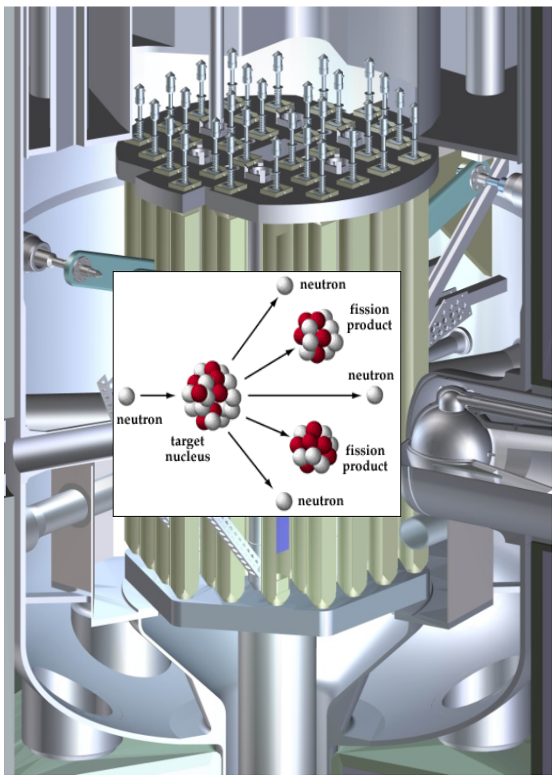

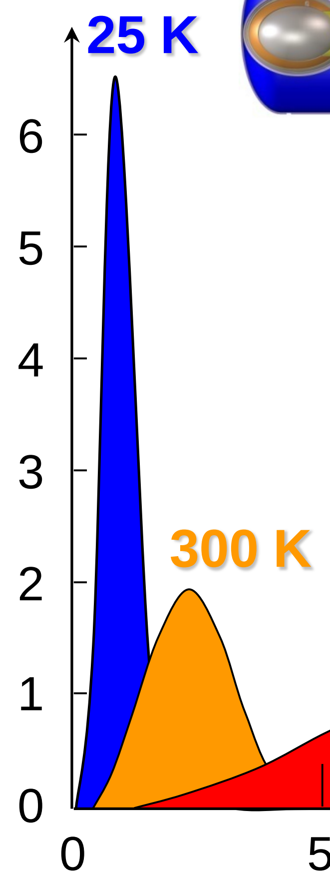

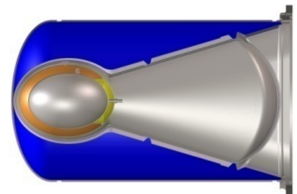

Liquid Hydrogen

Heavy Water (D_2O)

Hot Graphite

"Fast" neutrons: v = 20,000 km/sec

Neutron velocity v (km/sec)

Neutron and X-ray Scattering

- Both techniques collect data as functions of the energy and the momentum transferred from the system to the neutron or photon beam. The resulting five-dimensional data sets serve as powerful probes of materials. Elastic scattering elucidates the crystal structure, magnetic configuration, direction of the spins, symmetry of the magnetic state, spatial distribution of the magnetization density, and dependence of the order(s) parameter on thermodynamic fields such as temperature, pressure, magnetic and electric fields. Inelastic scattering determines the energies of the fundamental excitations which can be used to elucidate the nature, strength, and range of the interactions.
- Both techniques can measure crystal and magnetic structures and their dynamics.
- Neutron advantages:
  - Magnetic and structural scattering are comparable in strength; Elastic scattering yields quantitative information; energy resolution is orders-of-magnitude better than x-rays; simplicity of sample environment; low T accessible. Theory has solid theoretical basis.
- X-ray advantages:
  - High Flux → small samples; individual domains, topography; pump probe capability; resonant x-ray scattering →element specific; magnetic resonant x-ray scattering; RIXS

NCNR

Neutron Cross Sections

$$I_N(\mathbf{g}) = CM_{\tau}A(\theta_B)\left|F_N(\mathbf{g})\right|^2$$

$$\left|F_N(\mathbf{g})\right|^2 = \left|\sum_j b_j e^{i\mathbf{g}\cdot\boldsymbol{r}_j} e^{-W_j}\right|^2$$

$$I_M(\mathbf{g}_{hkl}) = C\left(\frac{\gamma e^2}{2mc^2}\right)^2 M_{\mathbf{g}}A(\theta_B)\left|F_M(\mathbf{g}_{hkl})\right|^2$$

$$F_M(\mathbf{g}_{hkl}) = \sum_{j=1}^{N} e^{i g\cdot \mathbf{r}_j}\hat{\mathbf{g}}\times\left[\boldsymbol{M}_j(\mathbf{g})\times\hat{\mathbf{g}}\right]e^{-W_j}$$

$$\left|F_M(\mathbf{g})\right|^2 = \left\langle 1-\left(\hat{\mathbf{g}}\cdot\hat{\boldsymbol{\eta}}\right)^2\right\rangle\left\langle \mu^z\right\rangle^2 f^2(\mathbf{g})\left|\sum_j \eta_j e^{i\mathbf{g}\cdot\boldsymbol{r}_j} e^{-W_j}\right|^2$$

Neutrons and X-rays are Complementary

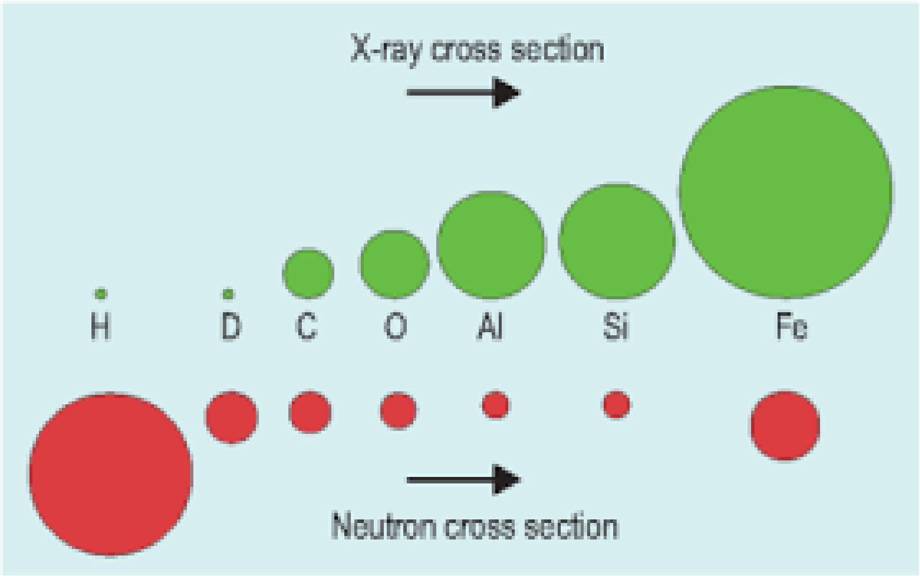

Nucleus looks like a point particle → b is just a constant independent of scattering angle.

Adjacent elements, heavy + light elements, isotope substitution

Neutrons and X-rays are Complementary

magnetic scattering amplitude for an ion is related to the Fourier Transform of the total magnetisation density, M(r)::

$$\mathrm{M}(\mathrm{q}) = \int \mathrm{M}(\mathrm{r}) \exp\left[i(\mathrm{q}\cdot\mathrm{r}) \right] d^3r$$

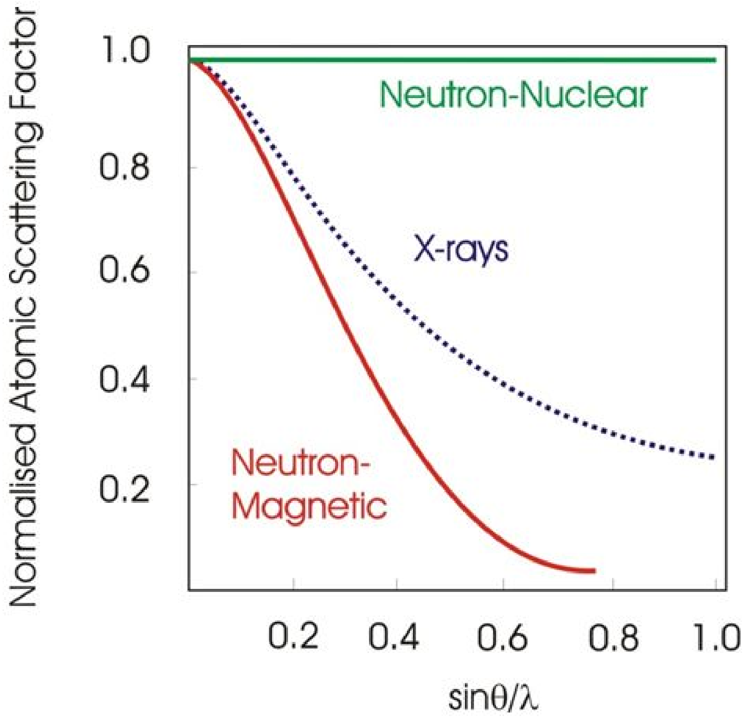

As the magnetism arises from unpaired electrons in *outer shells* and not the nucleus there is a dependence on intensity, similar to the sin(θ)/ λ used for x-rays

NCNR

Neutron Cross Sections

$$I_N(\mathbf{g}) = CM_{\tau}A(\theta_B)\left|F_N(\mathbf{g})\right|^2$$

$$\left|F_N(\mathbf{g})\right|^2 = \left|\sum_j b_j e^{i\mathbf{g}\cdot\mathbf{r}_j} e^{-W_j}\right|^2$$

$$I_M(\mathbf{g}_{hkl}) = C\left(\frac{\gamma e^2}{2mc^2}\right)^2 M_{\mathbf{g}}A(\theta_B)\left|F_M(\mathbf{g}_{hkl})\right|^2$$

$$F_M(\mathbf{g}_{hkl}) = \sum_{j=1}^{N} e^{i\mathbf{g}\cdot\mathbf{r}_j}\hat{\mathbf{g}}\times\left[\boldsymbol{M}_j(\mathbf{g})\times\hat{\mathbf{g}}\right]e^{-W_j}$$

$$\left|F_M(\mathbf{g})\right|^2 = \left\langle 1-\left(\hat{\mathbf{g}}\cdot\hat{\boldsymbol{\eta}}\right)^2\right\rangle\left\langle\mu^z\right\rangle^2 f^2(\mathbf{g})\left|\sum_j \eta_j e^{i\mathbf{g}\cdot\mathbf{r}_j} e^{-W_j}\right|^2$$

Magnetic X-ray Cross Sections

$$F_j(E) = \sigma^{(0)}(E)\, \varepsilon_i \cdot \varepsilon_o^* + \sigma^{(1)}(E)\, \varepsilon_i \times \varepsilon_o^* \cdot M_j + \sigma^{(2)}(E) \left(\left(\varepsilon_i \cdot M_j\right)\left(\varepsilon_o^* \cdot M_j\right) - \frac{1}{3} \varepsilon_i \cdot \varepsilon_o^* \right)$$

$$I = \left| \sum_j e^{ig \cdot r_j} \sigma_j^{(1)}(E)\, \varepsilon_i \times \varepsilon_o^* \cdot M_j \right|^2$$

Reciprocal Space for Powder

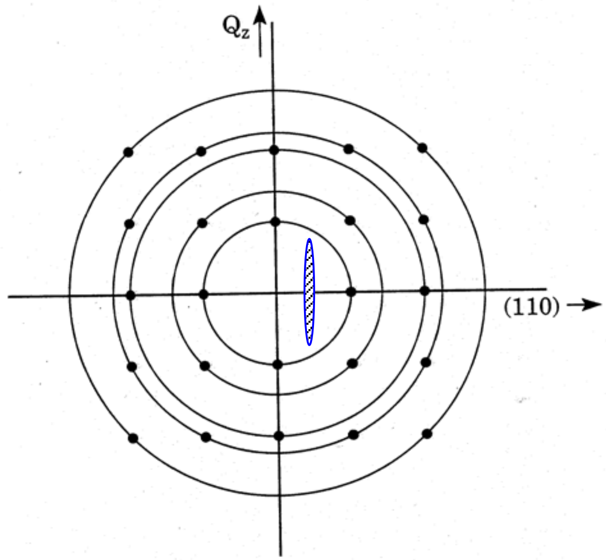

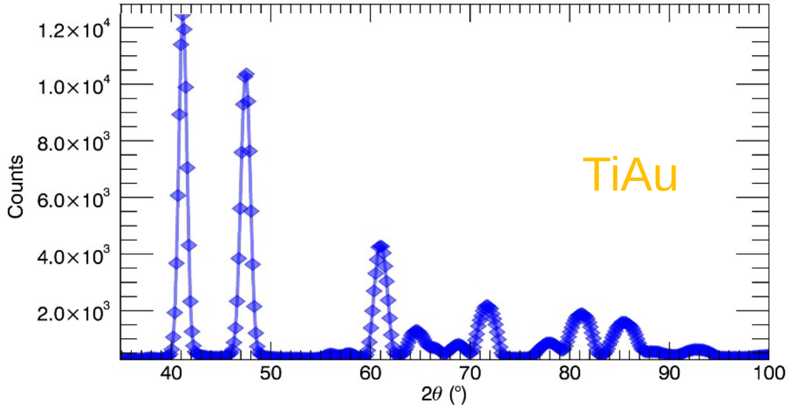

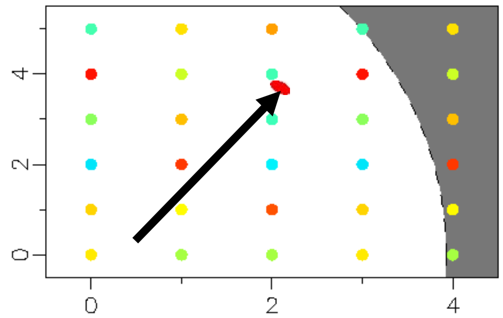

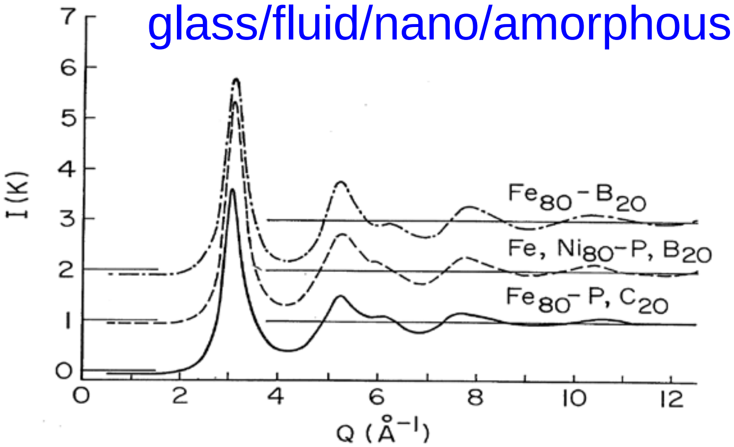

Review

The scattered neutron flux $\Phi(\vec{Q},\hbar\omega)$ is proportional to the space ($\vec{r}$) and time (t) Fourier transform of the probability $G(\vec{r},t)$ of finding one or two atoms (*spins*) separated by a particular distance (*angle*) at a particular time.

$$\Phi \propto \frac{\partial^2\sigma}{\partial\Omega\partial\omega} \propto \iint e^{i(\vec{Q}\cdot\vec{r}-\omega t)} G(\vec{r},t)\, d^3\vec{r}\, dt$$

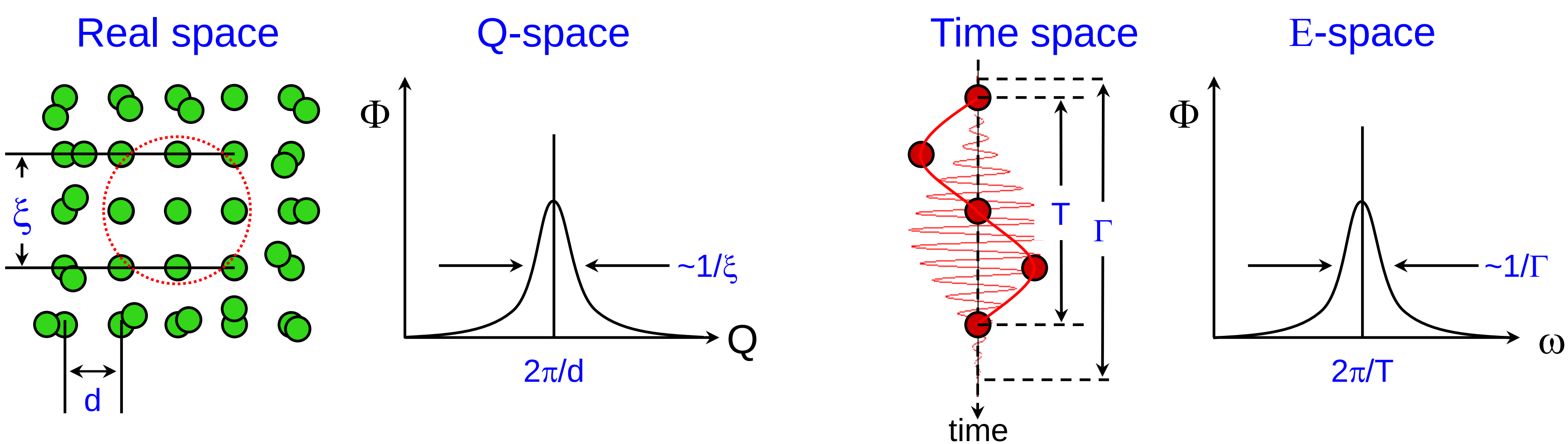

Neutron Scattering Techniques

Diffraction

- **Crystallography**–powder, single crystal
  Atomic positions, site occupancies, lattice parameters, bond distances, mean-square vibrations as a function of T, H, P
- **Magnetism**
  Magnetic structure, order parameter, spin directions, spin density distribution
  Phase Transitions and Critical Phenomena (Scaling, Universality)
- **Small Angle Neutron Scattering (SANS)**
  Ferromagnetic Correlations, Vortex Structures, Domain Structures, Grain boundaries, twin boundaries, defect structures, nanoparticles, skyrmions, …
- **Thin Film Reflectometry**
  Density profiles, Magnetic structures, Magnetization profiles, Surface and Interface properties (flatness, roughness)

Inelastic Scattering

Lattice Dynamics

Phonon Dispersion, Density of States
Interatomic Force constants
Mean-square vibrations
Diffusion

Spin Dynamics

Magnon Dispersion, Exchange interactions
Magnetic Anisotropy
Magnetic Fluctuation Behavior
Crystal Field Levels
Magnetic-Structural Coupling

NIST Center for Neutron Research

May 2017

RESEARCH PARTICIPANTS

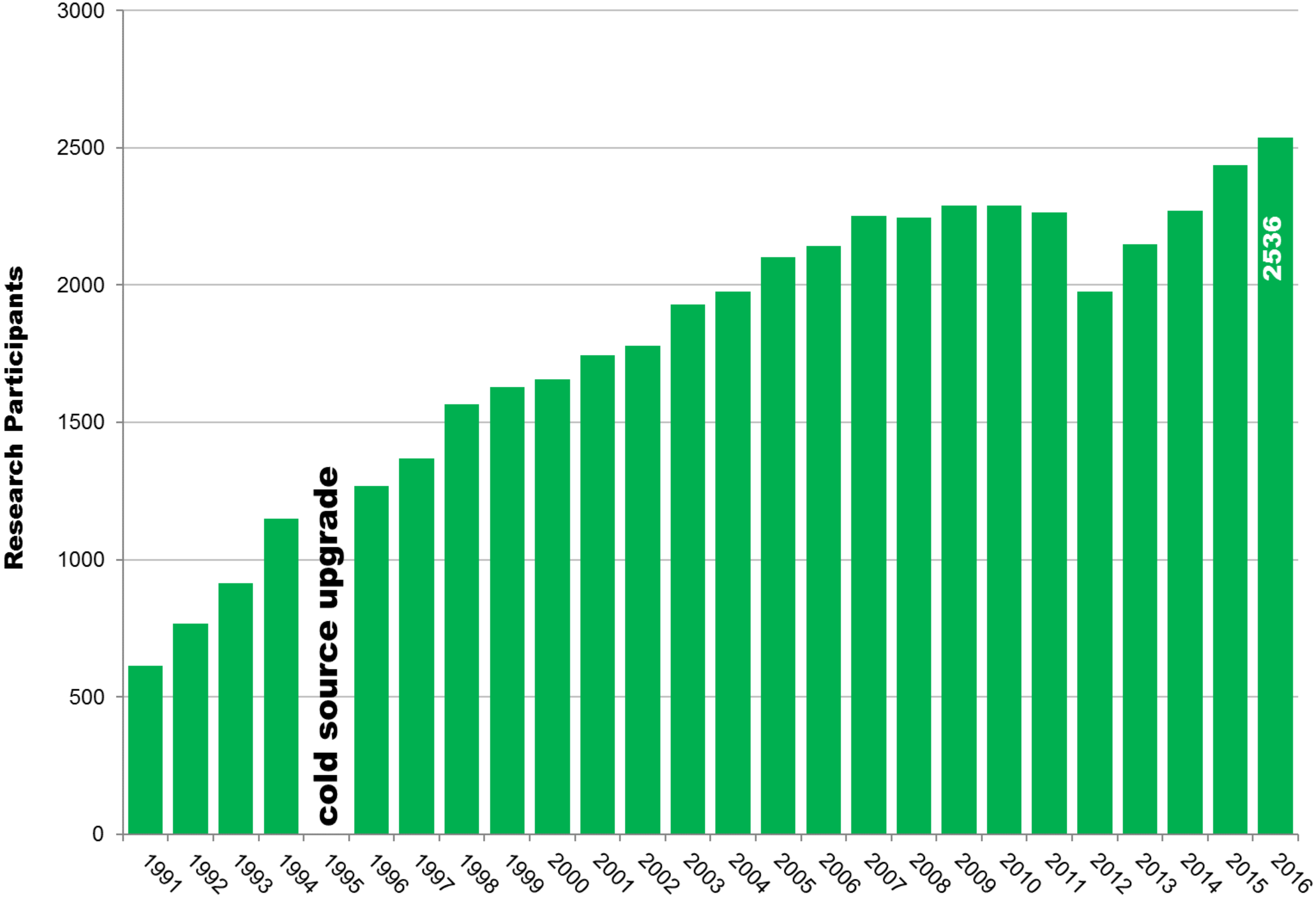

Oak Ridge National Laboratory

High Flux Isotope Reactor

Spallation Neutron Source

Different Spectrometers Cover Different Regions of Phase Space

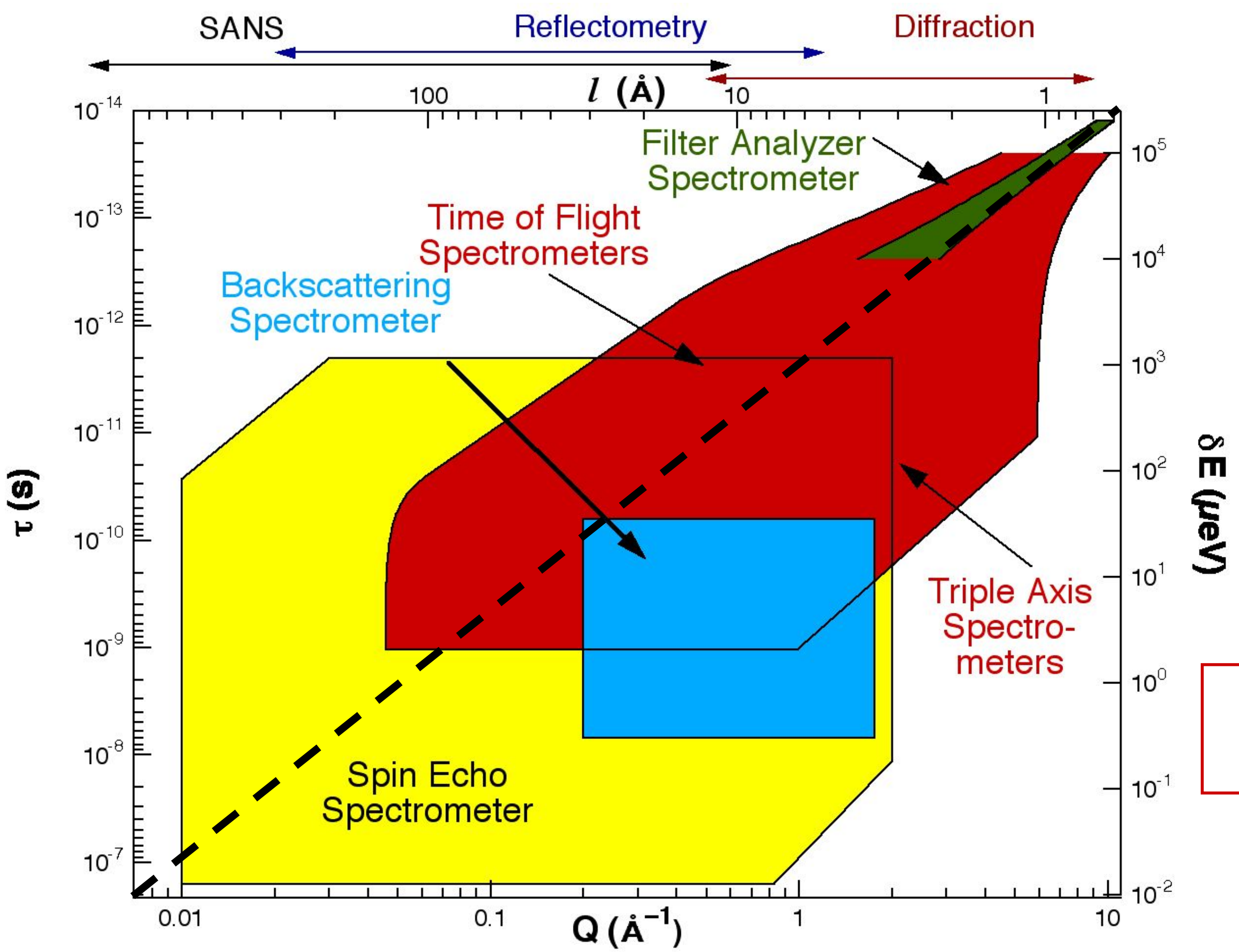

Larger "objects" tend to exhibit slower motions.

Materials that are both Magnetic and Superconducting

Magnetic Impurities Cause Spin depairing

Magnetic Fields and Superconductivity are Antagonists

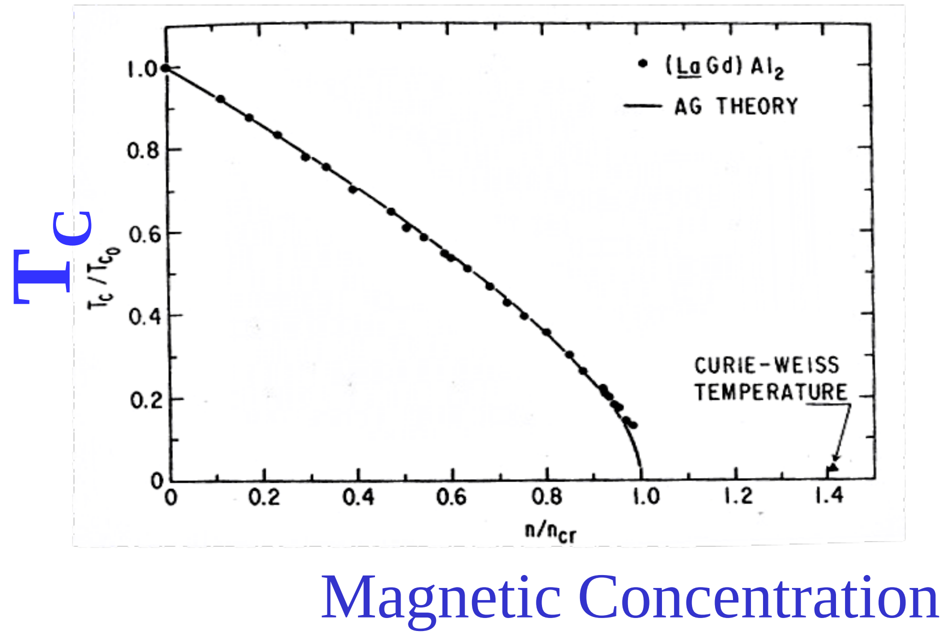

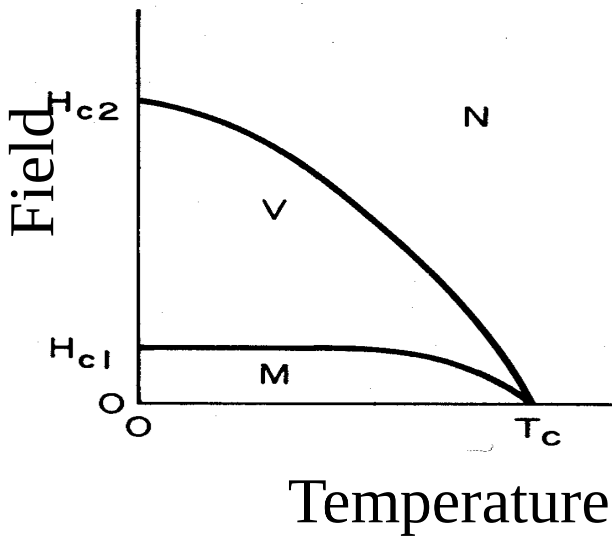

M. B. Maple, Appl. Phys. **9**,179 (1976)

Magnetic Superconductor History

$(k\uparrow; -k\downarrow)$

- Pure Superconductors (1911→ …)
- **X** Magnetic Impurities **X**
- Concentrated Magnetic Systems (Exceptions to the Rule!)
  C-15 Cubic Laves phase (Ce-Ho)Ru_2 ('60's-'70's)
- Magnetic Sublattice—Long Range Order
  Chevrel Phase $DyMo_6S_8$ ('70's)
- Ferromagnets—Competition & Coexistence ⇐
  - Chevrel Phase $HoMo_6(S\text{-}Se)_8$, $ErRh_4B_4$ ('70's – 80's)
- High T_C cuprates—Cu spin order & fluctuations
  Cuprates $RBa_2Cu_3O_7$ [123], R_2CuO_4 [214] ('80's→…)
- Borocarbides
  - $HoNi_2B_2C$, $ErNi_2B_2C$ ('90's→…)
- New Ferromagnetic Superconductors
  - Ruthenates $RuSr_2GdCu_2O_8$, $RuSr_2(Eu\text{-}Ce)_2Cu_2O_{10}$; $ZrZn_2$, UGe_2 (2000's →…) ⇐
- Sodium cobaltates (Magnetic, thermoelectric, and Superconducting) 2000's→…
  - Na_xCoO_2 (+ H_20) [just add water for superconductivity !]
- Iron-based superconductors (2008→…)
  - $R(O_{1-x}F_x)FeAs$; $Sr_{1-x}K_xFe_2As_2$; LiFeAs; $Fe(Se_{1-x}Te_x)$
  - 1:1:1:1 1:2:2 1:1:1 1:1

NCNR

Magnetic Structures

Ferromagnet

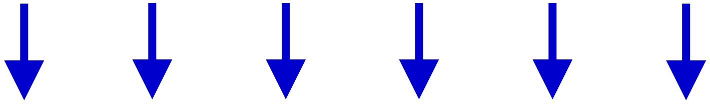

Antiferromagnet

Spin Density Wave

Magnetic Structures

Ferromagnet

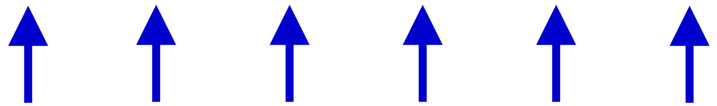

Antiferromagnet

Spin Density Wave

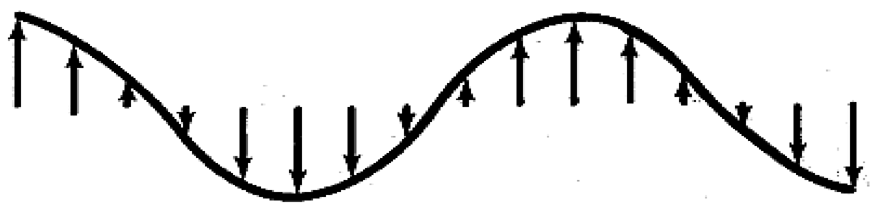

Ferromagnetic Superconductor

$RuSr_2GdCu_2O_8$

- T(Ru) = 136 K
- T(Superconductivity) = 35 K
- T(Gd) = 2.5 K
- J. W. Lynn, B. Keimer, C. Ulrich, C. Bernhard, and J. L. Tallon, Phys. Rev. B**61**, 14964 (2000)

^{160}Gd order

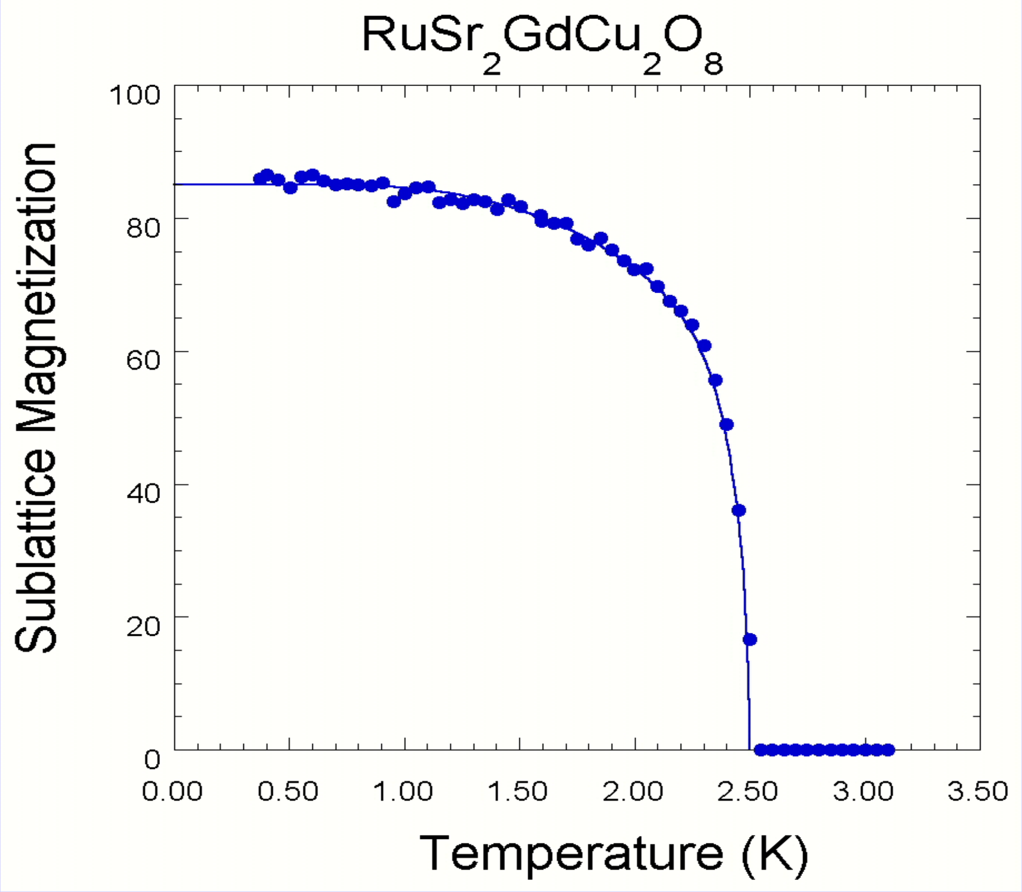

Antiferromagnetic Order

Phys. Rev. B**61**, 14964 (2000)

Ru order

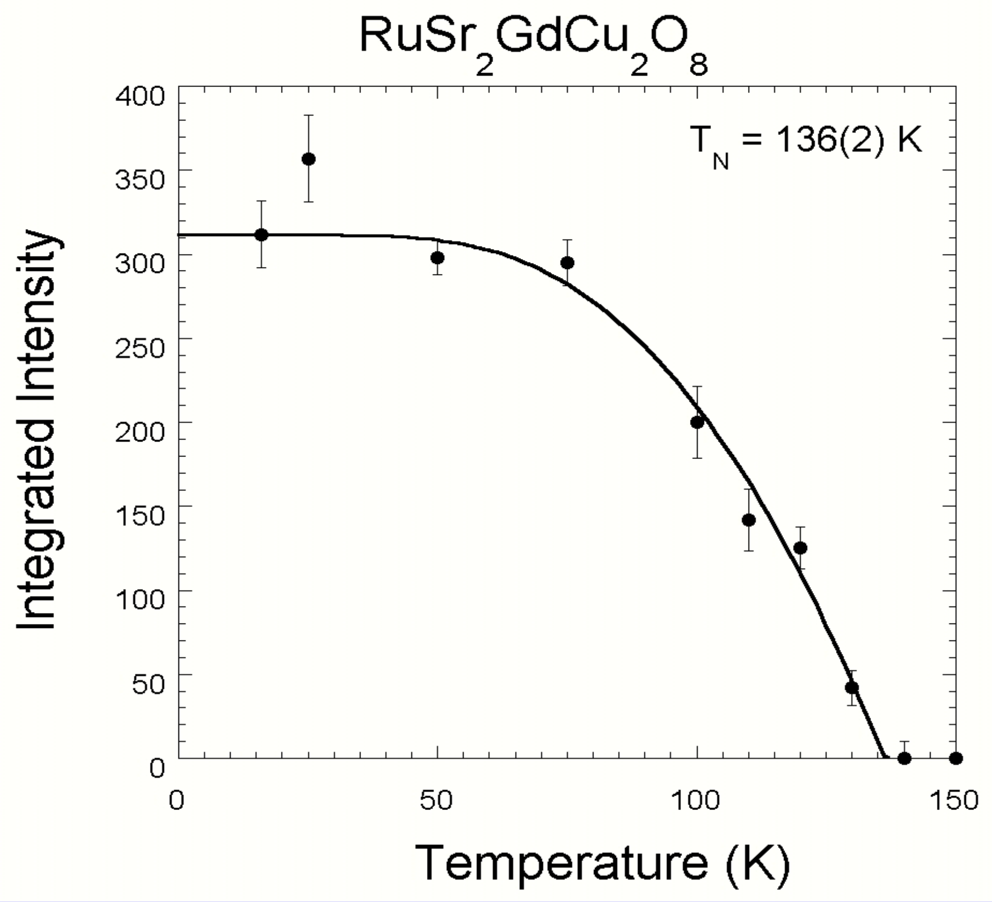

Phys. Rev. B**61**, 14964 (2000)

Magnetic Structure

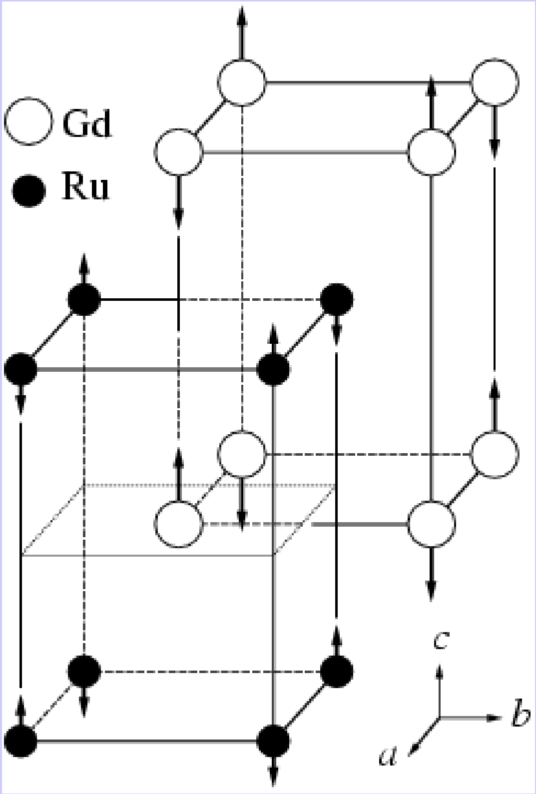

$RuSr_2GdCu_2O_8$

*Anti*ferromagnetic Order

Phys. Rev. B**61**, 14964 (2000)

Chevrel Phase Superconductors

	$HoMo_6S_8$,	$HoMo_6Se_8$,	$ErRh_4B_4$
T_{super}	= 1.8 K	5.6 K	8.6 K
T_{ferro}	= 0.7 K	0.5 K	0.9 K
$T_{reentrant}$	= 0.7 K	< 0 K	0.9 K

[$(HoS_8)Mo_6$ Magnetic Lattice Isolated]

$HoMo_6S_8$ Magnetic Diffraction Pattern

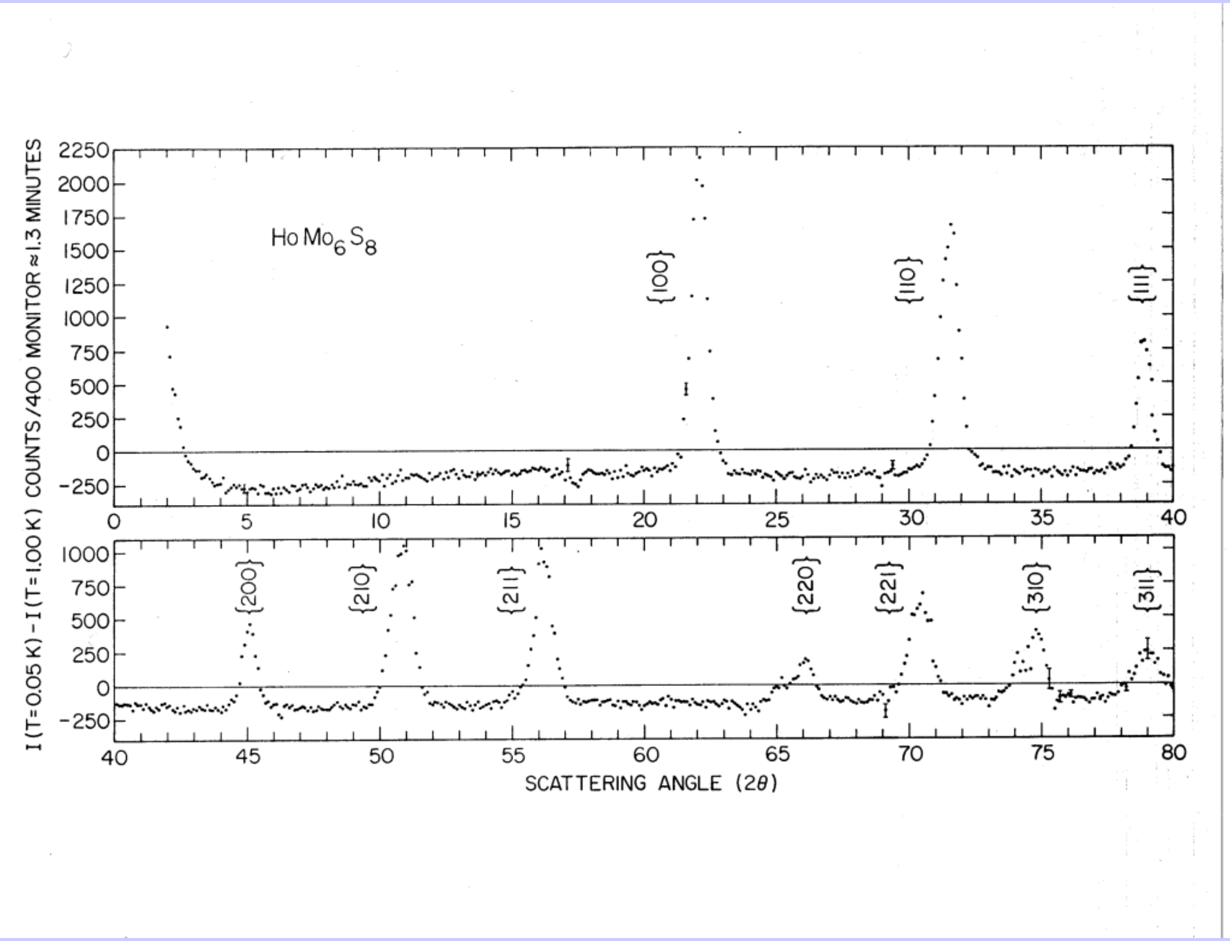

Direct Observation of Long Range Ferromagnetic Order in the Reentrant Superconductor $HoMo_6S_8$, J. W. Lynn, D. E. Moncton, W. Thomlinson, G. Shirane and R. N. Shelton, Sol. St. Comm. **26**, 493 (1978).

NCNR

Small Angle Neutron Scattering

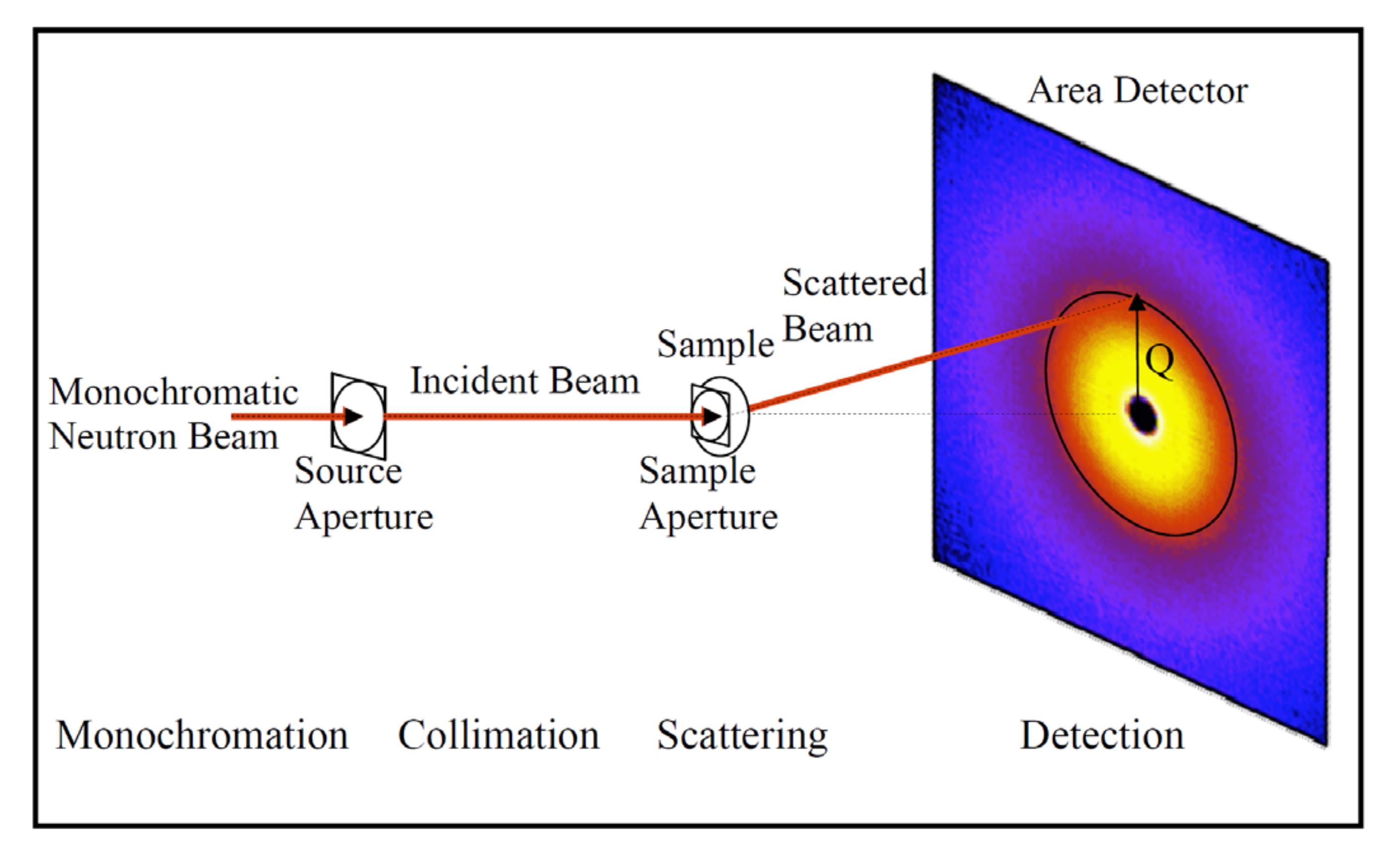

$HoMo_6S_8$

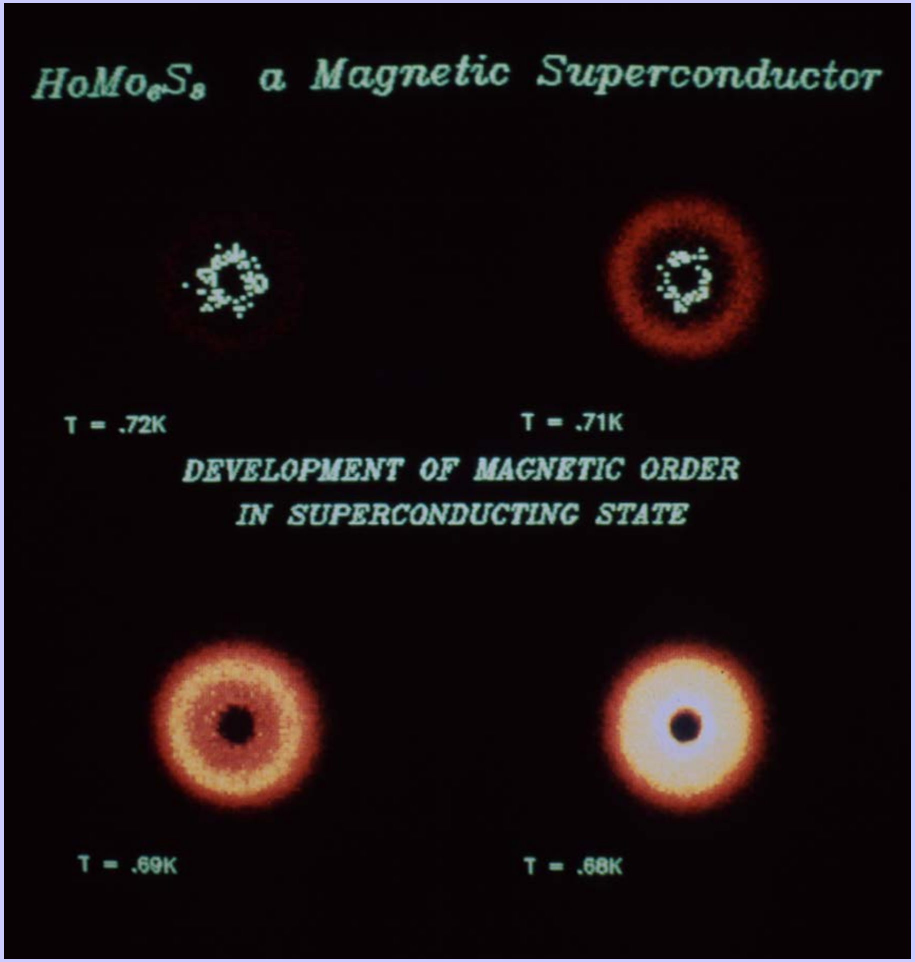

Oscillatory Magnetic State with ≈200 Å repeat distance

Sol. St. Comm. **26**, 493 (1978); PRL **46**, 368 (1981);
J. de Physique Lettres **42**, L45 (1981); Phys. Rev. B**24**, 3817 (1981).

$HoMo_6S_8$ Order Parameter

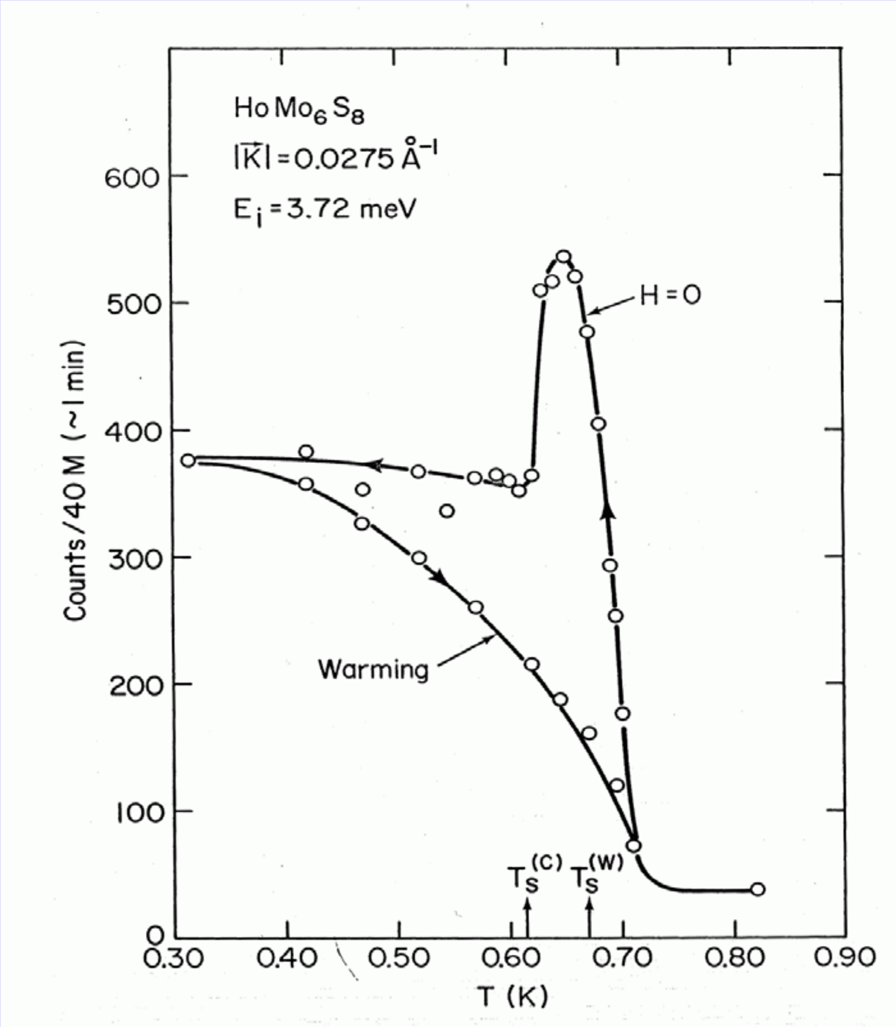

Sol. St. Comm. **26**, 493 (1978); Phys. Rev. Lett. **46**, 368 (1981); J. de Physique Lettres **42**, L45 (1981); Phys. Rev. B**24**, 3817 (1981).

$HoMo_6Se_8$

T_S=5.6 K

T_M=0.5K

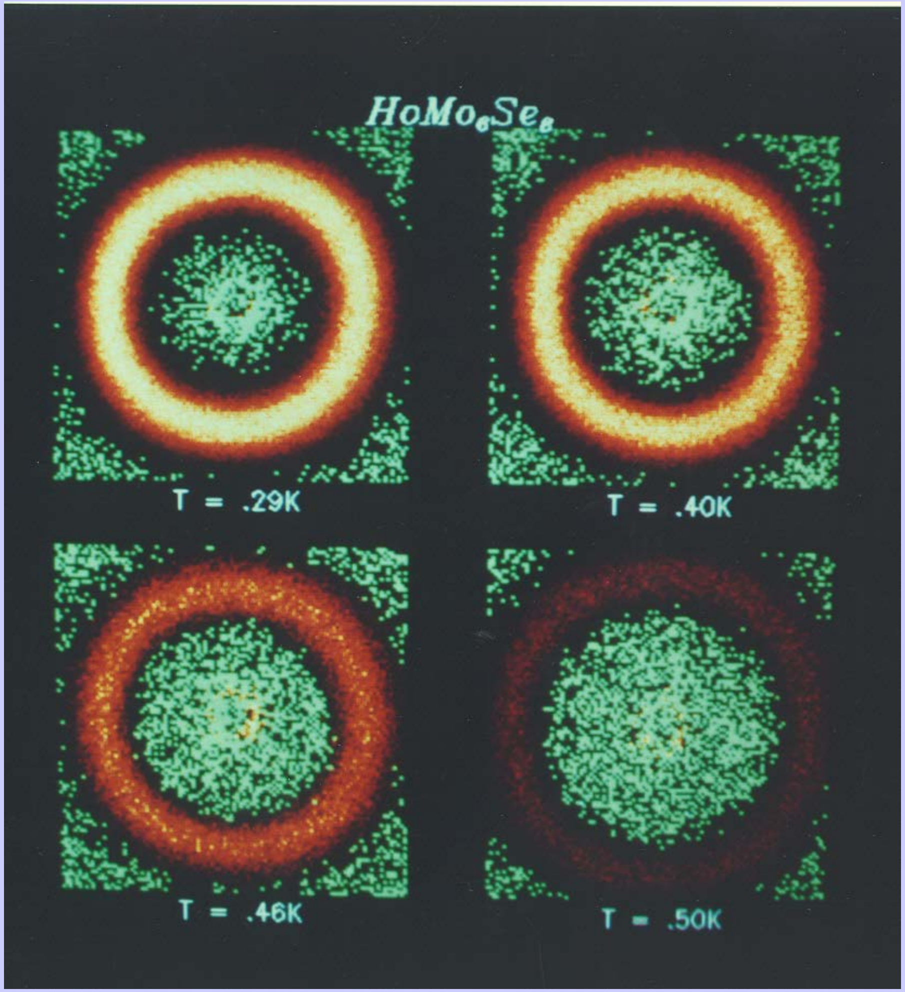

~100 Å
(10 nm)
periodicity

J. W. Lynn, J. A. Gotaas, R. W. Erwin, R. A. Ferrell, J. K. Bhattacharjee, R. N. Shelton and P. Klavins,
Phys. Rev. Lett. **52**, 133 (1984)

$HoMo_6Se_8$

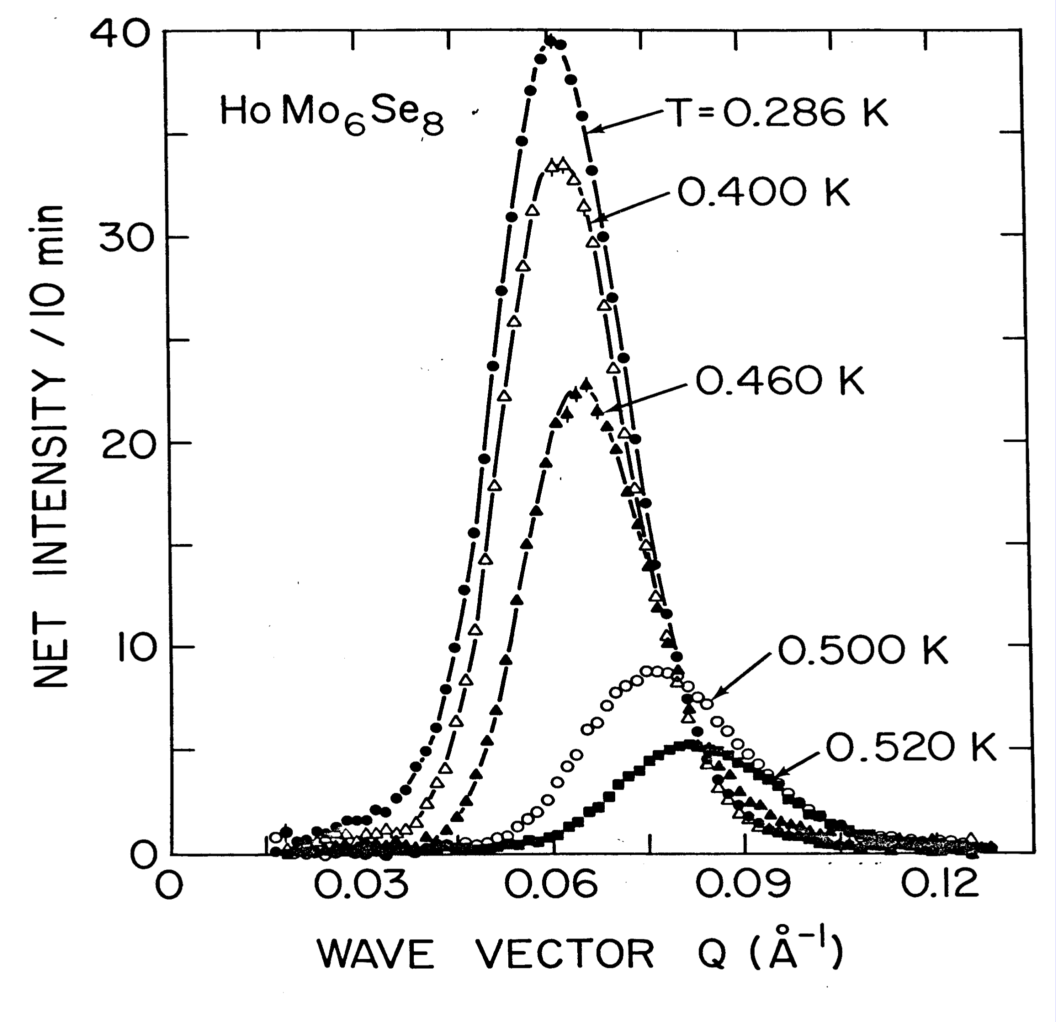

Center for Neutron Research

$HoMo_6Se_8$

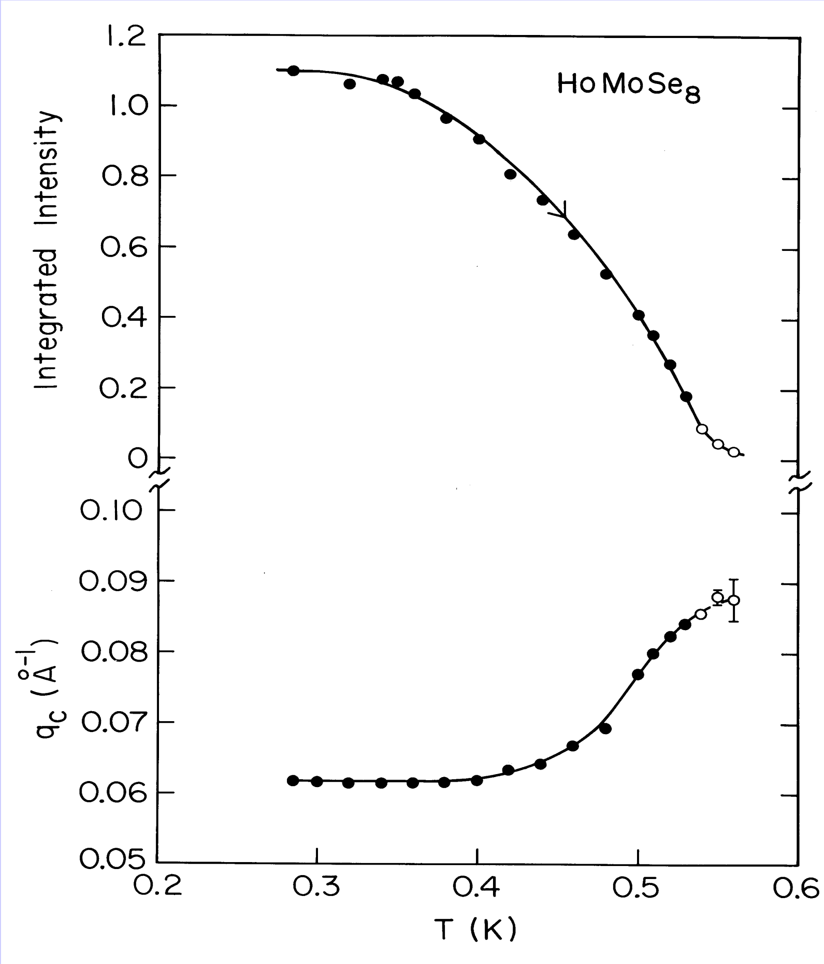

J. W. Lynn, J. A. Gotaas, R. W. Erwin, R. A. Ferrell, J. K. Bhattacharjee, R. N. Shelton and P. Klavins, Phys. Rev. Lett. **52**, 133 (1984)

$ErNi_2B_2C$ Spin Density Wave

T_C = 11 K

T_N = 6 K

T_M = 2.3 K

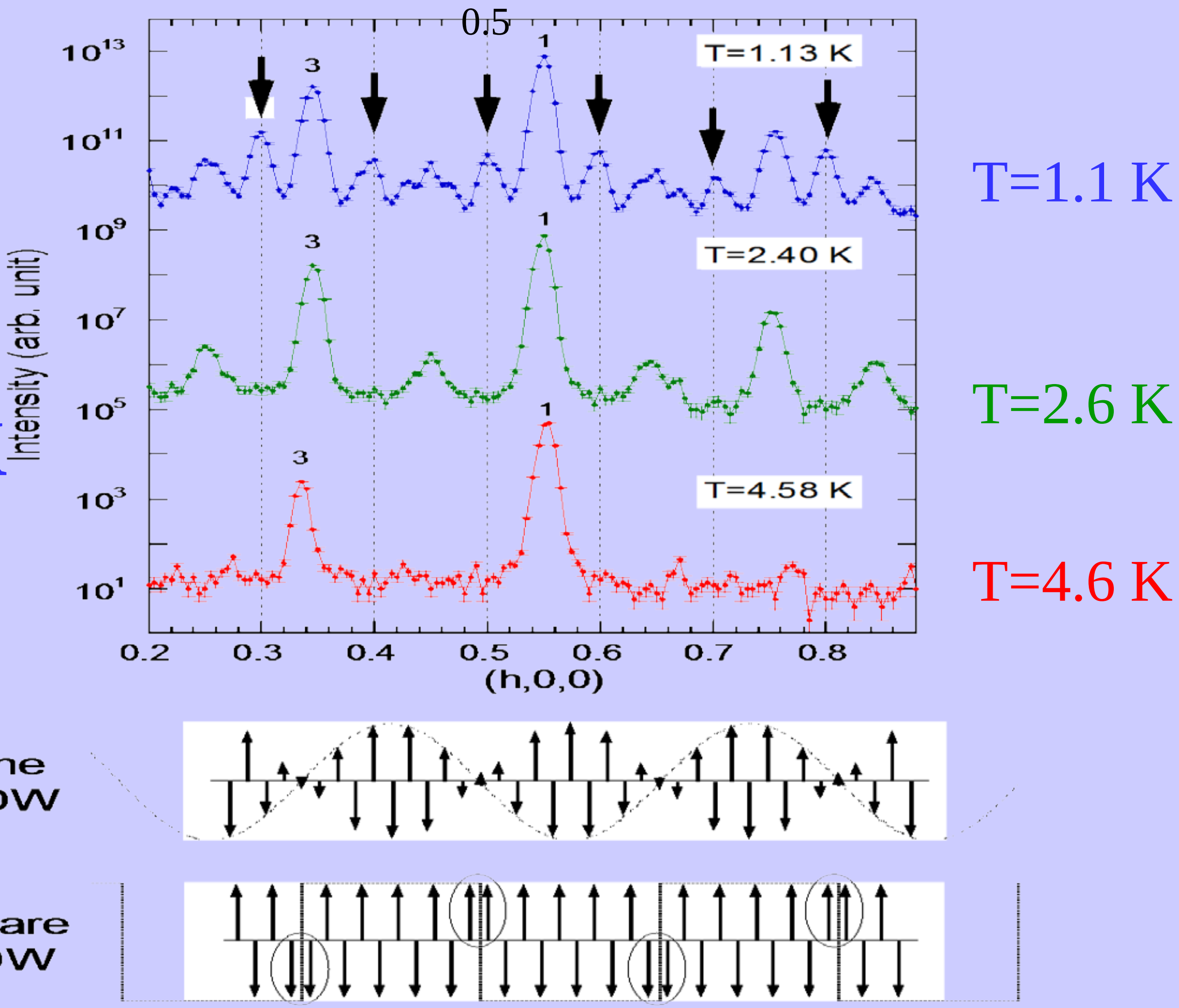

S. -M. Choi, J. W. Lynn, D. Lopez, P. L. Gammel, P. C. Canfield and S. L. Bud'ko, Phys. Rev. Lett. **86**, 712 (2001)

NCNR

Spontaneous Vortex Formation

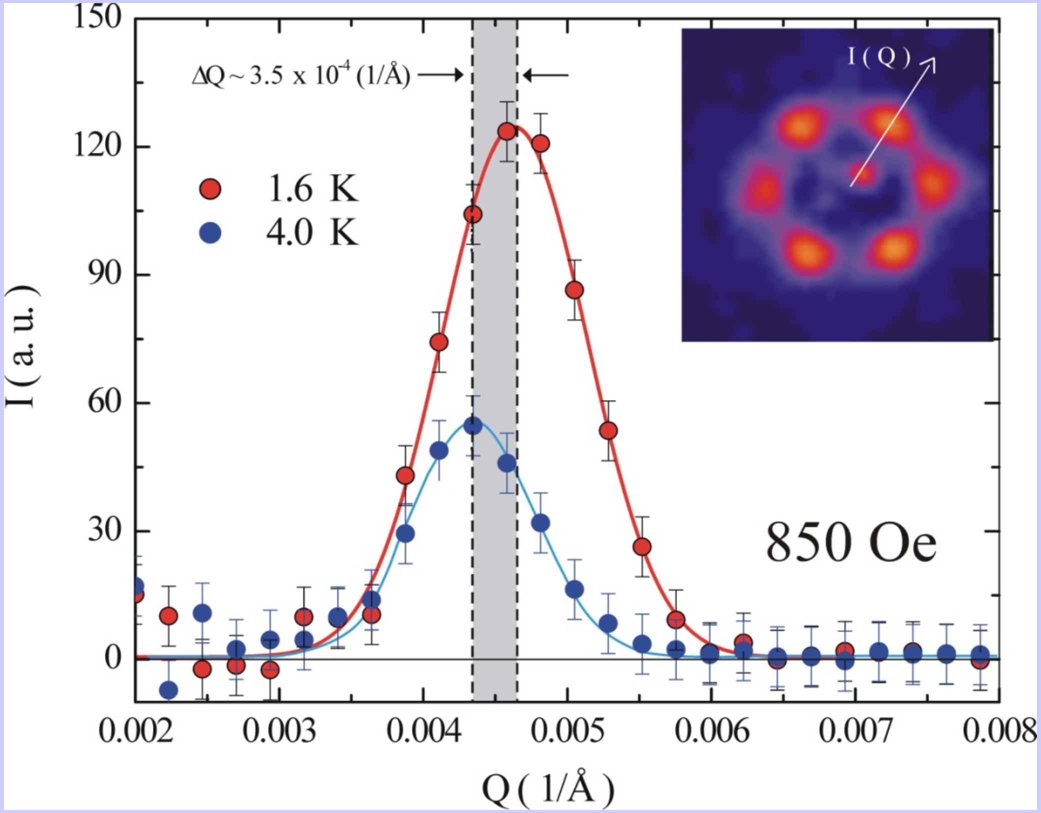

Vortex Matter in Superconductor Nb

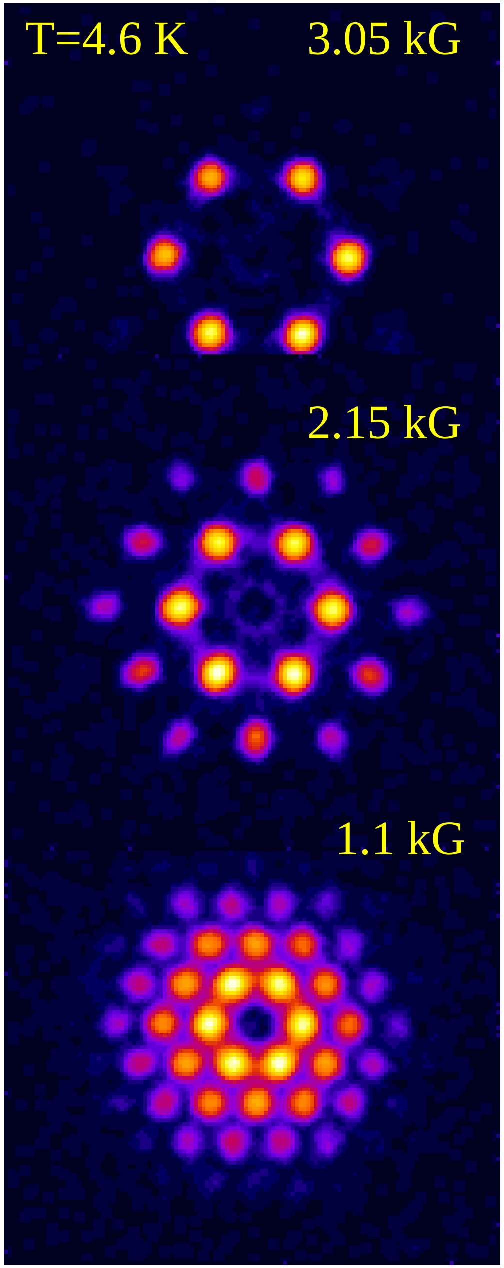

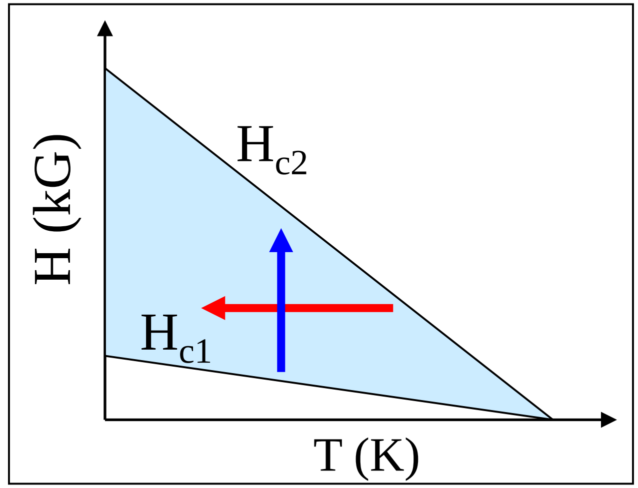

Real space depiction of vortex lattice

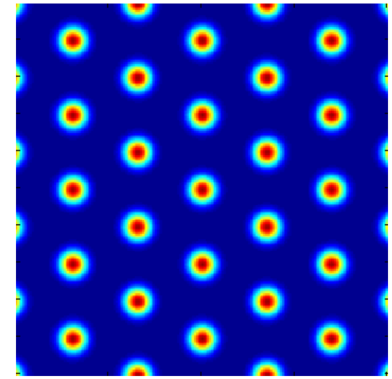

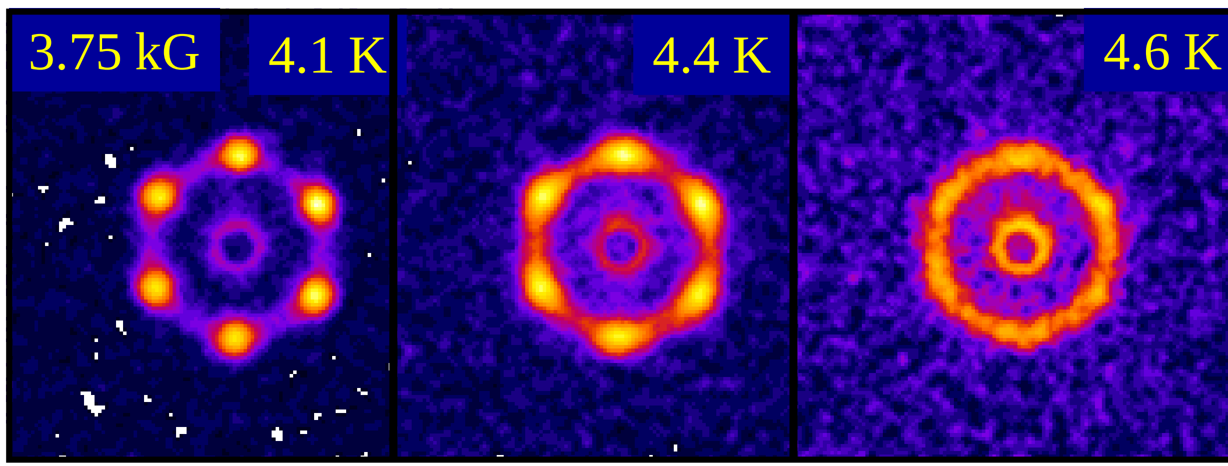

X. S. Ling and S.-R. Park (Brown University)
S.-M Choi, D. Dender and J. Lynn, (NCNR/NIST)
Phys. Rev. Lett. **72**, 3413 (1994); **86**, 712 (2001); **91**, 167003 (2003).

Iron-based High T_C Superconductors

Crystal Structure of La(O,F)FeAs

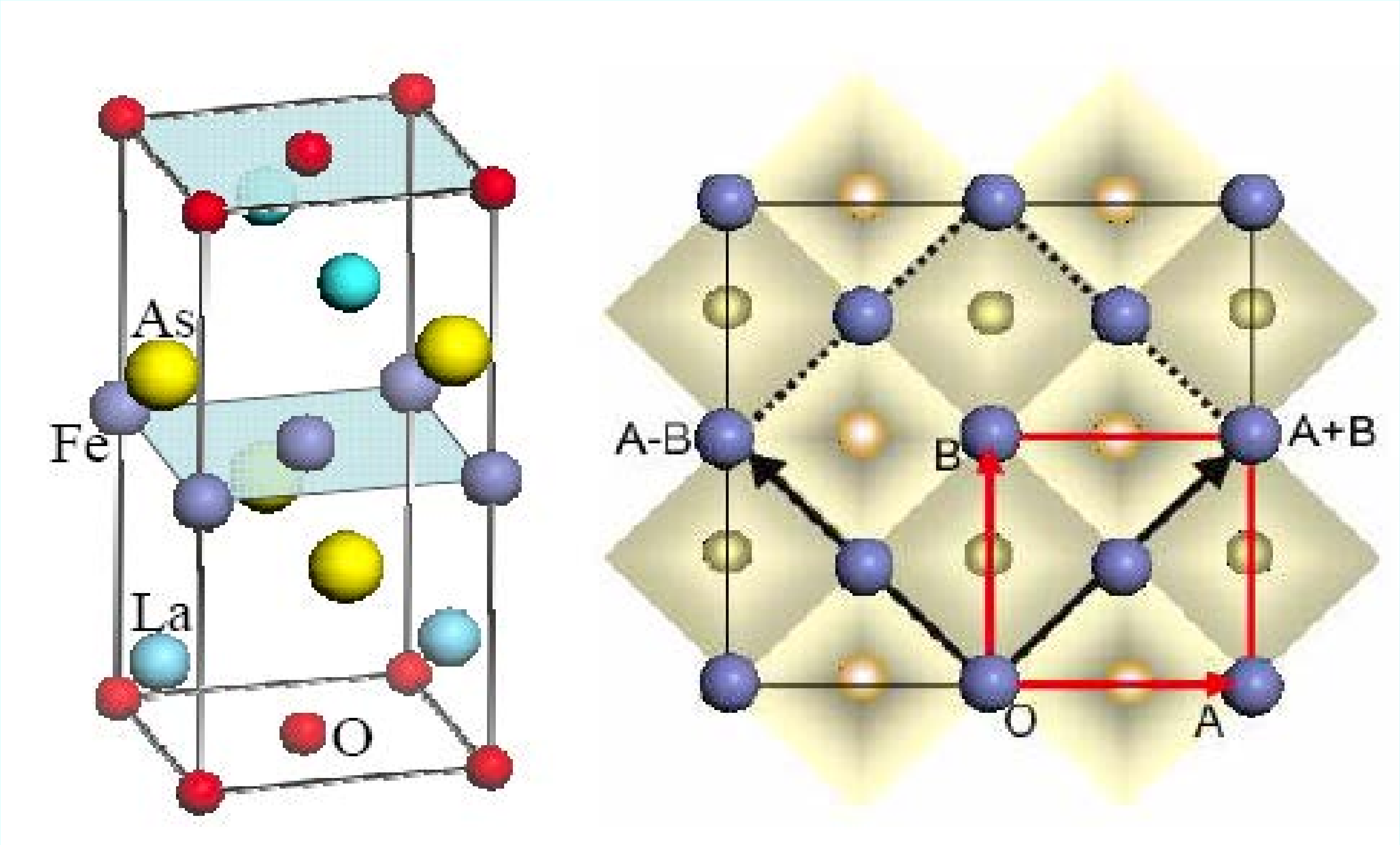

Magnetic Order Close to Superconductivity in the Iron-based Layered $La(O_{1-x}F_x)FeAs$ systems, C. de la Cruz, Q. Huang, J. W. Lynn, J. Li, W. Ratcliff II, J. L. Zarestky, H. A. Mook, G. F. Chen, J. L. Luo, N. L. Wang, and P. Dai,
Nature **453**, 899 (2008).

Basic Properties of Iron Superconductors

- Parent Materials
  - Metallic (poor metal)
  - Anisotropic (ranging from 5 – 30)
  - Have a structural distortion (T ~ 150 K)
  - Fe spins are antiferromagnetically ordered (T_N ~ 140 K)
- Superconductors
  - T_C as high as 56 K in bulk; ~100 K? in thin films
  - Anisotropic (but not nearly as much as the cuprates)
  - Very high (isotropic) upper critical fields 300 T

Iron-based superconductors under Investigation at the NCNR

- FeSe, Fe_{1+x}(Se-Te), $K_xFe_{2-y}Se_2$ (1:1)
- LiFeAs (1:1:1)
- $LaO_{1-x}F_xFeAs$ LaOFeAs (1:1:1:1)
- $CeO_{1-x}F_xFe$(As,P) CeOFeAs
- $NdO_{1-x}F_xFeAs$ Nd…
- $PrO_{1-x}F_xFeAs$ Pr…
- $BaFe_2As_2$, $SrFe_2As_2$, $CaFe_2As_2$ (1:2:2)
- $CaFe_2As_2$, Under Pressure; doping
  - http://www/ncnr.nist.gov/staff/jeff

Neutron Powder Diffraction

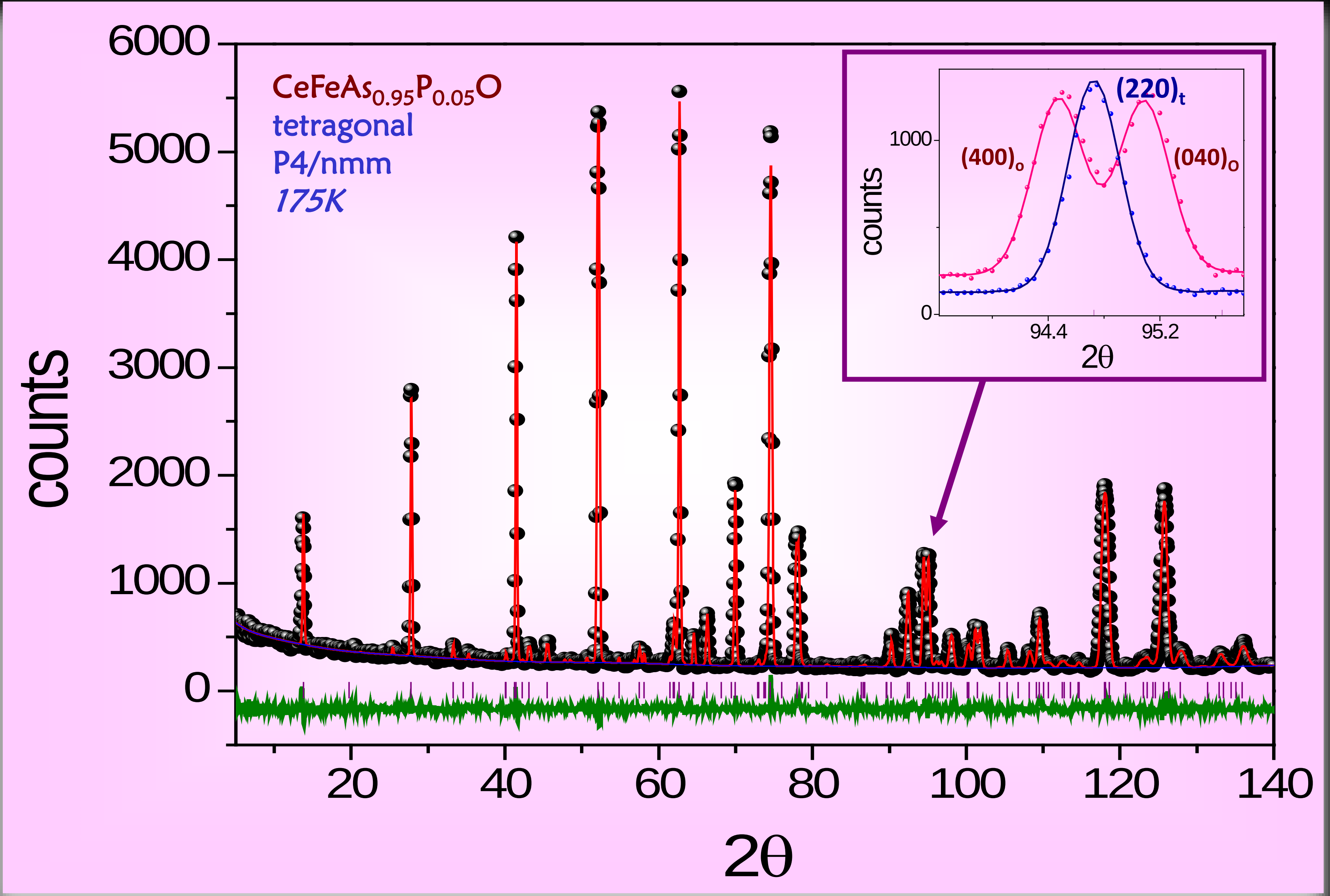

Crystal Structure of LaOFeAs

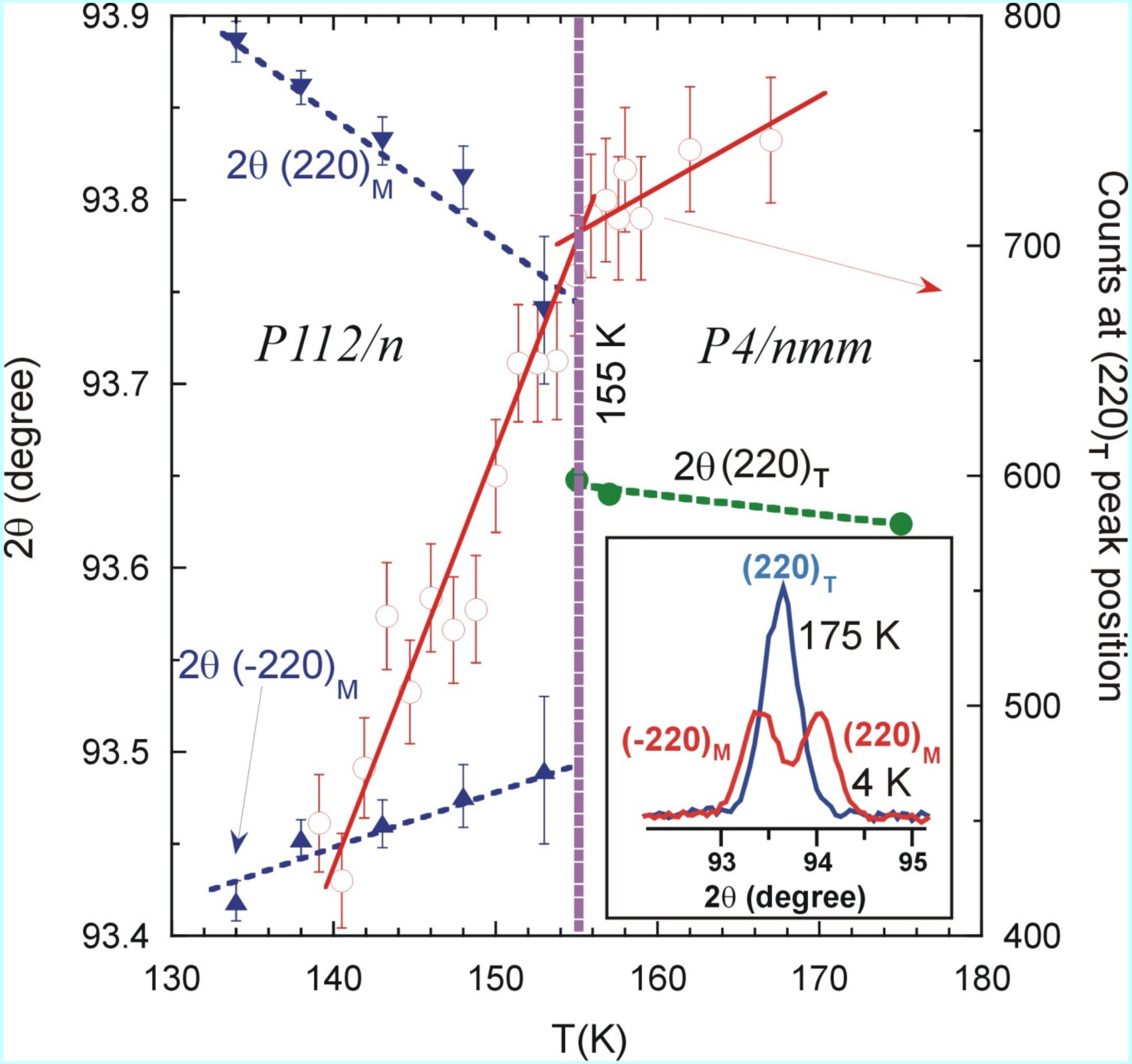

Magnetic Scattering from La(O,F)FeAs

PSD on BT-7

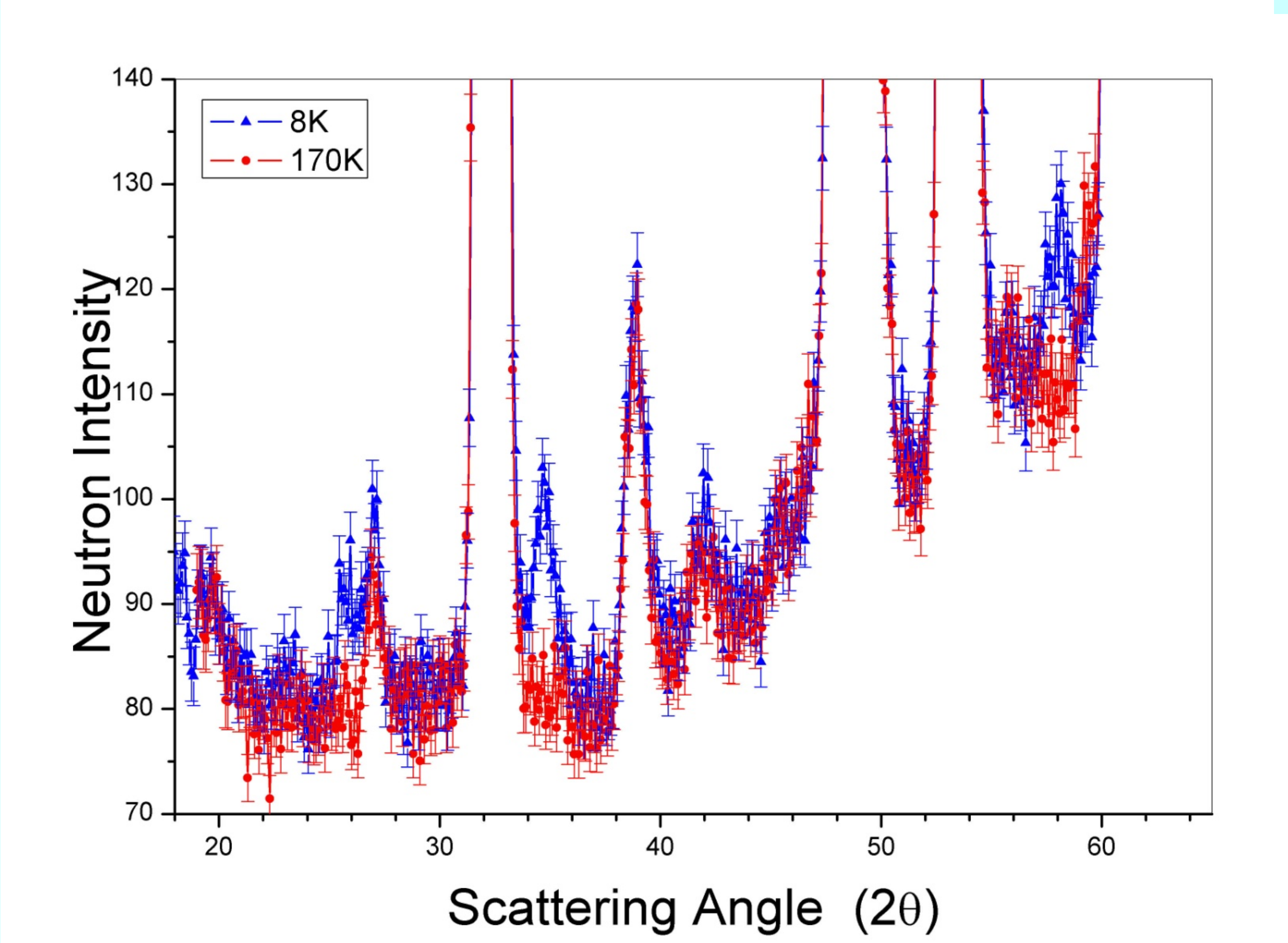

C. de la Cruz, Q. Huang, J. W. Lynn, J. Li, W. Ratcliff II, J. L. Zarestky, H. A. Mook, G. F. Chen, J. L. Luo, N. L. Wang, and P. Dai,
Nature **453**, 899 (2008).

Magnetic Structure of La(O,F)FeAs

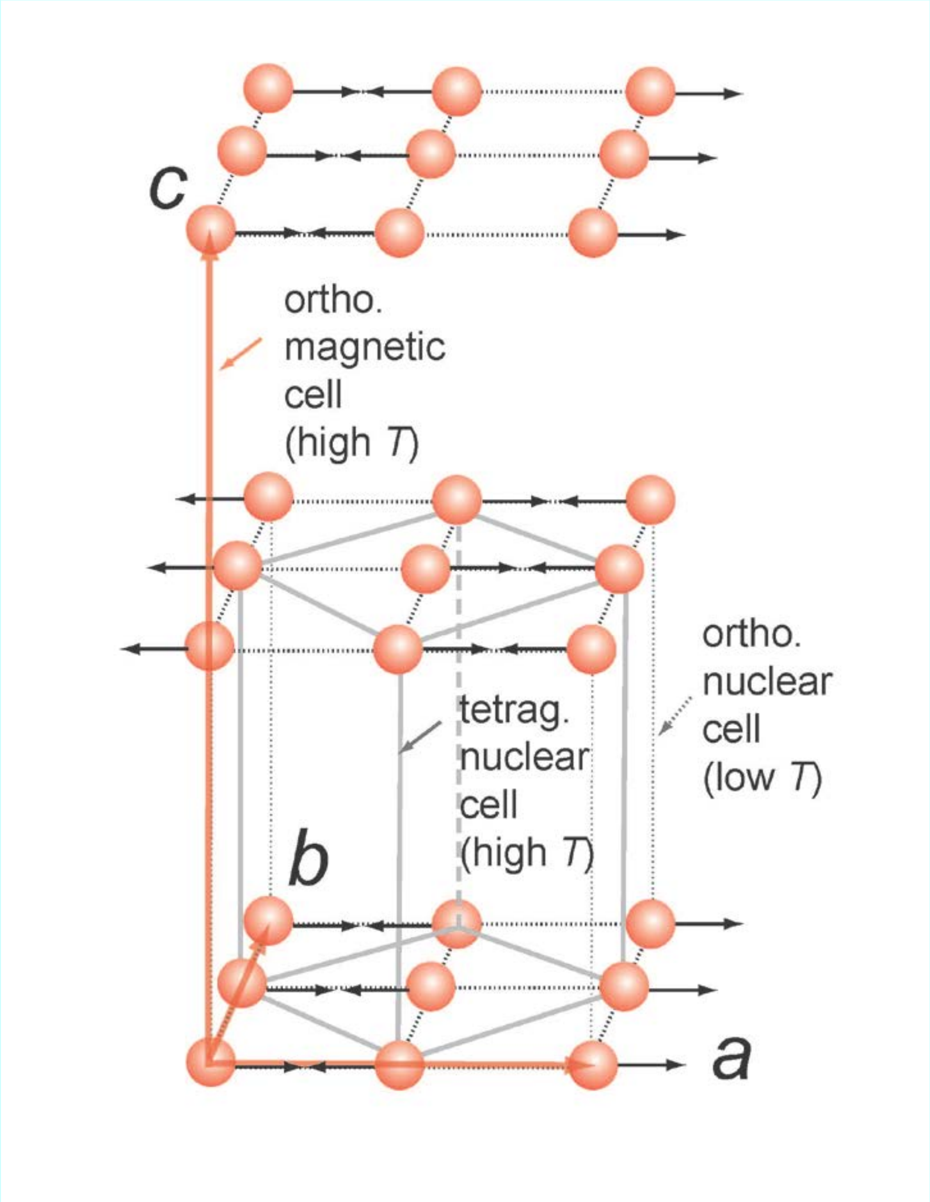

Antiferromagnetic Order LaOFeAs

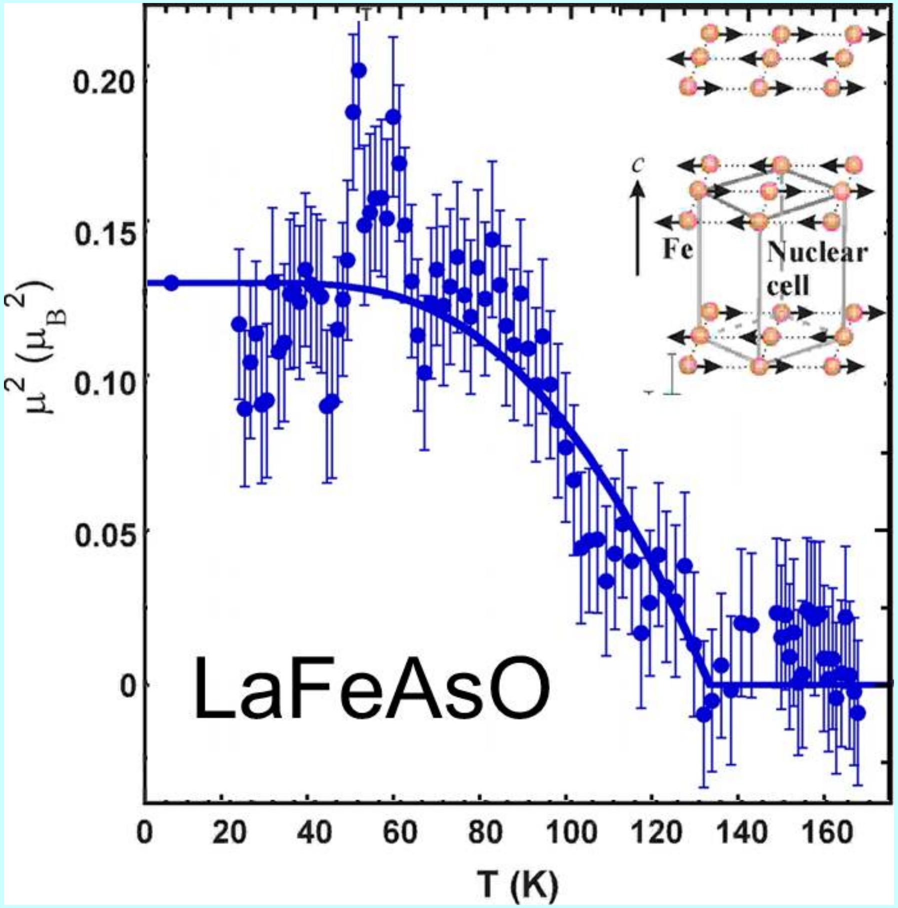

Single Crystal $SrFe_2As_2$

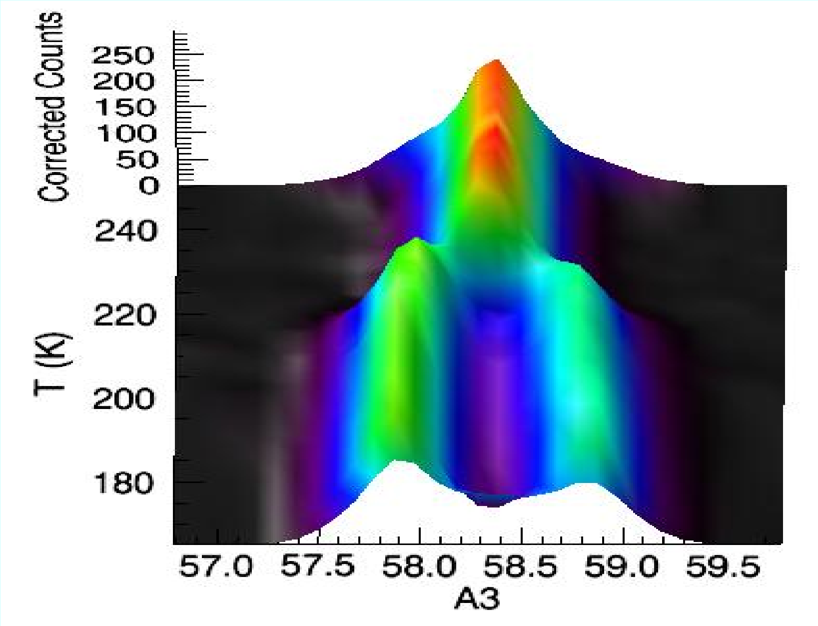

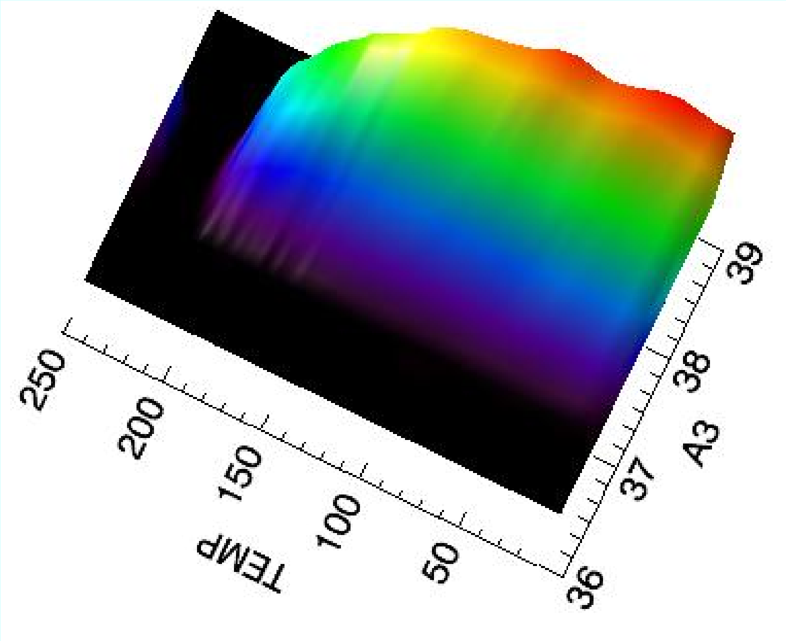

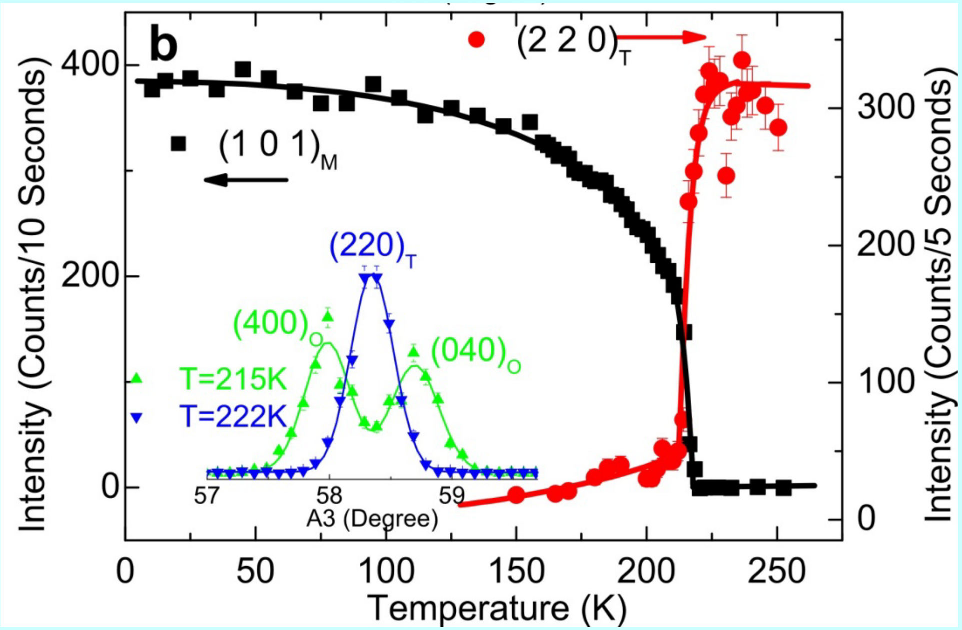

Spin and Lattice Structure of Single Crystal $SrFe_2As_2$, Jun Zhao, W. Ratcliff-II, J. W. Lynn, G. F. Chen, J. L. Luo, N. L. Wang, Jiangping Hu, and Pengcheng Dai, Phys. Rev. B **78,** 140504(R) (2008).

NIST Center for Neutron Research DAVE Data Analysis and Visualization Environment

NCNR

F- doping Phase diagrams

J. Zhao (2008)

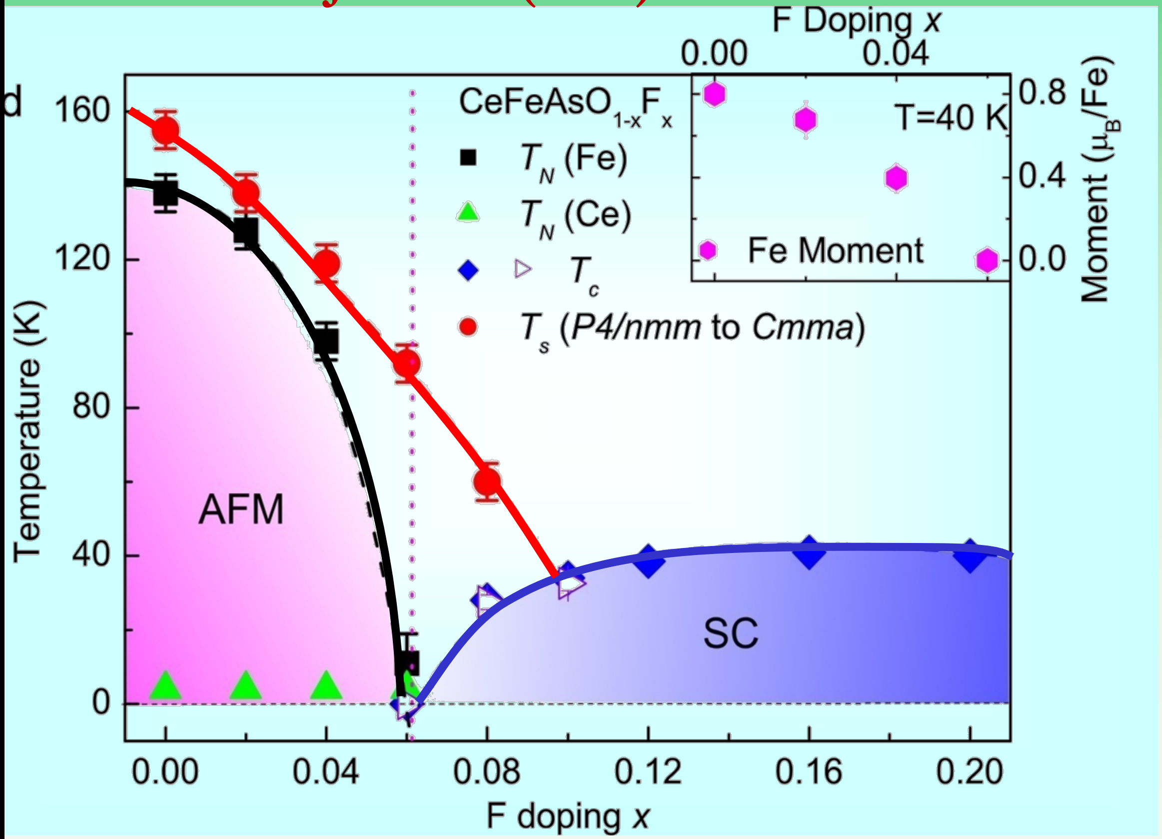

$CeFeAsO_{1-x}F_x$

J. Zhao, Q. Huang, C. de la Cruz, S. Li, J. W. Lynn, Y. Chen, M. A. Green, G. F. Chen, G. Li, Z. Li, J. L. Luo, N. L. Wang, and P. Dai, Nature Materials **7**, 953 (2008).

F- doping Phase diagrams

J. Zhao (2008)

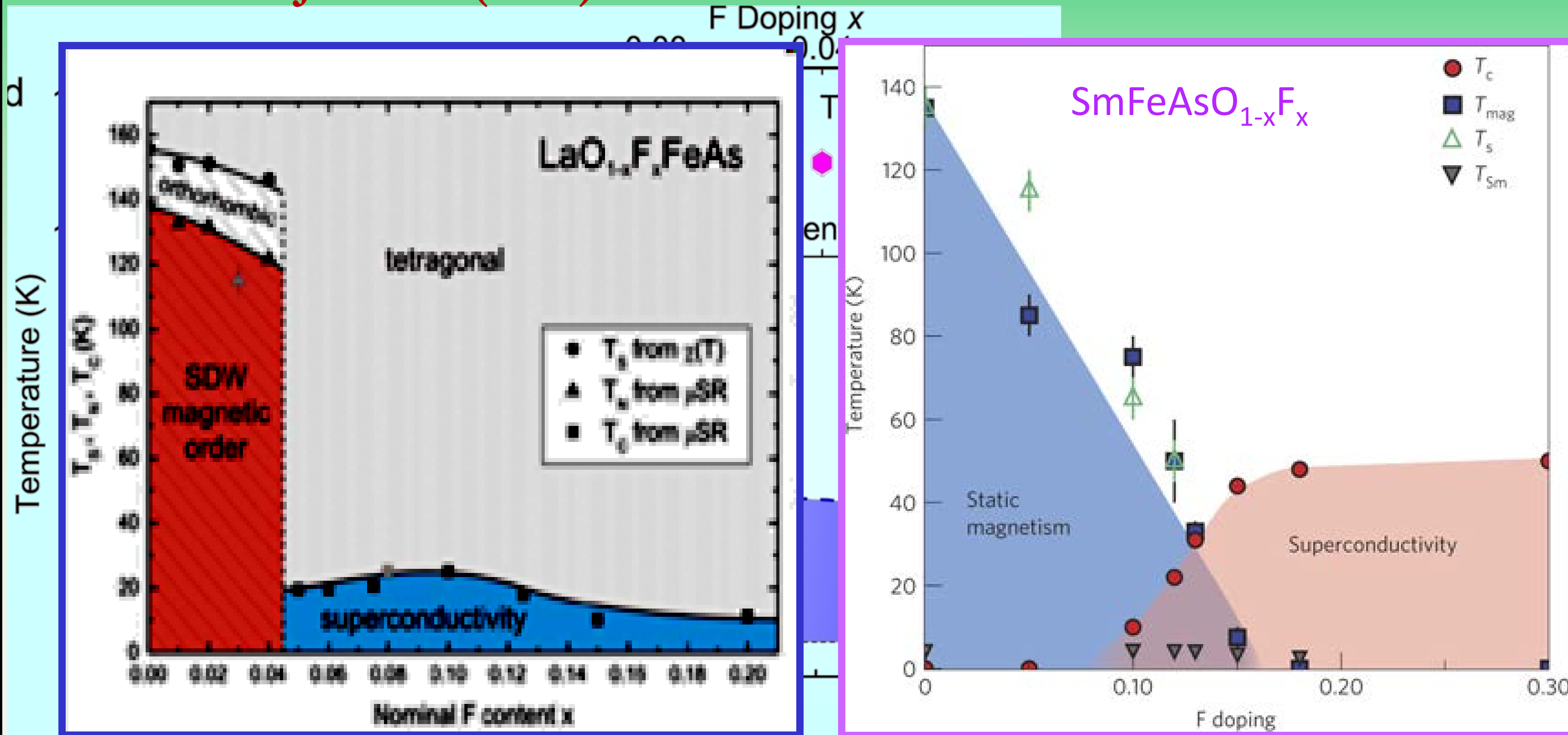

H. Luetkens (2008)

(Drew 2009)

Inelastic Scattering
Spin Waves

Low energy spin waves and magnetic interactions in $SrFe_2As_2$,

Jun Zhao, Dao-Xin Yao, S. Li, Tao Hong, Y. Chen, S. Chang, W. Ratcliff II, J. W. Lynn, H. A. Mook, G. F. Chen, J. L. Luo, N. L. Wang, E. W. Carlson, J. Hu, and P. Dai,

Phys. Rev. Lett. **101**, 167203 (2008).

NCNR

Spin Waves In $SrFe_2As_2$

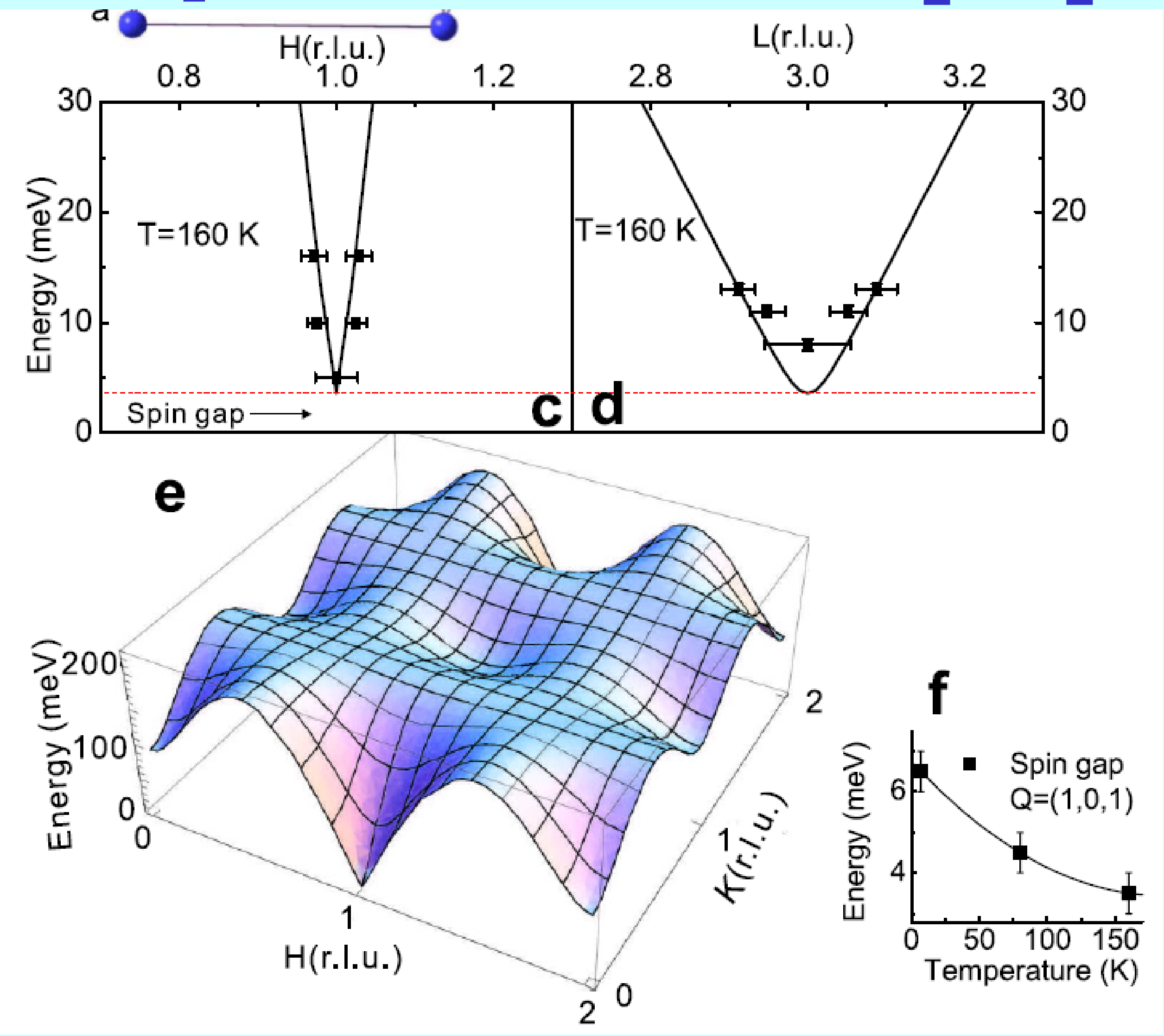

Jun Zhao, Dao-Xin Yao, S. Li, Tao Hong, Y. Chen, S. Chang, W. Ratcliff II, J. W. Lynn, H. A. Mook, G. F. Chen, J. L. Luo, N. L. Wang, E. W. Carlson, J. Hu, and P. Dai, Phys. Rev. Lett. **101**, 167203 (2008).

Spin Resonance in $Fe(Se_{0.4}Te_{0.6})$

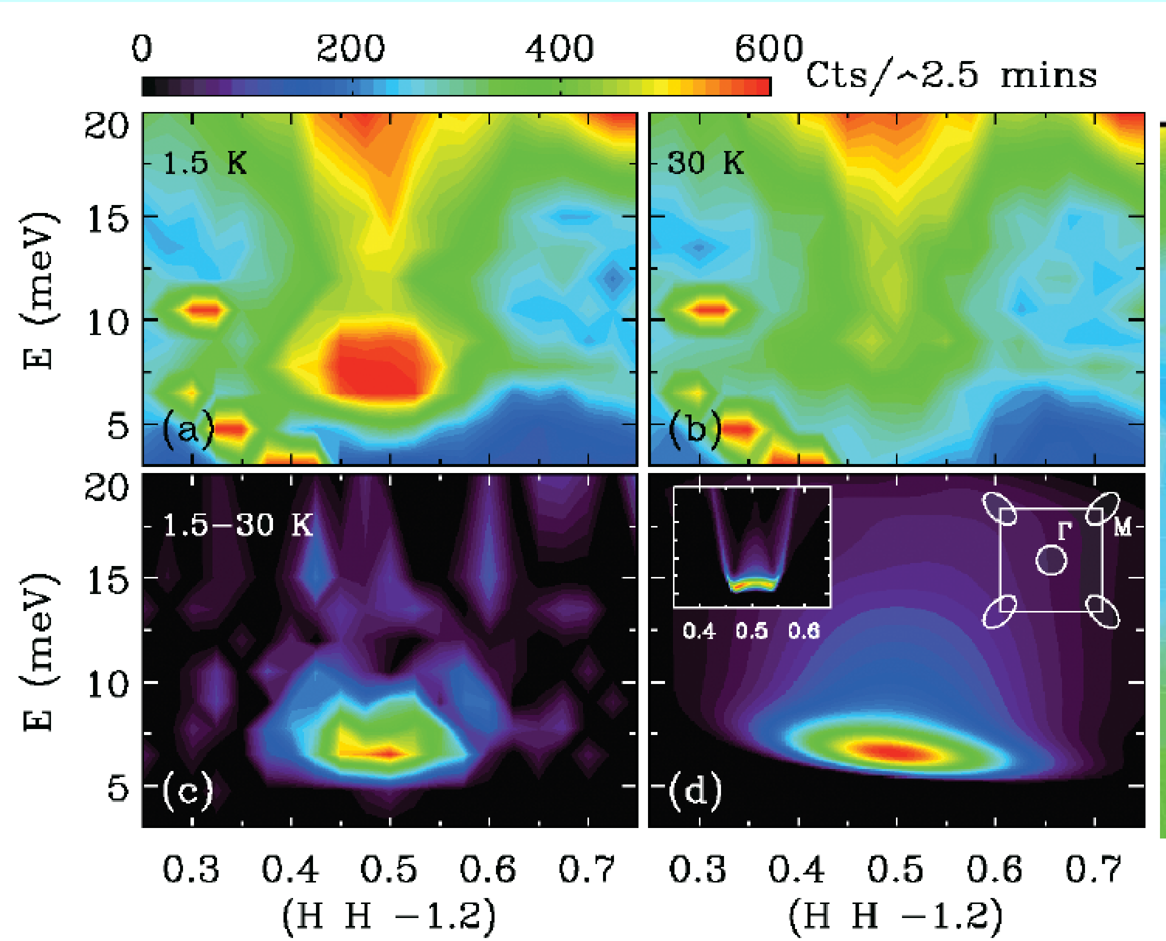

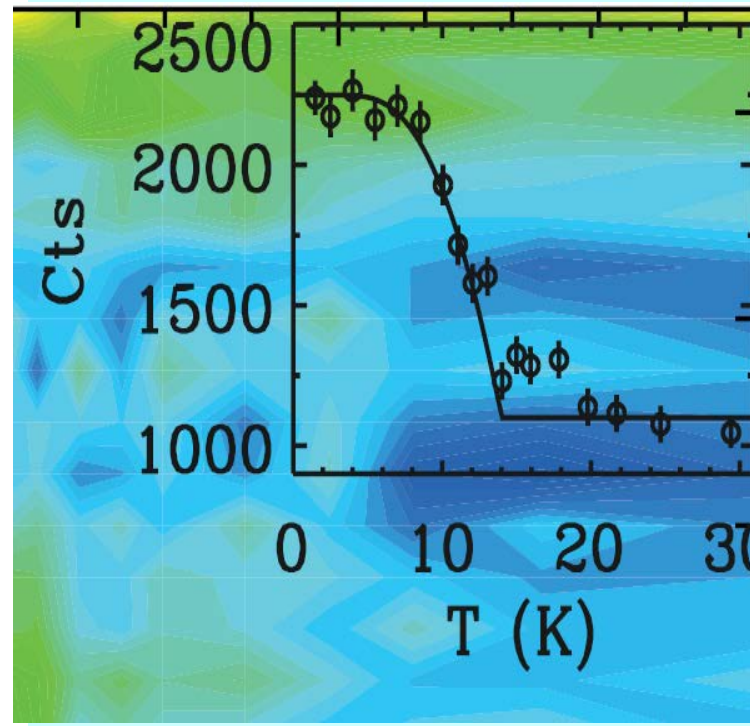

Y. Qiu, W. Bao, Y. Zhao, C. Broholm, V. Stanev, Z. Tesanovic, Y.C. Gasparovic, S. Chang, J. Hu, B. Q., M. Fang, and Z. Mao, Phys. Rev. Lett. **103**, 067008 (2009).

Spin Resonance Symmetry Crossover $K_xFe_{2-y}Se_{1-z}S_z$

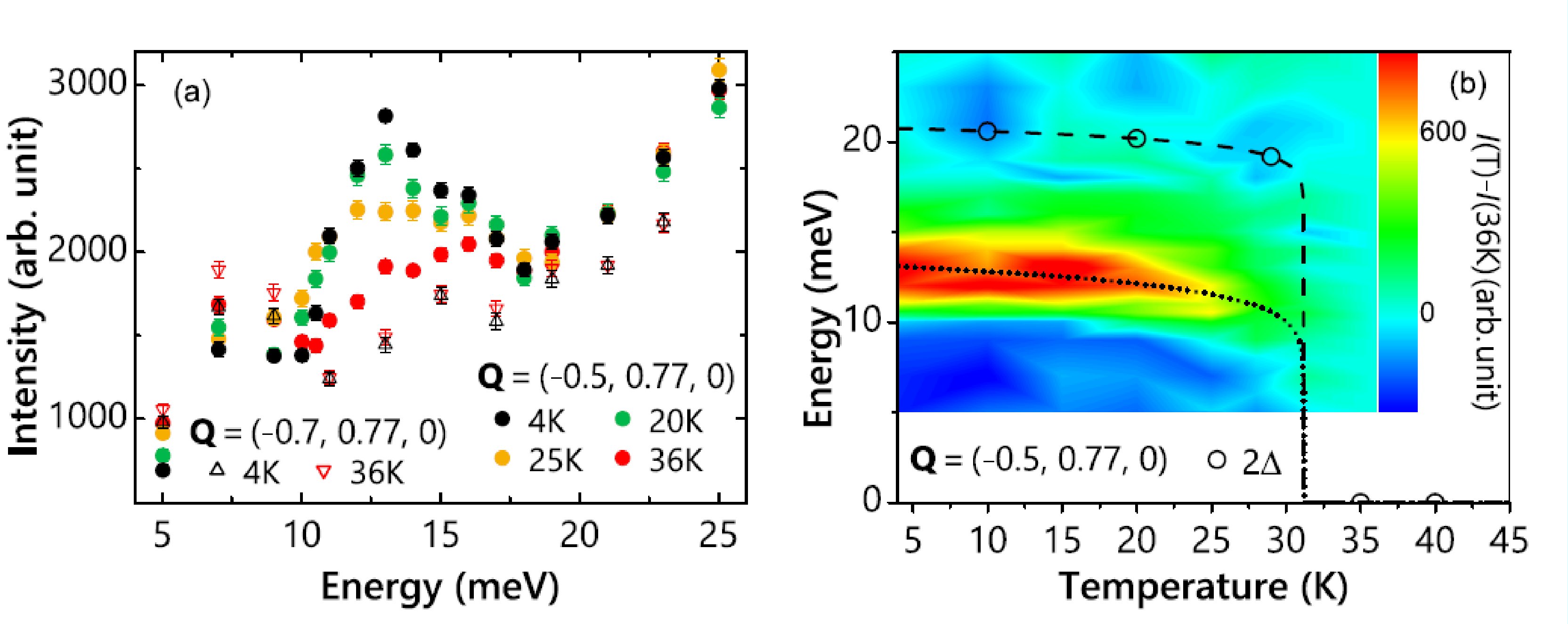

Transition from Sign-reversed to Sign-preserved Cooper-pairing Symmetry in Sulfur-doped Iron Selenide Superconductors,
Qisi Wang, J. T. Park, Yu Feng, Yao Shen, Yiqing Hao, Bingying Pan, J. W. Lynn, A. Ivanov, Songxue Chi, M. Matsuda, Huibo Cao, R. J. Birgeneau, D. V. Efremov, and Jun Zhao,
Phys. Rev. Lett. **116**, 197004 (2016).

Spin Resonance Symmetry Crossover

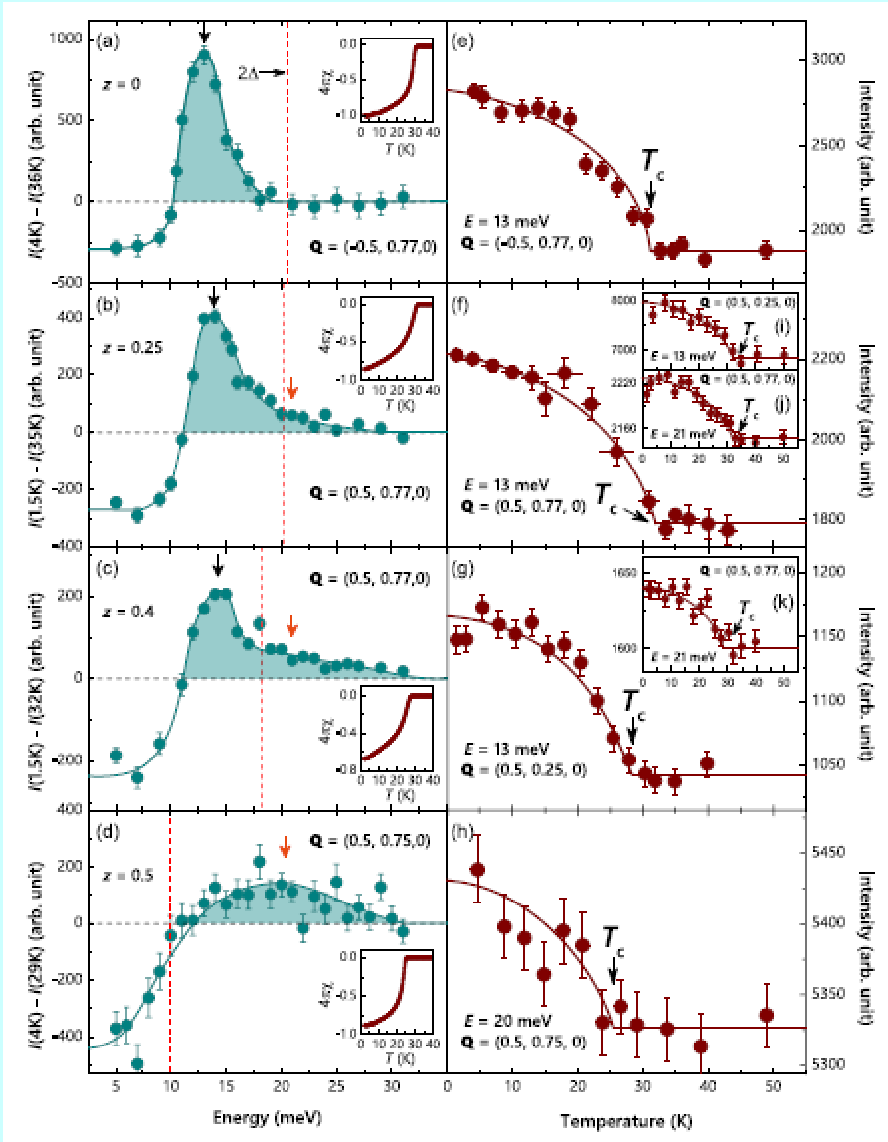

$^{7}Li_{1-x}Fe_xODFeSe$

Neutron Investigation of the Magnetic Scattering in an Iron-based Ferromagnetic Superconductor

Jeffrey W. Lynn[1], Xiuquan Zhou[2], Christopher K. H. Borg[2], Shanta R. Saha[3], Johnpierre Paglione[3], and Efrain E. Rodriguez[2]
(Phys. Rev. B **92**, 060510(R) (2015)

The Preparation and Phase Diagram of Superconducting ($^{7}Li_{1-x}Fe_xOD$)FeSe

Xiuquan Zhou[2], Christopher K. H. Borg[2], Jeffrey W. Lynn[1], Shanta R. Saha[3], Johnpierre Paglione[3], and Efrain E. Rodriguez[2]
J. Materials Chem. C **4**, 3934 (2016).

[1]NIST Center for Neutron Research, Gaithersburg, MD (USA)
[2]Department of Chemistry and Biochemistry, University of Maryland, College Park, MD (USA)
[3]Department of Physics, University of Maryland, College Park, MD (USA)

(Li-Fe)OHFeSe Ferromagnetic Superconductor

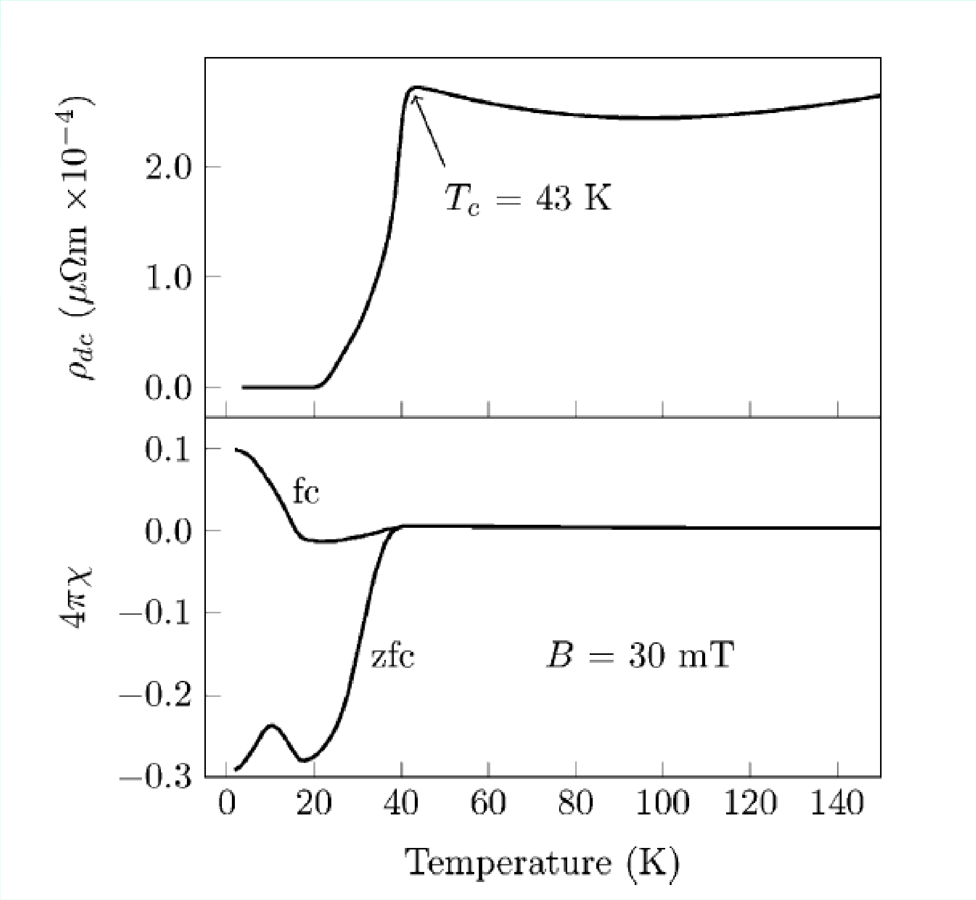

T_C=43 K

T_C=10 K

Coexistence of 3d-ferromagnetism and superconductivity in $[(Li_{1-x}Fe_x)OH](Fe_{1-y}Li_y)Se$, Ursula Pachmayr, Fabian Nitsche, Hubertus Luetkens, Sirko Kamusella, Felix Bruckner, Rajib Sarkar, Hans-Hennig Klauss, and Dirk Johrendt, Angew. Chem. Int. Ed. **54**, 293 (2015)

(Li-Fe)OHFeSe Ferromagnetic Superconductor

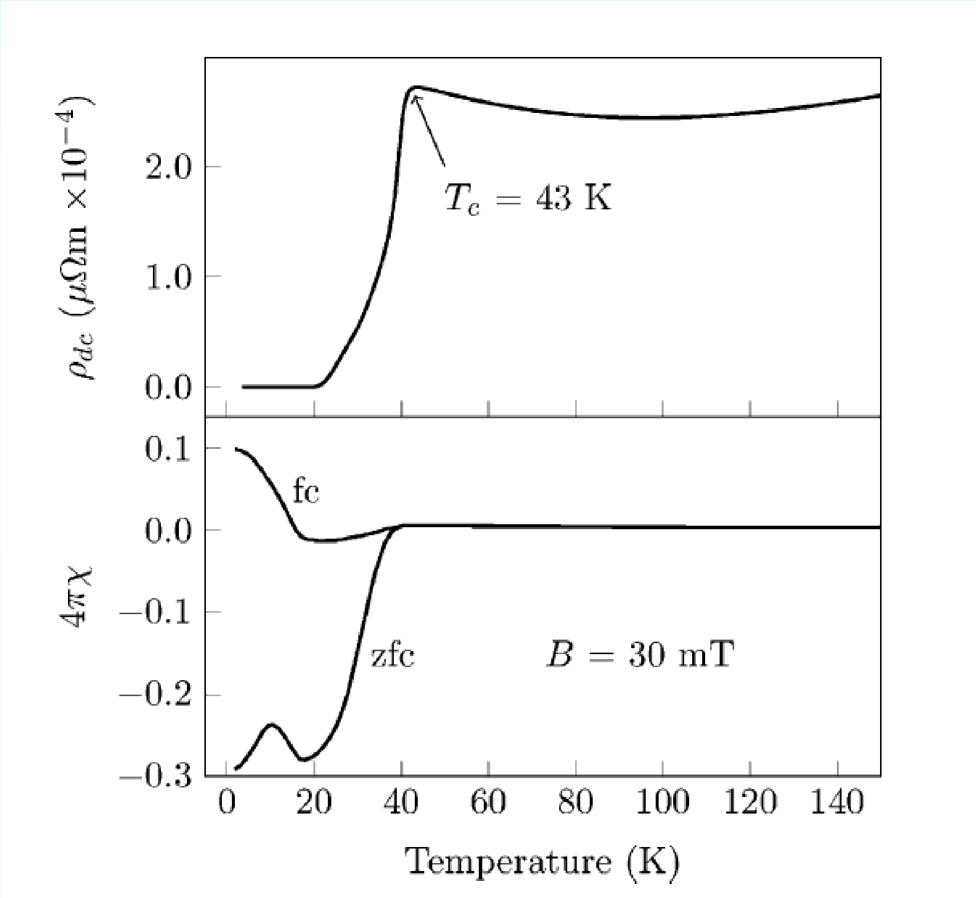

T_S=43 K

T_F=10 K

Coexistence of 3d-ferromagnetism and superconductivity in $[(Li_{1-x}Fe_x)OH](Fe_{1-y}Li_y)Se$, Ursula Pachmayr, Fabian Nitsche, Hubertus Luetkens, Sirko Kamusella, Felix Bruckner, Rajib Sarkar, Hans-Hennig Klauss, and Dirk Johrendt, Angew. Chem. Int. Ed. **54**, 293 (2015)

Crystal Structure

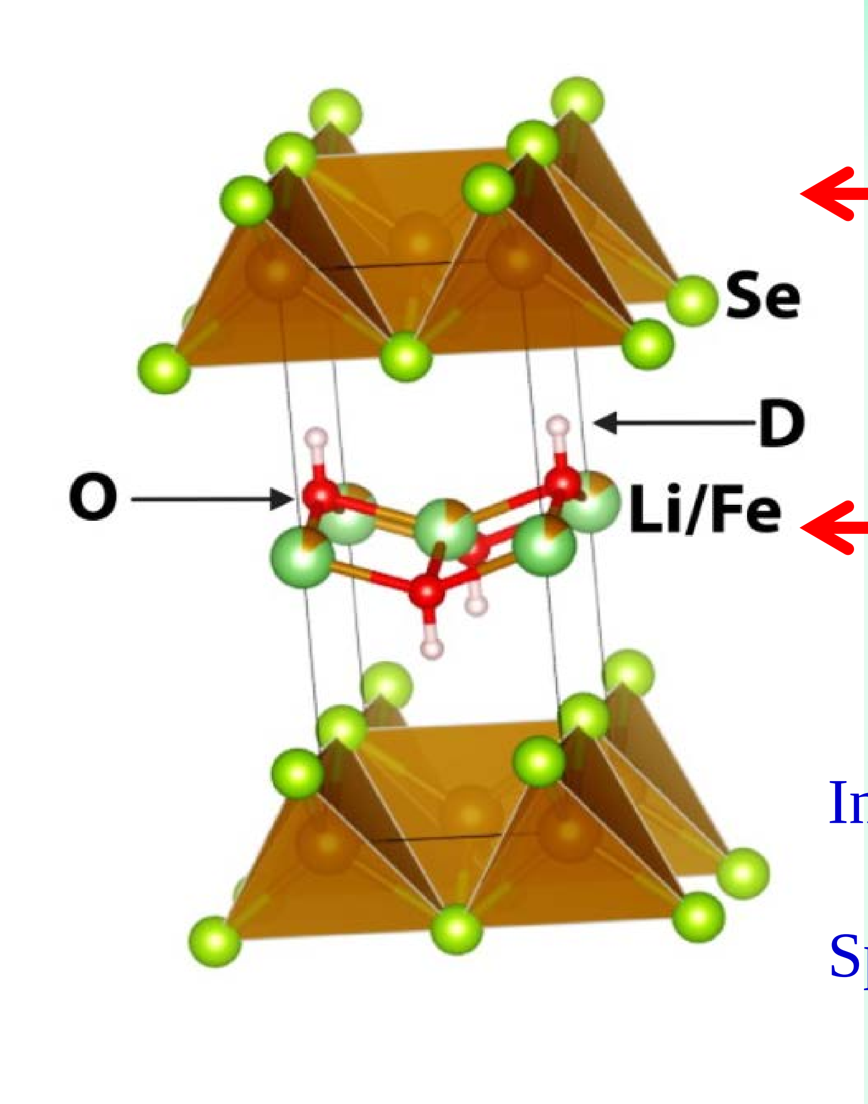

FeSe Superconducting Layer

Magnetic Layer

Incommensurate Long wavelength Ordered state?

Spontaneous Vortex Lattice?

Phase Diagram For (Li-Fe)OHFeSe

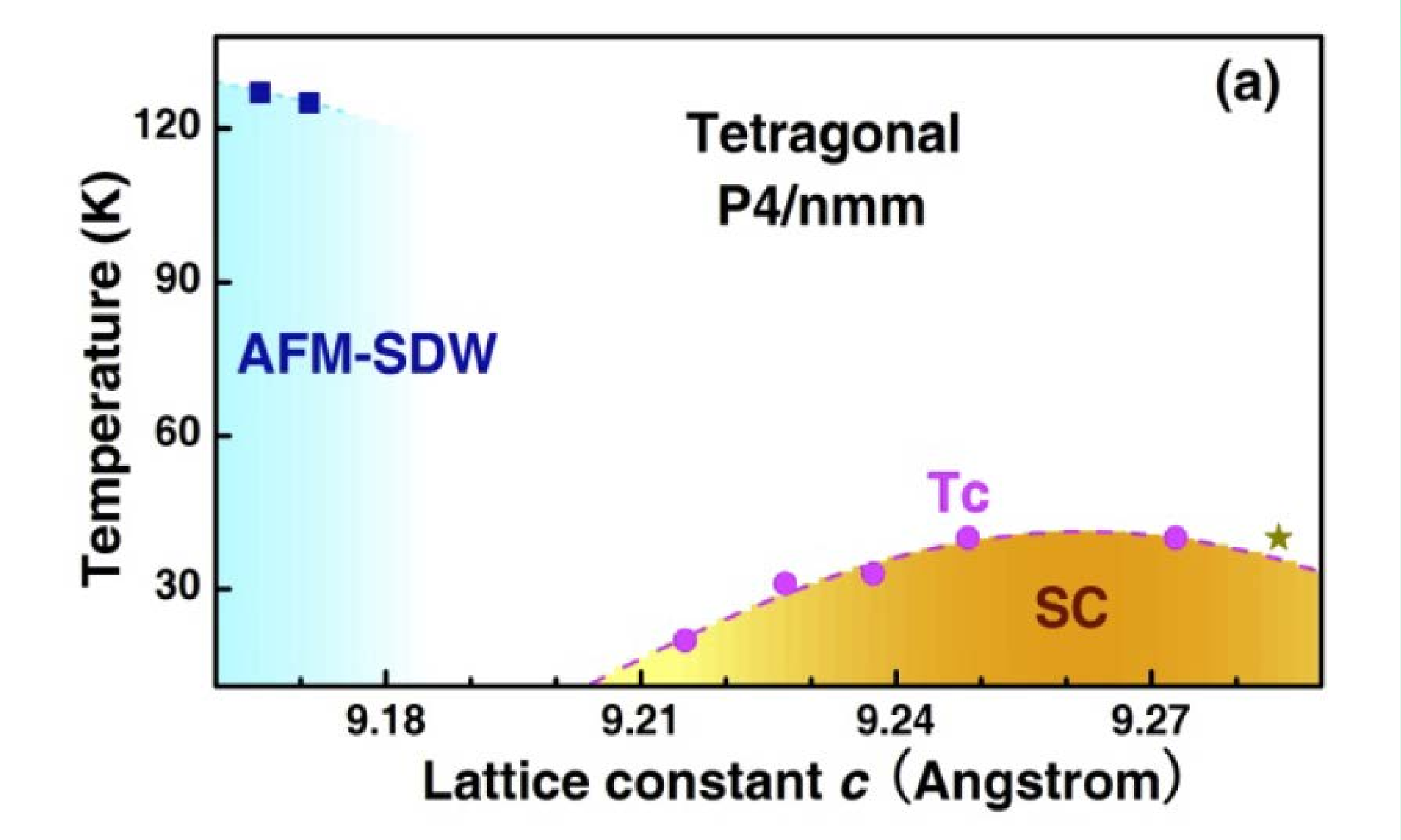

X. Dong, H. Zhou, H. Yang, J. Yuan, K. Jin, F. Zhou, D. Yuan, L. Wei, J. Li, X. Wang, G. Zhang, and Z. Zhao, J. Am. Chem. Soc. **137**, 66 (2014); X. F. Lu, *et al*., Nat. Mat **14**, 325 (2015).

Neutron Diffraction

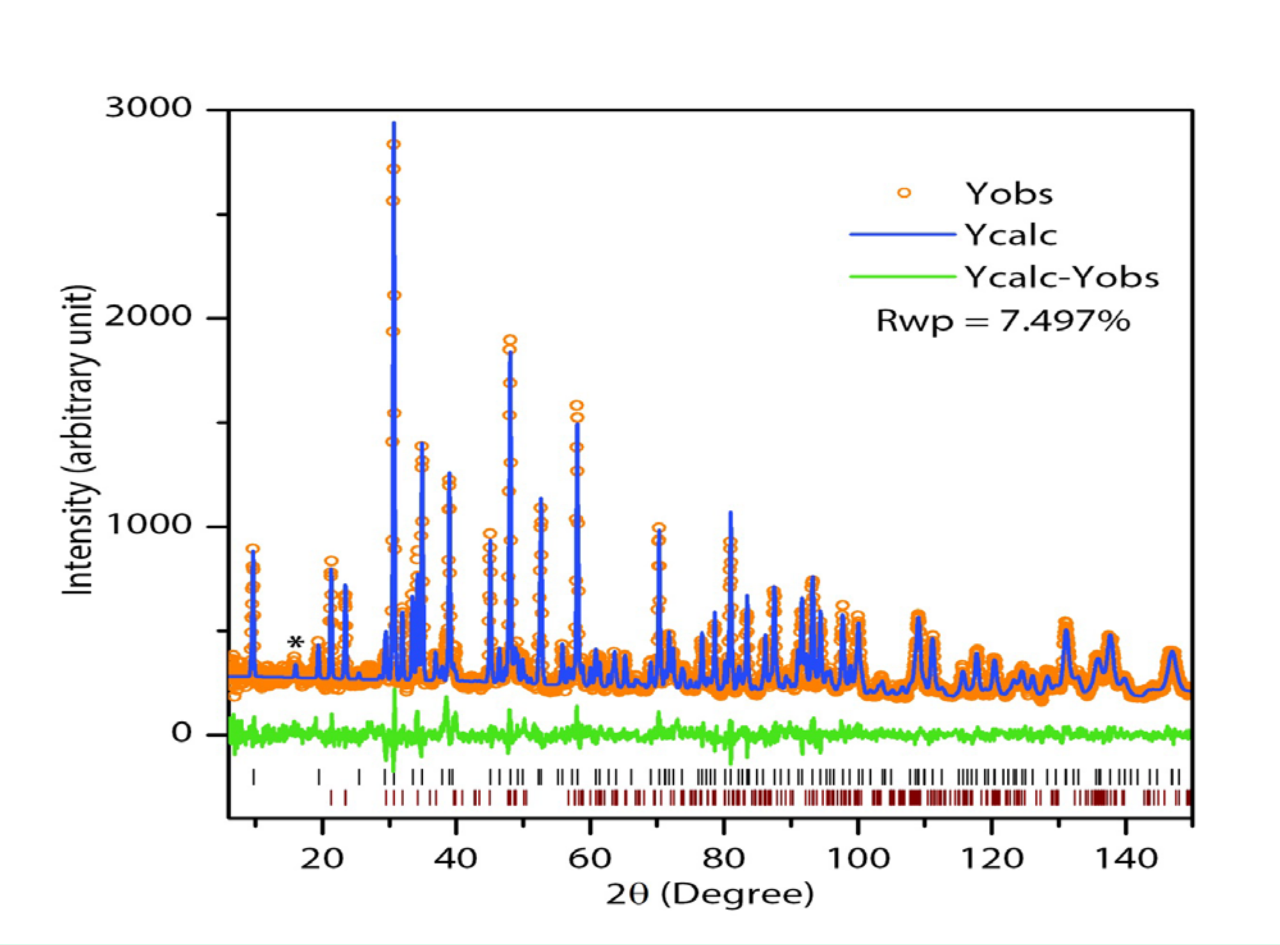

Neutron

T = 4 K

a= 3.7827(1) Å

c= 9.1277(3) Å

$^{7}Li_{1-x}Fe_{x}ODFeSe$ (x ≈ 0.18)

Phase Diagram

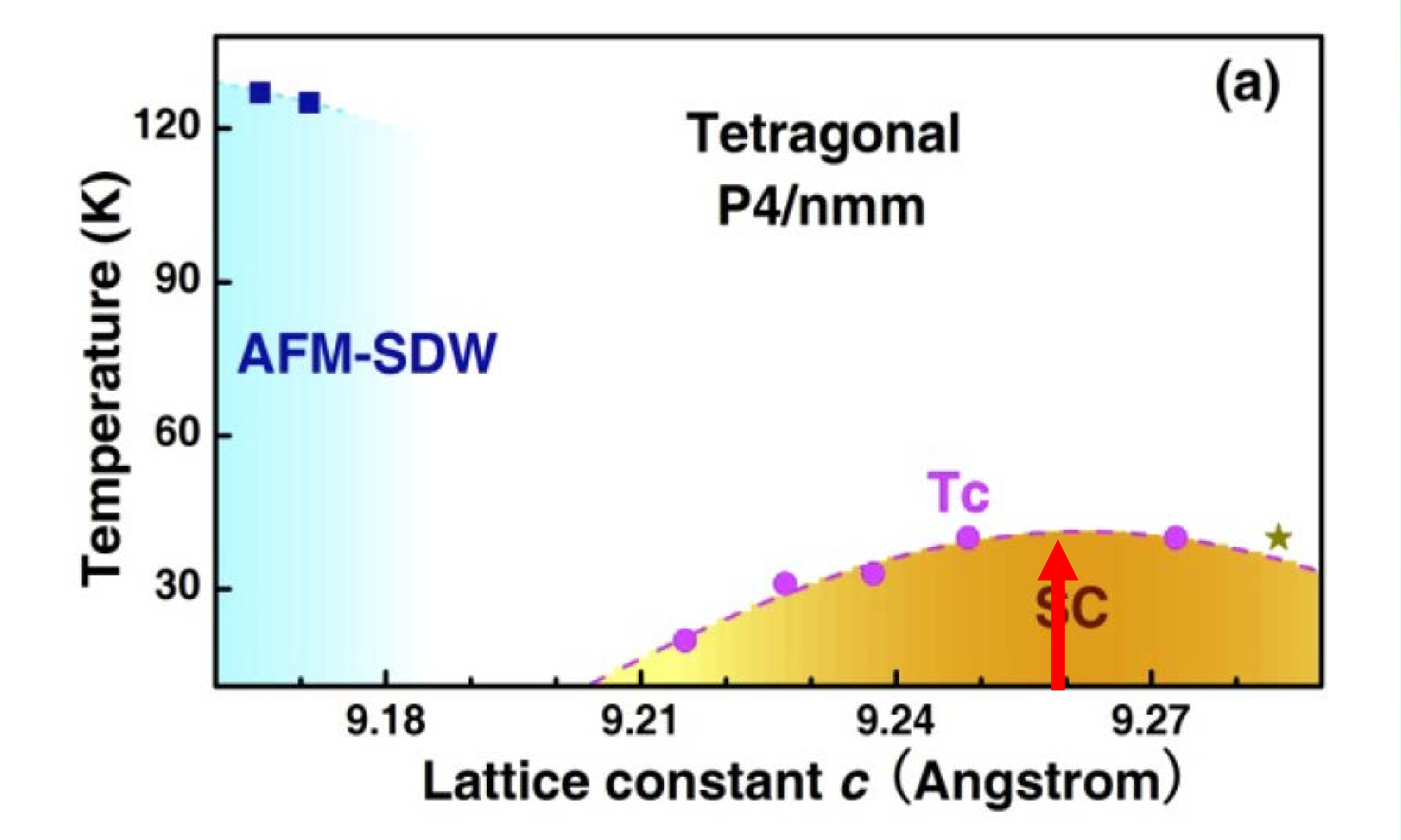

X. Dong, H. Zhou, H. Yang, J. Yuan, K. Jin, F. Zhou, D. Yuan, L. Wei, J. Li, X. Wang, G. Zhang, and Z. Zhao, J. Am. Chem. Soc. **137**, 66 (2014).

Phase Diagram for Deuterium

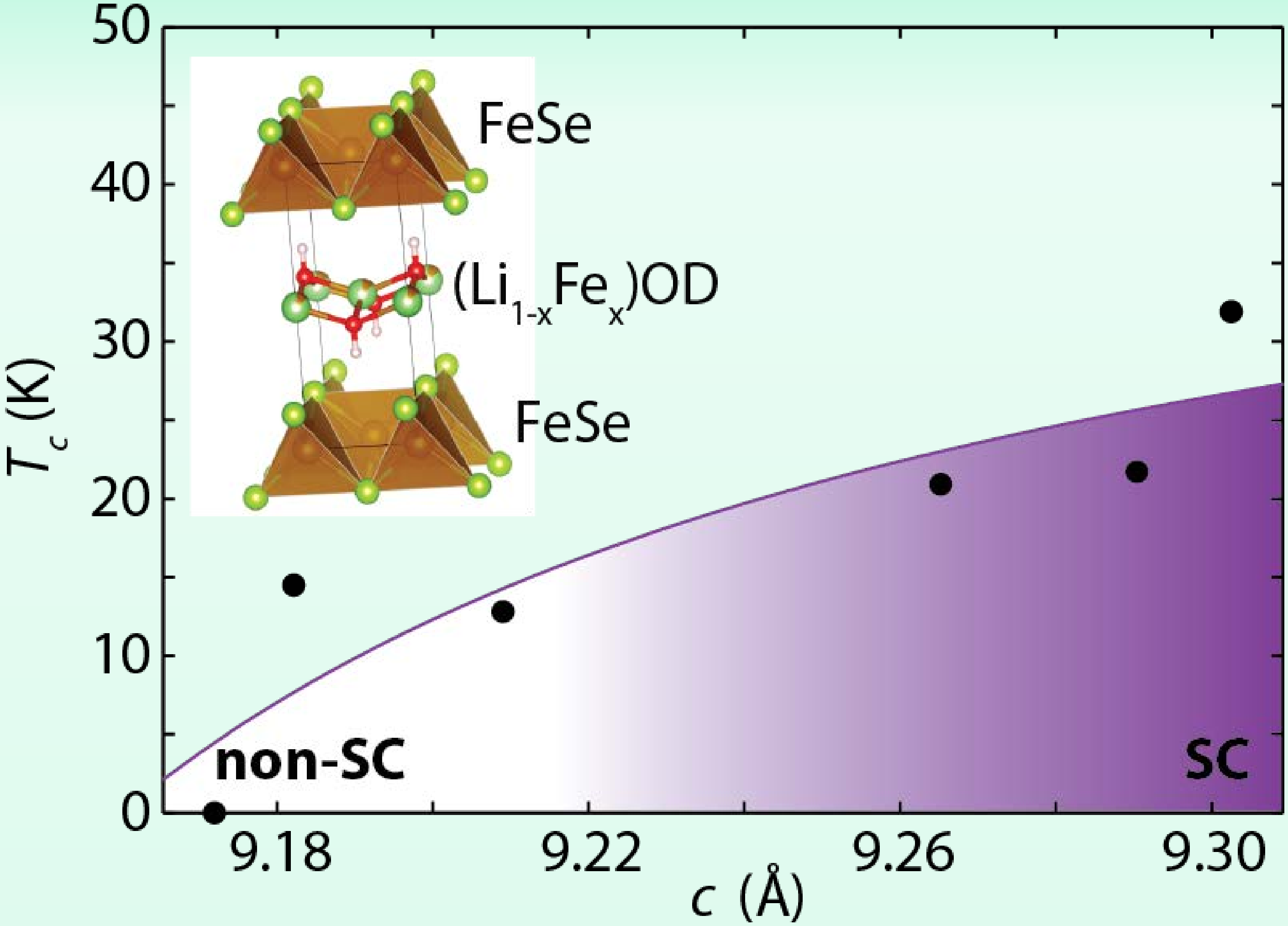

Magnetization for Tc = 18 K
(polycrystalline sample)

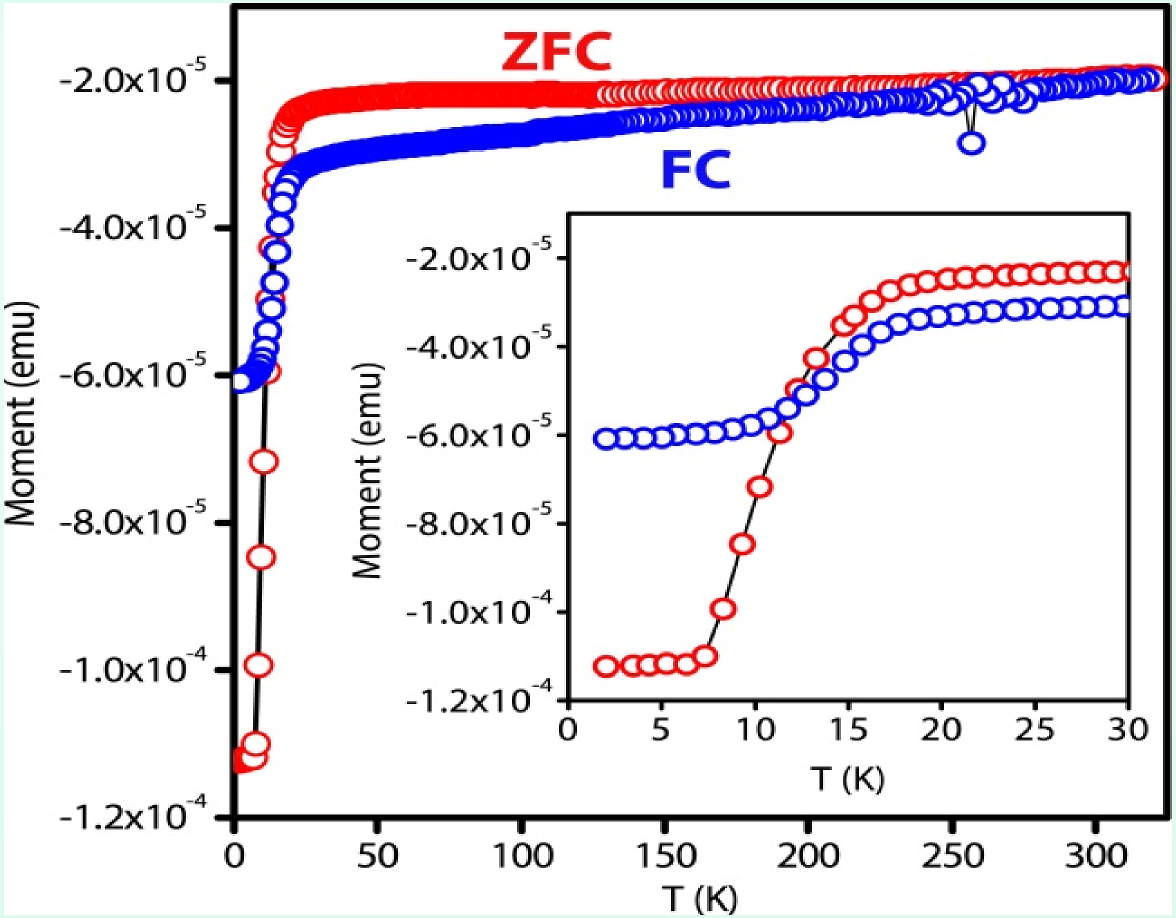

Ferromagnetic Magnetization

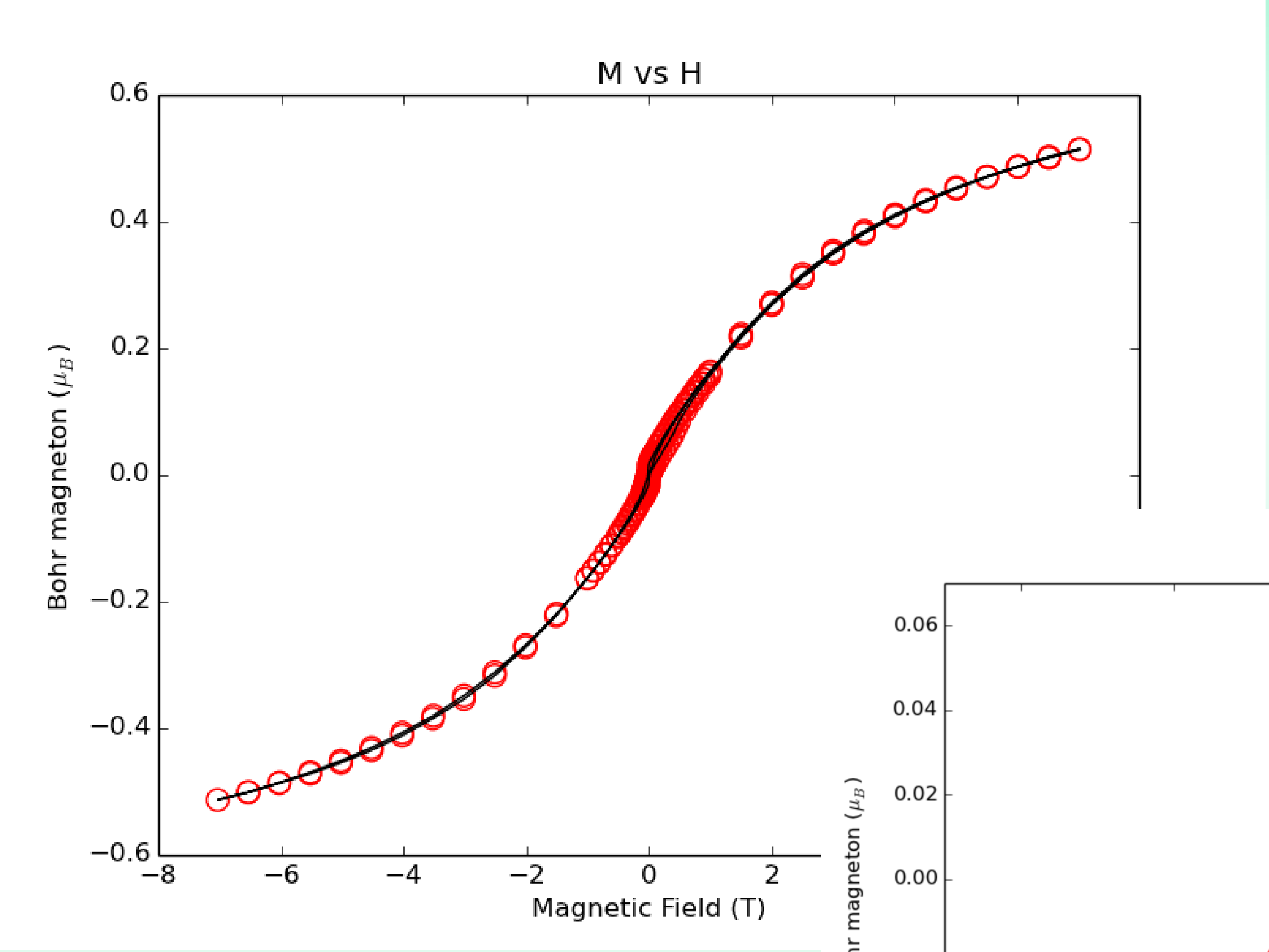

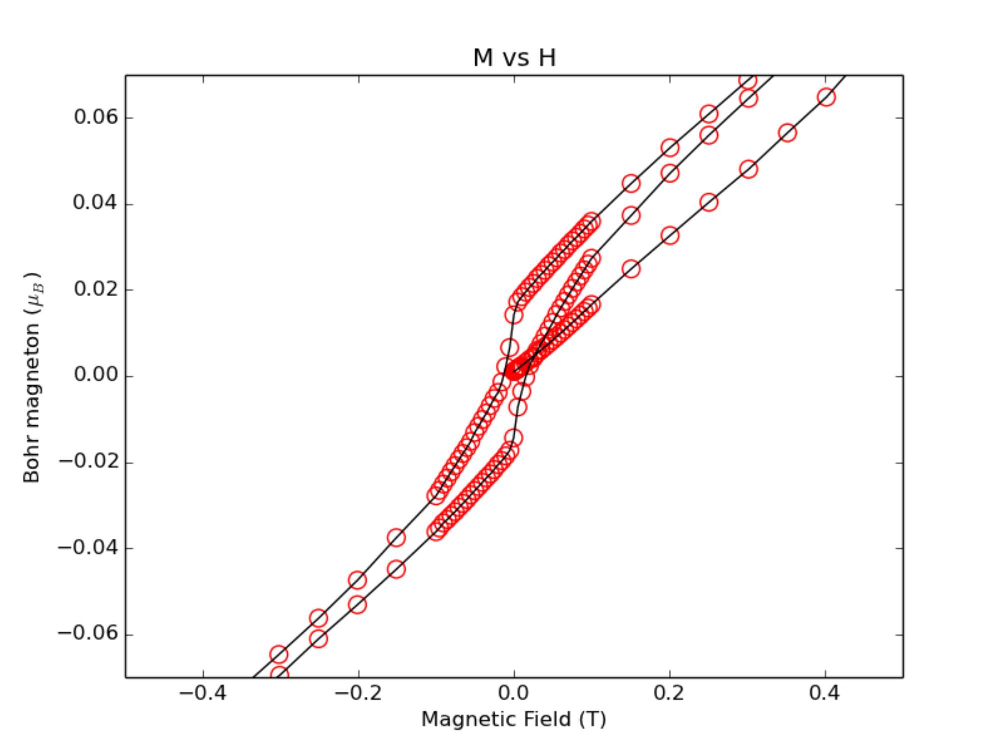

Neutron Diffraction at 2.5 K

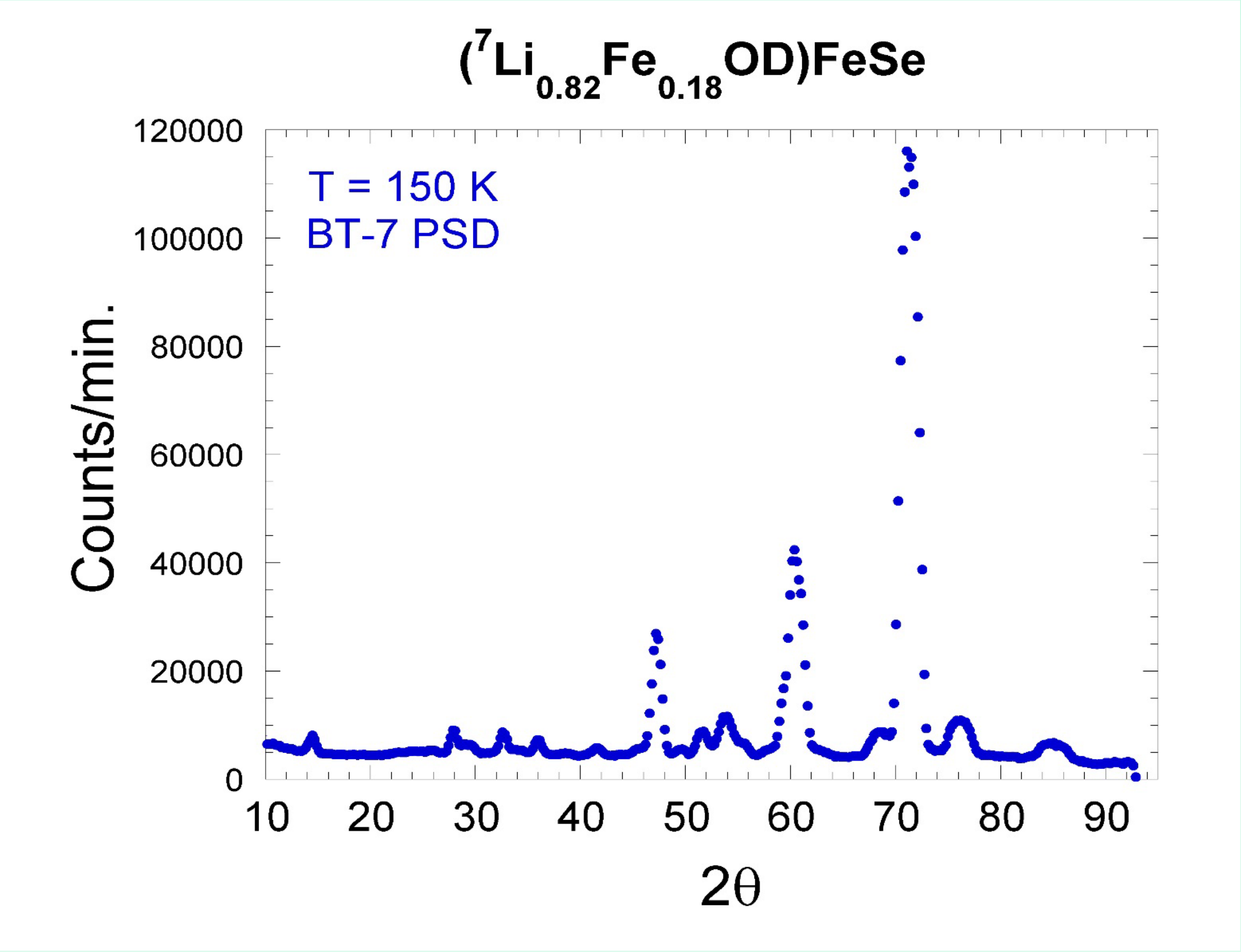

Difference Data (2.5 K – 50 K)

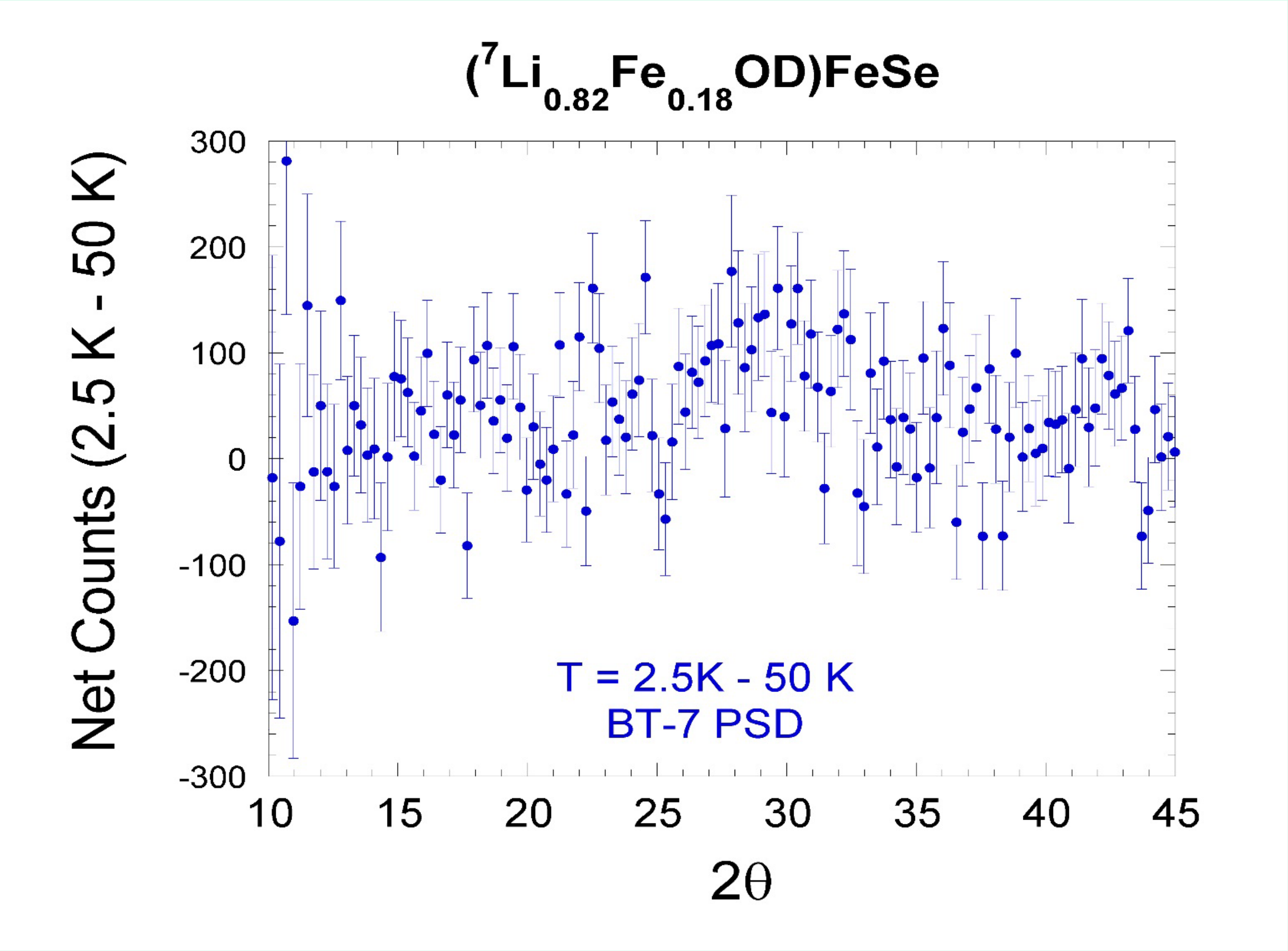

SANS I(5 K) – I(25) K

T_C = 18 K

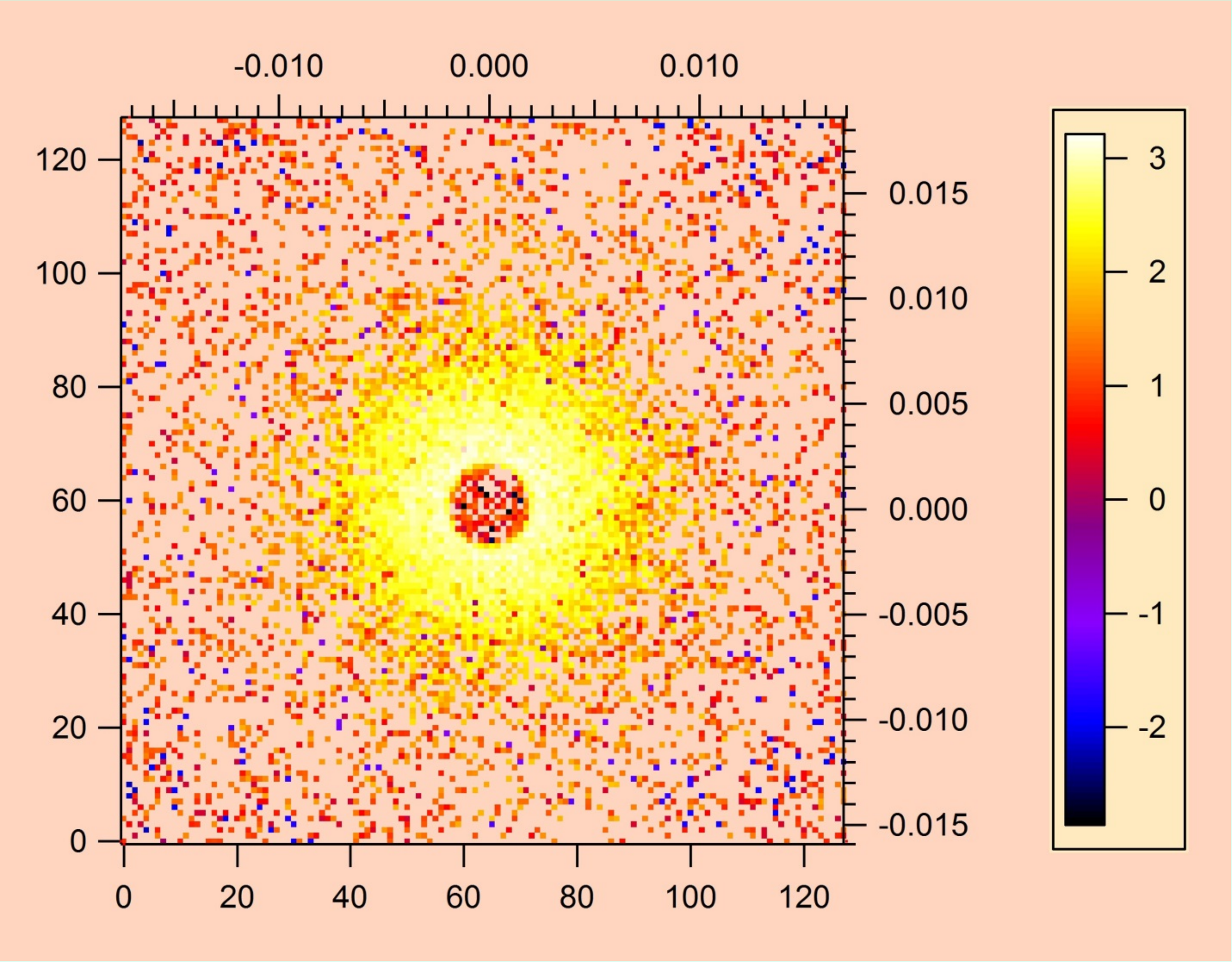

No Applied Magnetic Field

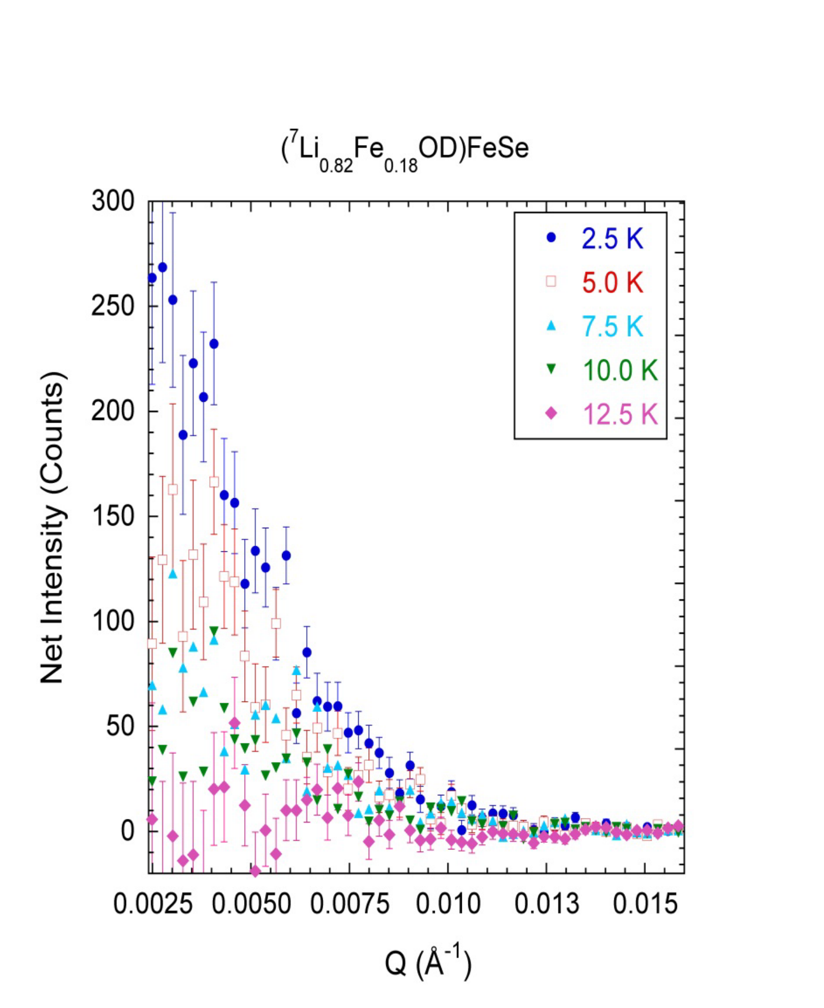

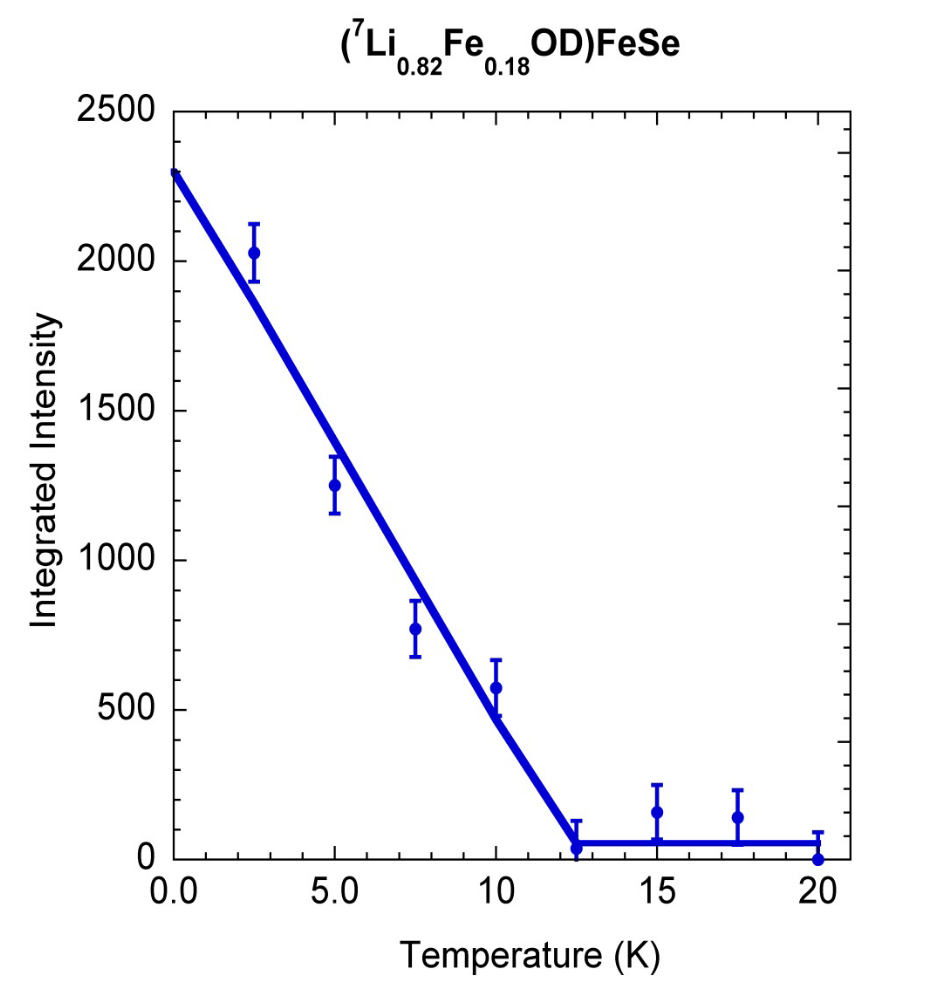

B = 0.4 T

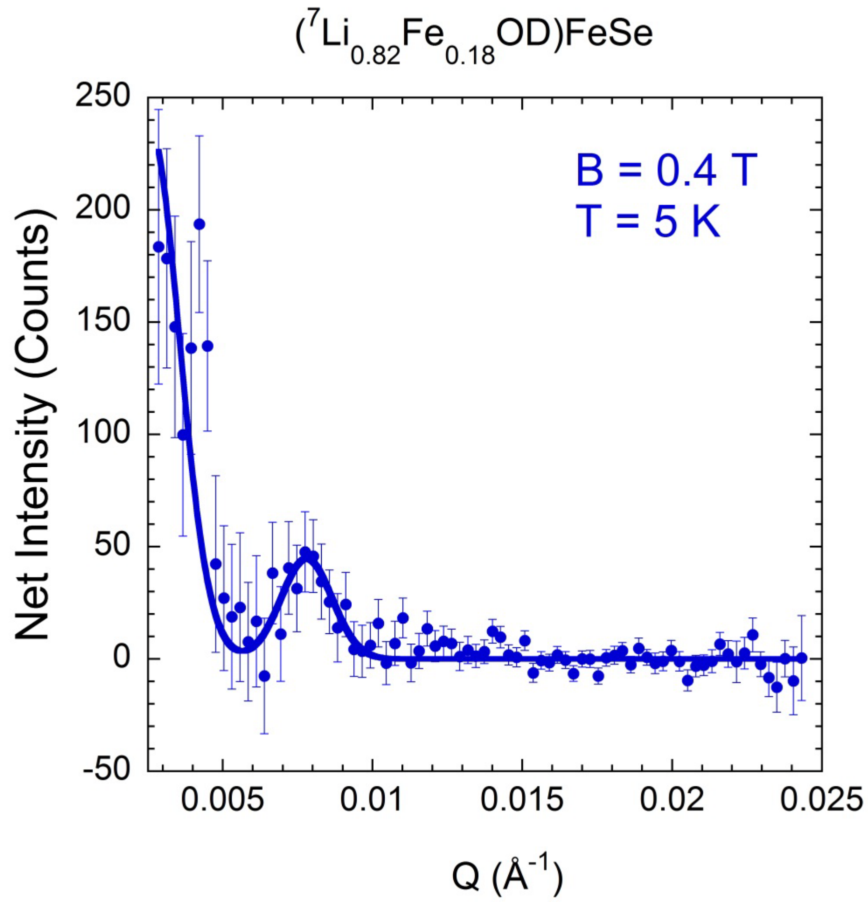

($^7Li_{0.82}Fe_{0.18}OD$)FeSe
B = 0.4 T
T = 5 K
Net Intensity (Counts)
Q (Å^{-1})
250
200
150
100
50
0
-50
0.005
0.01
0.015
0.02
0.025

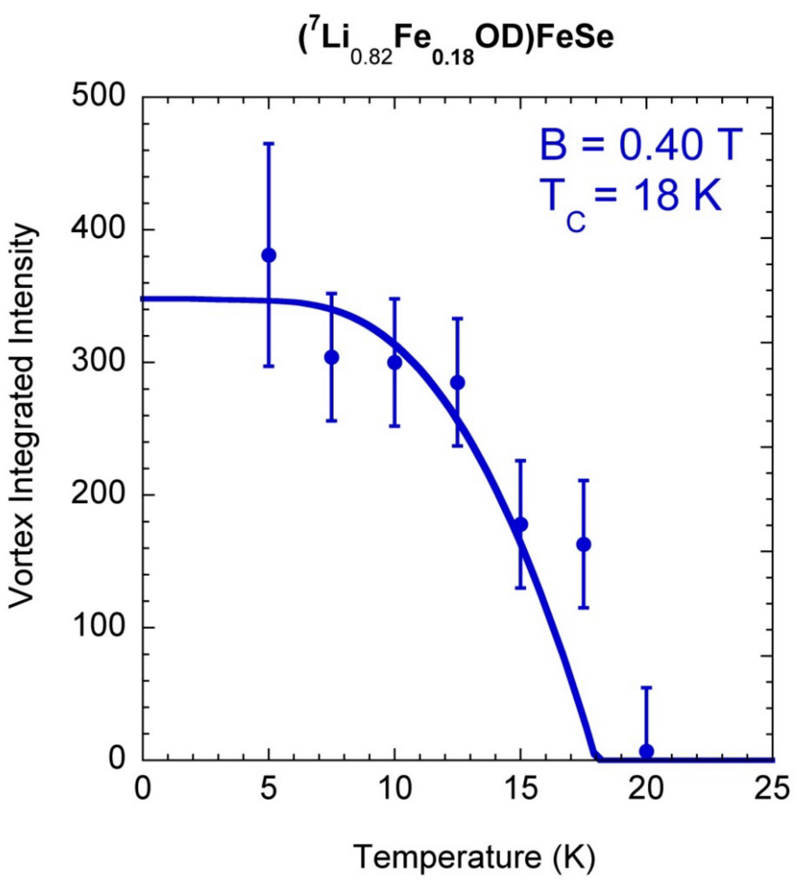

($^7Li_{0.82}Fe_{0.18}OD$)FeSe
B = 0.40 T
T_C = 18 K
Vortex Integrated Intensity
Temperature (K)
500
400
300
200
100
0
0
5
10
15
20
25

Magnetic Superconductors

- Magnetic Superconductors have a rich and interesting history, ranging from "***shouldn't have magnetic spins in the lattice***" to "***must have magnetic spins in the lattice***" for High Tc
- The iron-based superconductors exhibit a similar phase diagram to the cuprates. The 'parent' systems exhibit a ubiquitous structural transition, below which long range antiferromagnetic occurs. The magnetic energetics is ~200 meV, also similar to the cuprates. The role of spin fluctuations in the superconducting pairing is clear.

$La_{1-x}Ca_xMnO_3$

Phase Diagram

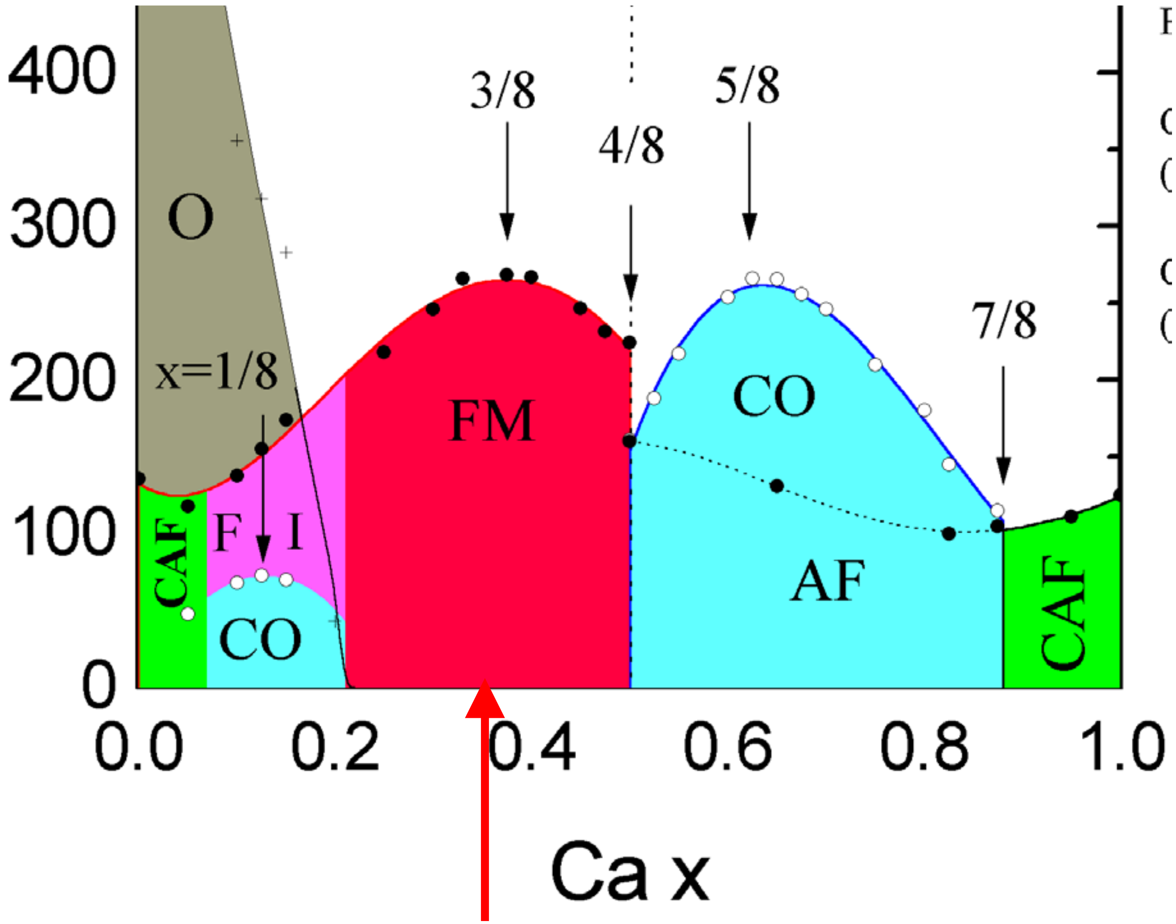

S-W. Cheong and C. H. Chen
Colossal Magnetoresistance, Charge Ordering, and Related Properties of Manganese Oxides (World Scientific, 1998), p. 241 (Ed. by Raveau and Rao)

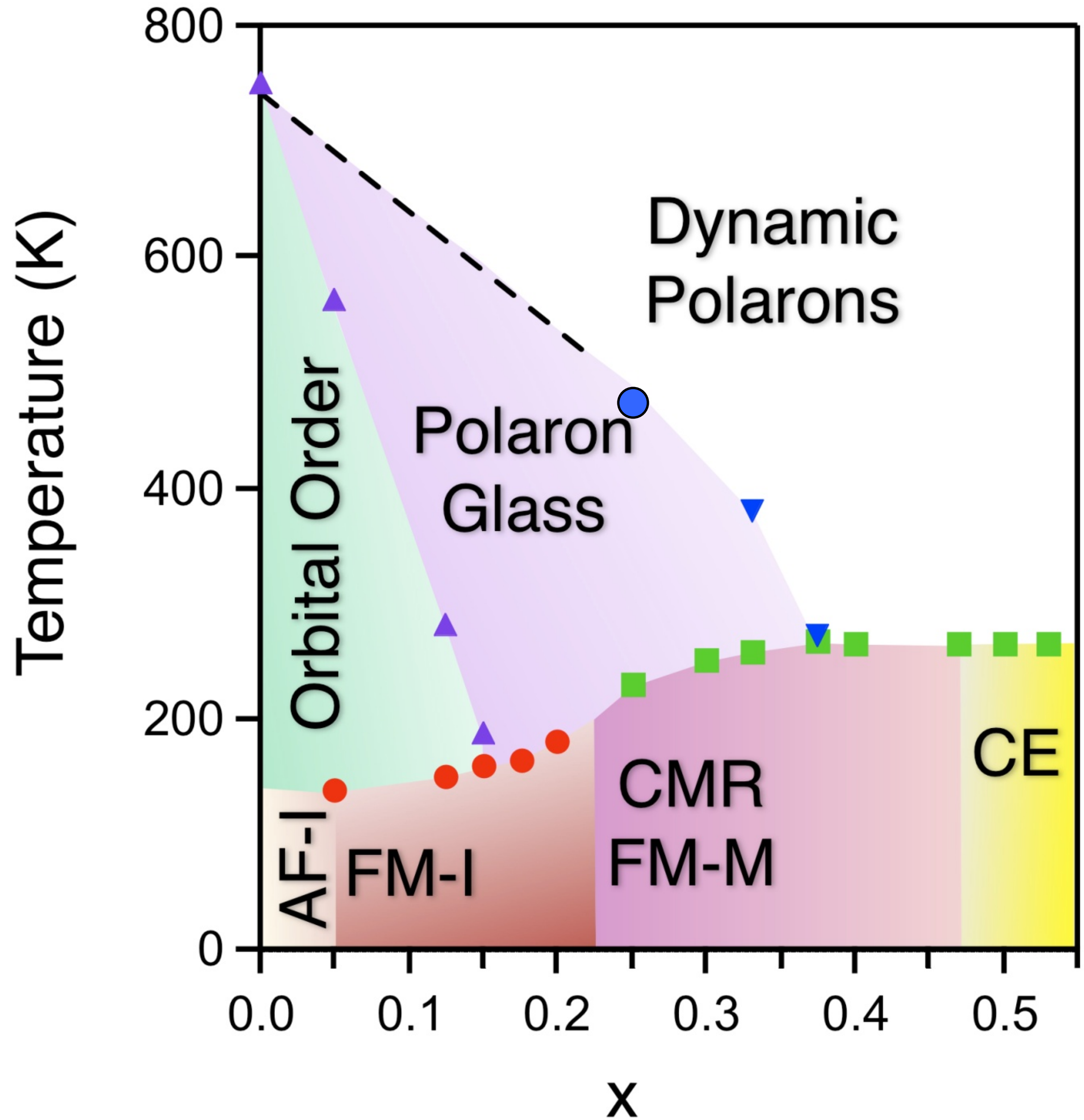

J. W. Lynn, D. N. Argyriou, Y. Ren, Y. Chen, Y. M. Mukovskii, and D. A. Shulyatev, Phys. Rev. B**76**, 014437 (2007)

NCNR

Polaron Dynamics in CMR $La_{0.7}Ca_{0.3}MnO_3$

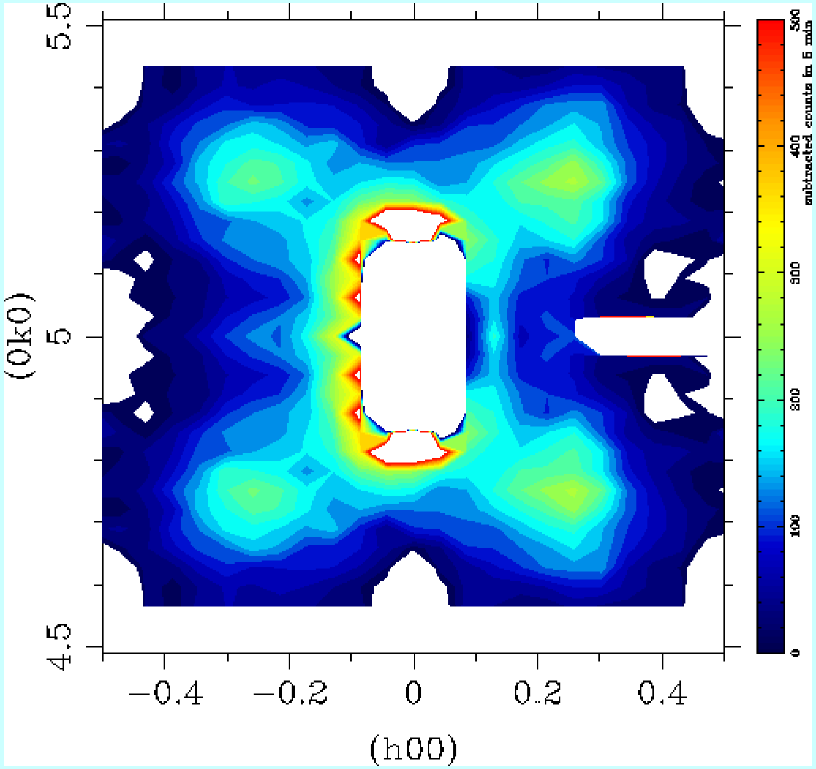

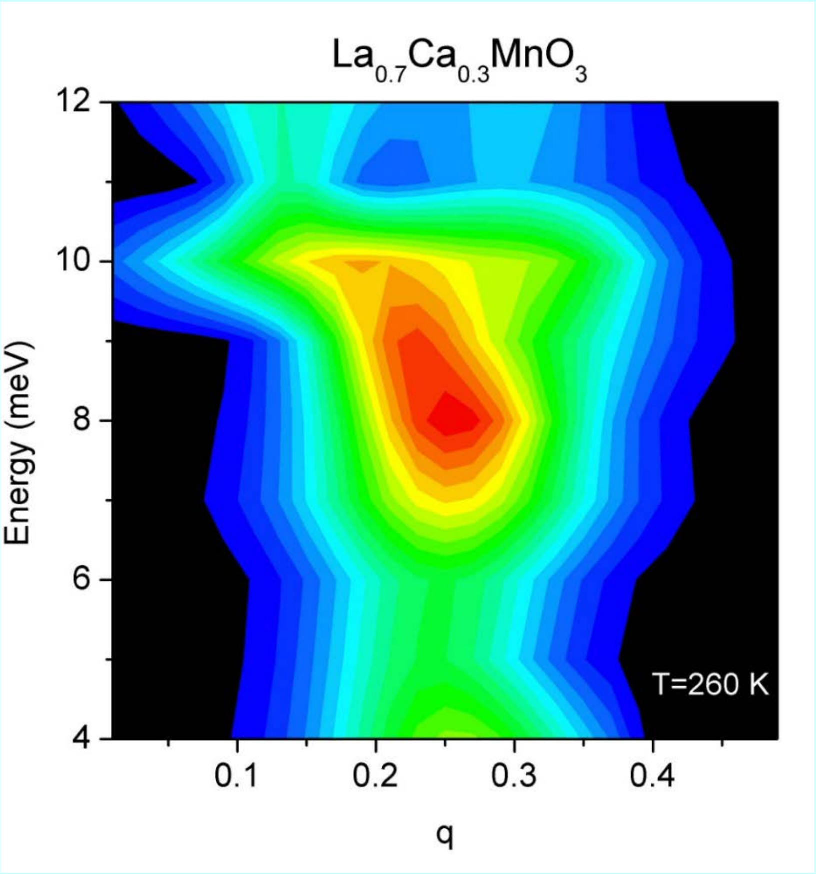

J. W. Lynn, D. N. Argyriou, Y. Ren, Y. Chen, Y. M. Mukovskii, and D. A. Shulyatev, Phys. Rev. B**76**, 014437 (2007)

Polarized Neutron Scattering Data (BT7)

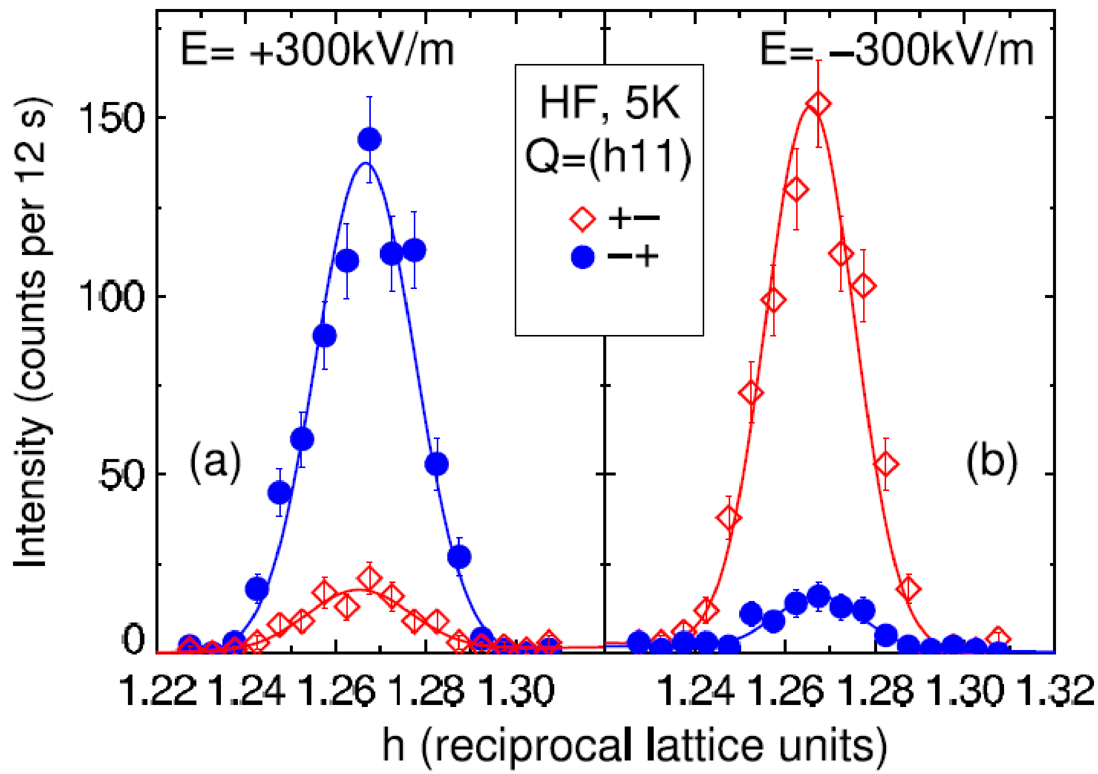

Coupled Magnetic and Ferroelectric Hysteresis in Multiferroic $Ni_3V_2O_8$, I. Cabrera, M. Kenzelmann, G. Lawes, Y. Chen, W. C. Chen, R. Erwin, T. R. Gentile, J. B. Leao, J. W. Lynn, N. Rogado, R. J. Cava, and C. Broholm, Phys. Rev. Lett. 103, 087201 (2009).

Thin Films and Multilayers

***Specular reflection**: incident ∠ = reflected ∠*

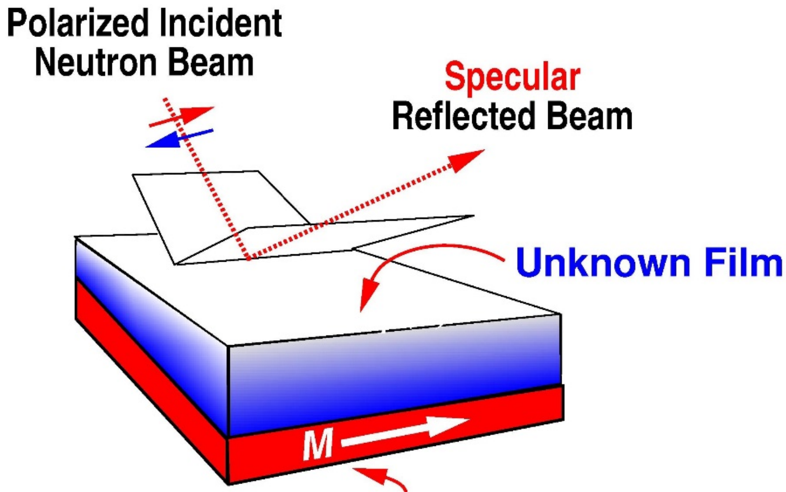

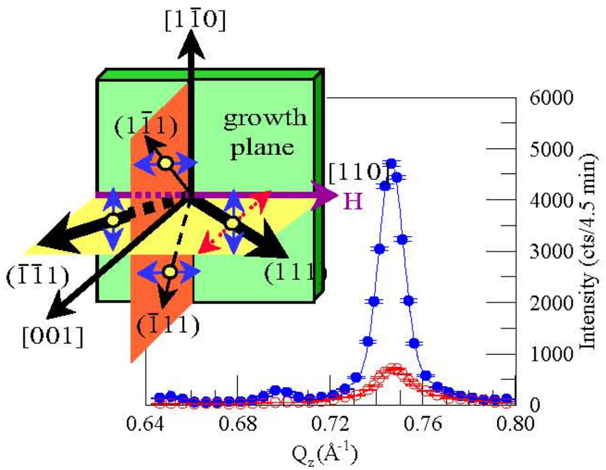

Doping Ferromagnetism in Antiferromagnetic Manganite Superlattices

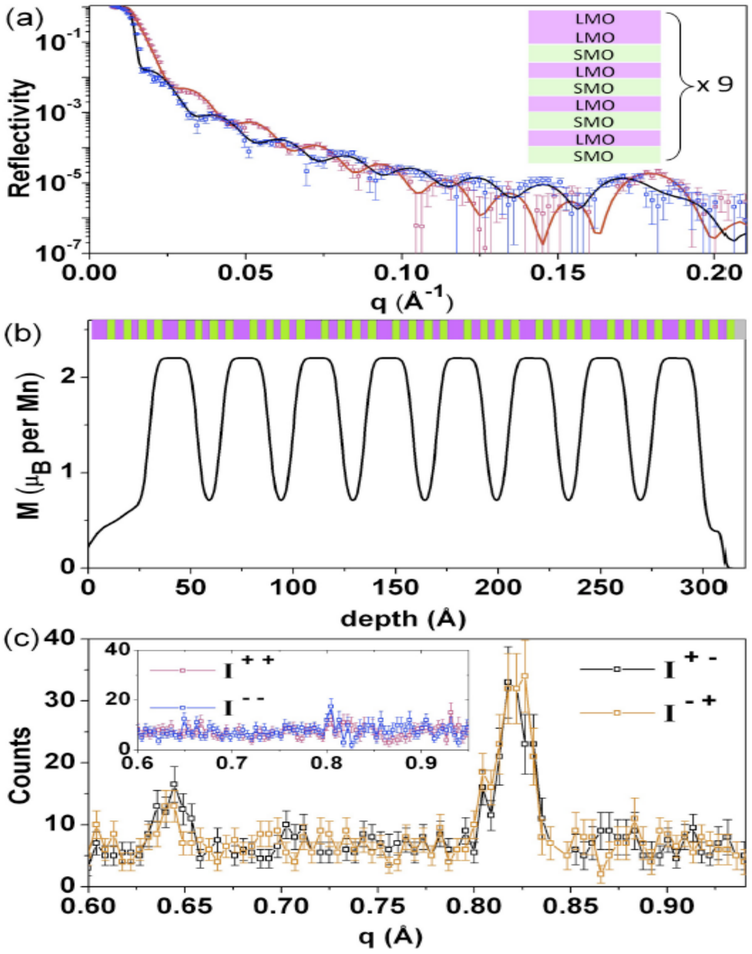

T. S. Santos, B. J. Kirby, S. Kumar, S. J. May, J. A. Borchers, B. B. Maranville, J. Zarestky, S. G. E. Te Velthuis, J. van den Brink and A. Bhattacharya,
Phys. Rev. Lett. **107**, 167202 (2011).

Interfacial Magnetism Example

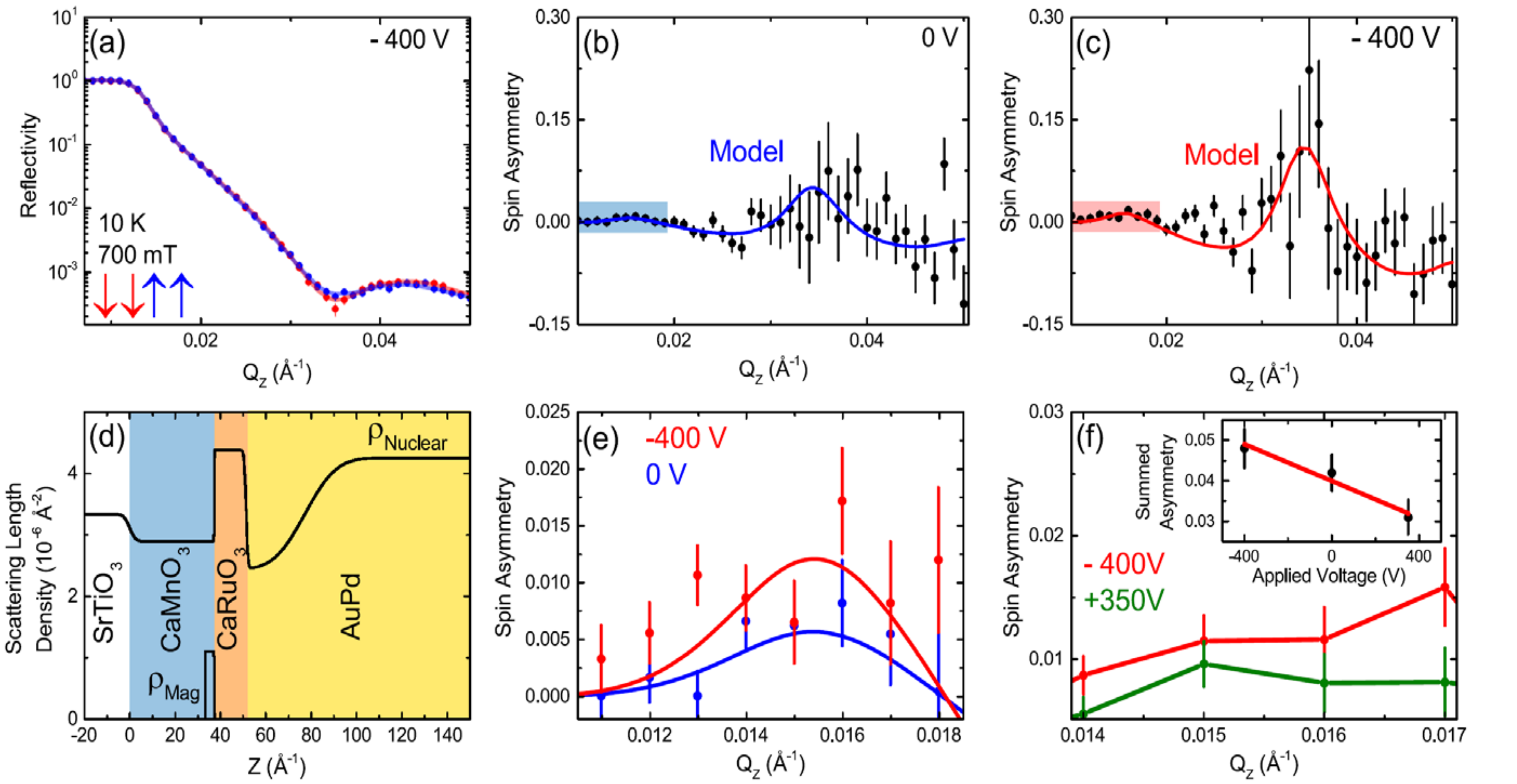

A. J. Grutter, B. J. Kirby, M. T. Gray, C. L. Flint, U. S. Alaan, Y. Suzuki, and J. A. Borchers, Phys. Rev. Lett. 115, 047601 (2015).

Spin Ice and Magnetic Monopoles

- Observation of Magnetic Monopoles in Spin Ice, Hiroaki Kadowaki, Naohiro Doi, Yuji Aoki, Yoshikazu Tabata, Taku J. Sato, J. W. Lynn, K. Matsuhira, and Z. Hiroi, J. Phys. Soc. Japan **78**, 103706 (2009).
- Quantum Spin Fluctuations in the Spin Liquid State of $Tb_2Ti_2O_7$, H. Kadowaki, H. Takatsu, Y. Tabata, T. J. Sato, J. W. Lynn, J. Phys. Cond. Matr. **24**, 052201 (2012).
- Quadrupole Order in the Frustrated Pyrochlore $Tb_{2+x}Ti_{2-x}O_{7+y}$, H. Takatsu, S. Onoda, S. Kittaka, A. Kasahara, Y. Kono, T. Sakakibara, Y. Kato, B. Fåk, J. Ollivier, J. W. Lynn, T. Taniguchi, M. Wakita, and H. Kadowaki, Phys. Rev. Lett. **116**, 217201 (2016).

$Dy_2Ti_2O_7$ Spin Ice

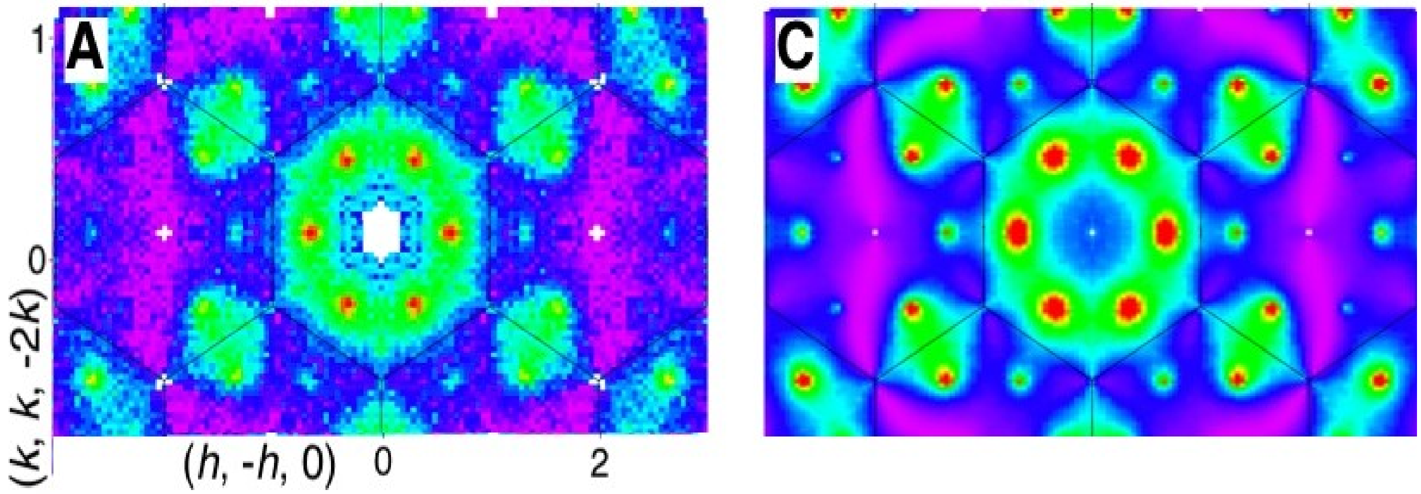

B = 0.5 T T = 0.43

Topological Systems

- Topological RPdBi half-Heusler semimetals: a new family of non-centrosymmetric magnetic superconductors, Y. Nakajima, R. Hu, K. Kirshenbaum, A. Hughes, P. Syers, X. Wang, K. Wang, R. Wang, S. Saha, D. Pratt, J.W. Lynn, and J. Paglione, Science Advances **1**, e1500242 (2015).
- Large Anomalous Hall Effect in a Half Heusler Antiferromagnet, T. Suzuki, R. Chisnell, A. Devarakonda, Y.-T. Liu, J. W. Lynn, and J. G. Checkelsky, Nature Physics (http://dx.doi.org/10.1038/NPHYS3831).

Polarized beam inelastic scattering

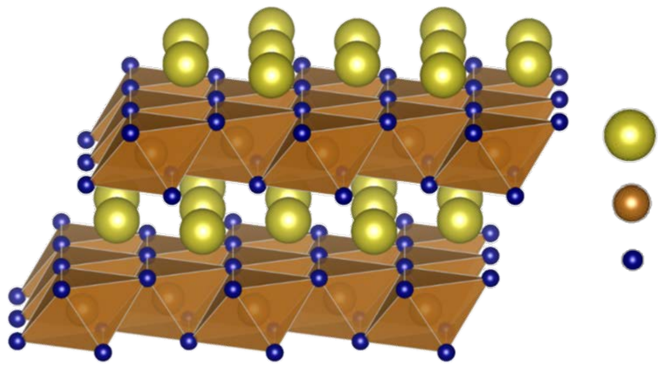

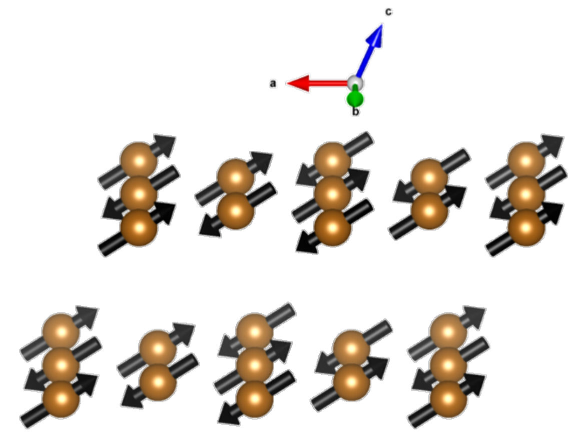

α-$NaMnO_2$
magnetic structure

Q || P

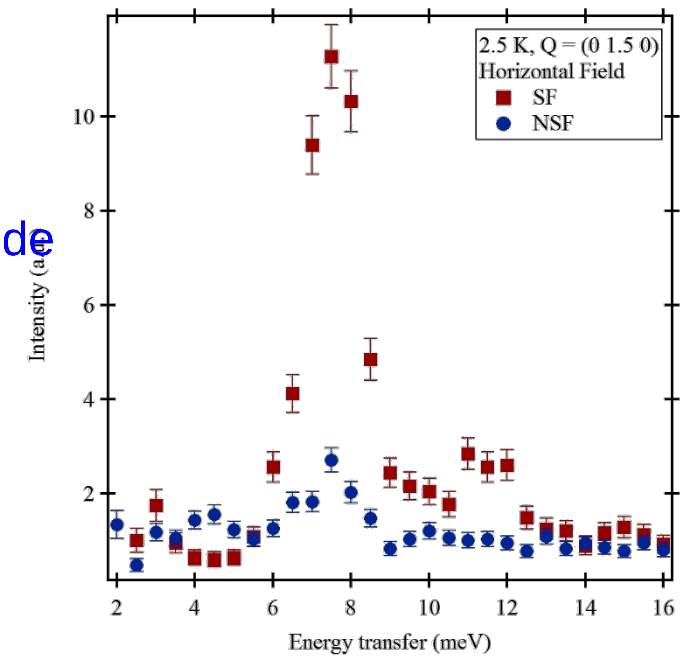

Q ⊥ P

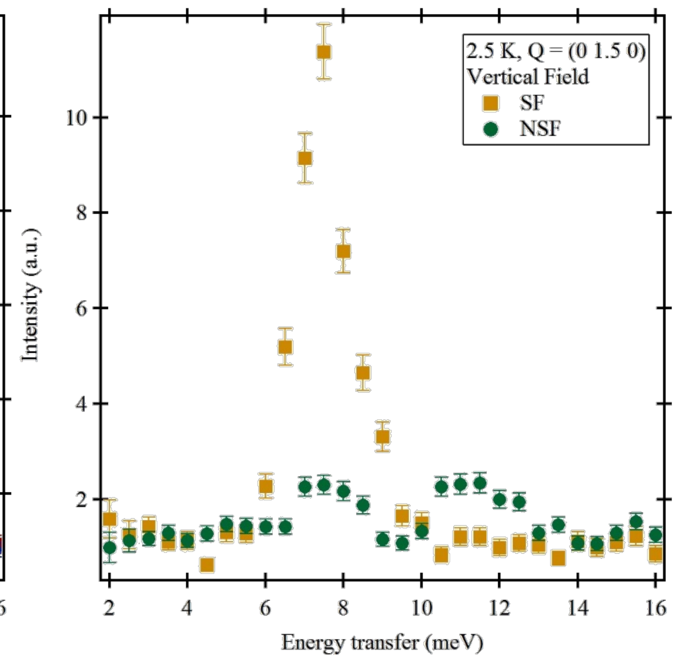

Amplitude (Higgs) Mode
Rebecca Dally, *et al.*,
Nature Comm.
(submitted)

BT-7

Spin Liquid Scattering in $ZnCu_3(OD)_6C_{l2}$

T = 1.6 K

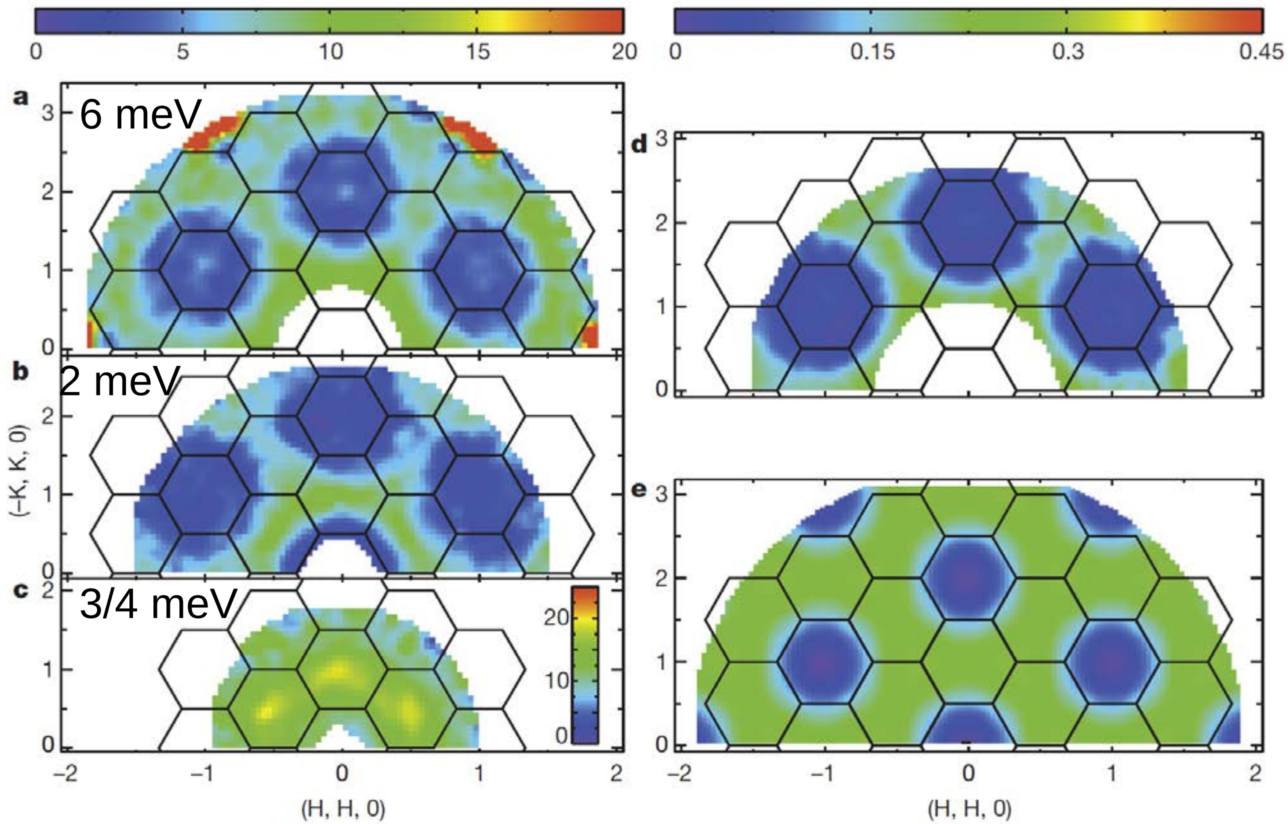

MACS

Tian-Heng Han, Joel S. Helton, Shaoyan Chu, Daniel G. Nocera, Jose A. Rodriguez-Rivera, Collin Broholm, and Young S. Lee, Nature **492**, 406 (2012).

Fractional Spin Excitations in Yb_2Pt_2Pb

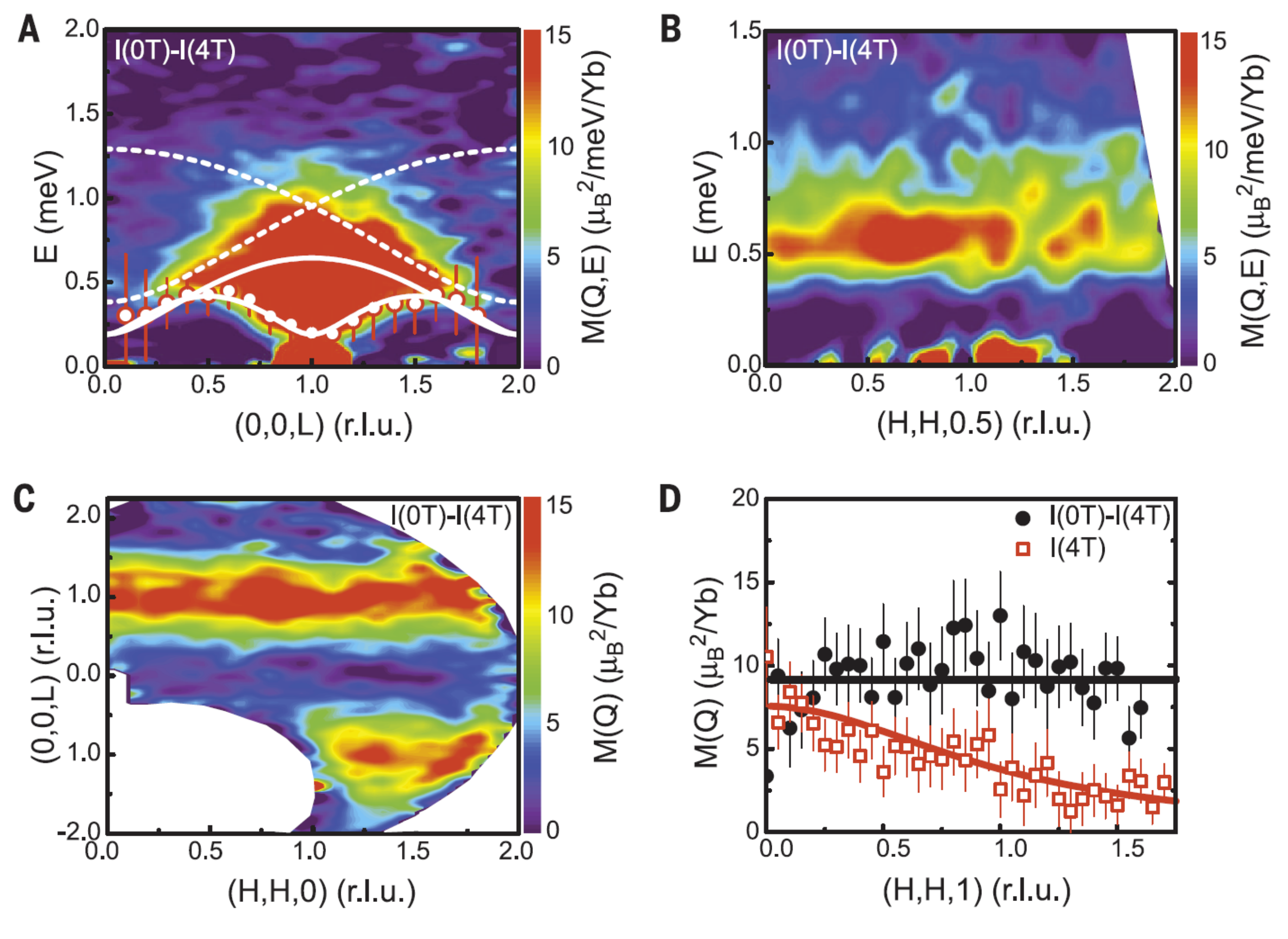

L. S. Wu, W. J. Gannon, I. A. Zaliznyak, A. M. Tsvelik, M. Brockmann, J.-S. Caux, M. S. Kim, Y. Qiu, J. R. D. Copley, G. Ehlers, A. Podlesnyak, M. C. Aronson, Science **352**, 1690 (2016).

NCNR

References:

S. W. Lovesey, Theory of neutron scattering from condensed matter, Oxford: Clarendon Press - Oxford, 1984.

E. Balcar and S. Lovesey, Theory of Magnetic Neutron and Photon Scattering, Oxford: Clarendon Press, 1989.

L. Ament, M. van Veenendaal, T. P. Devereaux, J. P. Hill and J. van den Brink, "Resonant inelastic s-ray scattering studies of elementary excitations," *Rev. Mod. Phys.*, vol. 83, p. 705, 2011.

G. E. Bacon, Neutron Diffraction, Third ed., Oxford: Oxford University Press, 1975.

Magnetic Scattering, Jeffrey W. Lynn and Bernhard Keimer, *in Handbook of Magnetism*, ed. by Michael Coey and Stuart Parkin

Neutron Nuclear Properties:

https://www.ncnr.nist.gov/resources/n-lengths/

https://www.ncnr.nist.gov/instruments/magik/Periodic.html

Magnetic Form Factors

https://www.ill.eu/sites/ccsl/ffacts/ffachtml.html

List of publications at http://www.ncnr.nist.gov/staff/jeff